Dynamic Matching on a Commuter Carpooling Platform*

Tracy Xiao Liu† Tsinghua University

Zhixi Wan‡ University of Hong Kong

Chenyu Yang§ University of Maryland

July 25, 2024

Abstract

We study dynamic matching using data from a large carpooling platform. The platform facilitates matching between commuting drivers and passengers. Drivers search for passengers with similar routes and departure times, while passengers wait to be matched. We estimate a dynamic matching model and simulate the effects of alternative market designs. Designs that require drivers or passengers to wait until they are matched or reach their departure times increase the number of matches and platform revenue but reduce the average surplus.

Keywords: market design, dynamic matching market, carpooling platform, two-sided market

JEL: C73, D47, D83, L92, R40

1 Introduction

We study the design of a dynamic matching market between drivers and passengers. Their decisions to wait, match, or leave affect future match opportunities. This dynamic externality is central to many online markets, such as ride-hailing and short-term apartment rental platforms. We consider market designs that leverage this dynamic externality and modify how much agents wait and which agents are matched.

Our empirical context is a commuter carpooling platform in China. This platform is interesting for two reasons. First, the platform is large, facilitating over 1 million rides per day in 2018. Second, researchers have found that common ride-hailing platforms such as Uber and Lyft often increase

*We thank seminar and conference participants at the AEA, APIOC, Boston College, DOJ, IIOC, INFORMS, Maryland, Michigan, NASMES, NBER Market Design meeting, NBER Summer Institute (IO and Digitization), SICS, SITE, SUFE IO Conference, Rochester and Western Ontario for valuable insights and comments. We thank Sueyoul Kim and Shu Wang for excellent research assistance. Xiao Liu gratefully acknowledges financial support by the National Natural Science Foundation of China (72222005, 72342032) and Tsinghua University (No. 2022Z04W01032). Chenyu Yang acknowledges the University of Maryland supercomputing resources (http://hpcc.umd.edu) made available for conducting the research reported in this paper. The paper was previously circulated under the title "The Efficiency of A Dynamic Decentralized Two-Sided Matching Market".dear

†School of Economics and Management, Tsinghua University; liuxiao@sem.tsinghua.edu.cn

‡Faculty of Business and Economics, University of Hong Kong; zhixiwan@hku.hk

§Department of Economics, University of Maryland; cyang111@umd.edu

congestion and air pollution (Barnes, Guo and Borgo, 2020; Diao, Kong and Zhao, 2021; Tarduno, 2021), as many people join the platform as full-time drivers (Chen, Rossi, Chevalier and Oehlsen, 2019). Our carpooling platform aims to increase car occupancy rates of existing car-driving commuters, which may lead to a more sustainable solution to urban transportation.

The matching works as follows. A passenger sends a request that specifies her route (origin and destination) and departure time. A commuting driver can then choose a request based on fares and similarities of routes and departure times. After the match, the driver meets the passenger at the passenger's location by the passenger's departure time to start the trip. Unmatched drivers and passengers can stop searching and leave the platform at any time. To comply with local regulations and discourage the participation of full-time drivers, the platform sets fares strictly based on distances that are about 50% lower than taxi fares, often lower than the fuel costs. In addition, a driver can choose at most two requests per day on this carpooling platform.

We empirically study market designs that may improve matching outcomes. The distance-based fares may not fully reflect heterogeneous driver and passenger preferences for matches and waiting costs. In our data, only about 50% of passengers that send requests on the carpooling platform are matched. Subject to the constraint on fares, we consider alternative market designs that exploit the dynamic externality in this two-sided market. One approach is to prolong the waiting time of one or both sides of the market. When drivers and passengers wait more on the platform, a driver can potentially see a bigger choice set of passengers, and a passenger may be considered by more drivers. Another approach is to directly change the set of passengers that a driver can see and choose, which can improve sorting. An important tradeoff of these market designs is that fewer drivers and passengers may decide to participate in the matching market if they are required to wait longer or face other limits on their choices. To quantify the net effects of these designs, we estimate drivers' and passengers' preferences for matches and waiting costs in a dynamic matching model.

We start with an illustrative model to explain our equilibrium notion and market designs. Drivers decide whether to match with a passenger, wait, or leave the market without a match by comparing the value of the match, the expected value of waiting and the value of an outside option. The expected value of waiting is based on the equilibrium distribution of passengers and the cost of waiting. Any unmatched driver reaching her departure time leaves the market. On the passenger side, a passenger forms a belief about the average match rate and sets an optimal leaving time no later than her departure time. The passenger would cancel her ride request and leave the market if she is not matched by the optimal leaving time. Drivers and passengers incur flow waiting costs.

We then define a tractable equilibrium for the matching market. Our equilibrium concept can be viewed as a continuous-time variation of the Non-stationary Oblivious Equilibrium (Weintraub, Benkard, Jeziorski and Van Roy, 2010). In the illustrative model, there is a continuum of two types of drivers and two types of passengers. They dynamically form matches and leave the market. Their beliefs are consistent with how their masses change over time.

We use the illustrative model to simulate counterfactual market designs. The first design is a driver commitment, which requires a driver to wait or match with a passenger. The driver cannot leave without a match until reaching her departure time. The second design is a passenger commit-

ment, which requires a passenger to wait till her departure time or when she is matched. In both designs, the arriving drivers and passengers can choose whether to accept the design or leave the market immediately. The third design shows a driver a selected set of passengers. We discuss the implementability of these designs and, in particular, how to ensure the truthful reports of departure. In numerical simulations, we find that these designs can increase the number of matches but have ambiguous effects on surplus. For example, the driver commitment can decrease driver surplus even though passenger surplus increases with a higher number of matches.

After extending the equilibrium concept to our full model with many types, we use data on drivers and passengers to estimate their preferences. Our data cover a period in the late afternoons of 20 weekdays in a Chinese city. On the driver side, we use a two-step approach. In the first step, we directly estimate driver preferences for matches and expected values of waiting in a choice model. The second step uses these estimates, the equilibrium distributions of passengers and the driver value functions to recover waiting costs. Two sources of variations are important for identification. First, the available passengers, thus driver choice sets, vary across drivers and time. Second, drivers with similar departure times arrive at different times. Our equilibrium model implies an important restriction that allows us to exploit these variations for identification. Namely, drivers do not use observed passengers to infer future choice sets. Therefore the variations of choice sets do not directly enter the expected value of waiting and can identify the driver preferences for matches. Conditional on a departure time, drivers arriving at different times have different planning horizons in their dynamic choice problems, which shifts expected values of waiting. These variations help to identify the driver waiting costs. On the passenger side, variations in passenger characteristics and arrival times similarly identify passenger preferences for matching and waiting costs. We find that the flow waiting costs are higher near the departure time for both drivers and passengers, with drivers' waiting costs markedly higher than passengers'.

We use the estimated model to simulate the effects of counterfactual market designs. For commitment designs, we find that the driver commitment increases the number of matches by 52.7%. The design decreases the share of drivers that wait in the market after arrival from 42.9% to 14.8%, but increases their waiting time by 84%. The design also decreases driver surplus and increases passenger surplus. The passenger commitment has a smaller effect, increasing the number of matches by 5.33%, increasing driver surplus and decreasing passenger surplus. Combining the two commitments, the number of matches increases by 54.86%. Across these scenarios, the average surplus falls. We also use an algorithm to maximize the total number of matches, revenue or average surplus by changing the set of passengers drivers can see. We cannot find any change that improves on these measures.

Contributions and Related Work

First, we contribute to the literature of dynamic matching. The market design literature studying the optimality of dynamic matching markets has identified the trade–offs between waiting time and match quality (Ashlagi, Burq, Jaillet and Manshadi, 2019; Baccara, Lee and Yariv, 2020; Akbarpour, Li and Gharan, 2020; Loertscher, Muir and Taylor, 2022; Doval, 2022). In particular, Akbarpour et al. (2020) considers a dynamic matching market where agents arrive exogenously. A pair of agents

are matched with a certain probability, and agents leave the market when they reach an exogenous departure time but are unmatched. A key insight in their paper is that the platform designer can thicken the market by prolonging the agents' waiting time. To do so, the platform delays matches until just before their departure times. Motivated by this insight, we consider various designs that constrain agent departures from the market and their choices.

We also add to the growing empirical literature on market design (Agarwal and Budish, 2021), especially the study of dynamic allocation mechanisms. Some examples include the allocation of deceased donors' kidneys (Agarwal, Ashlagi, Rees, Somaini and Waldinger, 2021), public housing assistance (Waldinger, 2021), and bear-hunting licenses (Reeling and Verdier, 2021).

In the transportation industry, a number of papers use dynamic models to study the taxi market (Lagos, 2003; Frechette, Lizzeri and Salz, 2019; Buchholz, 2022), ride-hailing platforms (Shapiro, 2018; Bian, 2020; Castillo, 2020; Rosaia, 2020; Gaineddenova, 2022) and dry bulk shipping (Brancaccio, Kalouptsidi and Papageorgiou, 2020; Brancaccio, Kalouptsidi, Papageorgiou and Rosaia, 2023). We define a tractable equilibrium with a large number of agents. Our solution concept is related to those in Jovanovic (1982), Hopenhayn (1992) and the non-stationary oblivious equilibrium in Weintraub et al. (2010).

Our paper is also related to empirical studies of peer-to-peer platforms (Einav, Farronato and Levin, 2016). Some examples include estimating matching on an online dating website (Hitsch, Hortaçsu and Ariely, 2010), the heterogeneous competitive effects of Airbnb (Farronato and Fradkin, 2022), and the determinants of a platform's growth (Cullen and Farronato, 2020). In addition, a number of papers study how search strategies respond to experimental variations in information on market thickness (Bimpikis, Elmaghraby, Moon and Zhang, 2020; Li and Netessine, 2020; Fong, 2024). More broadly, there is a large literature studying market design using experimental methods (Roth, 2016; Chen, Cramton, List and Ockenfels, 2021; Chen, 2023). Finally, our paper is related to the large literature on two-sided markets (Rysman, 2009; Jullien, Pavan and Rysman, 2021). We consider market designs that leverage a dynamic externality in such a market.

Road Map In Section 2, we describe the setting and our data. Section 3 uses an illustrative model to explain the agent decision models and equilibrium concept. We also conduct numerical simulations of the matching market designs. In Section 4, we present the full model. We discuss the identification and estimation of the driver and passenger decision models in Sections 5 and 6. Section 7 compares the equilibrium effects of various market designs, and we conclude in Section 8.

2 Background and Data

We first discuss the workings of the platform in more detail. Then using results from interviews, we highlight features of driver and passenger decisions. Finally, we present our data and provide reduced form evidence on determinants of matches.

2.1 Matching on the Carpooling Platform

The carpooling platform operates without a centralized dispatch system. A prospective passenger sends a ride request to the platform, where waiting drivers decide whether to choose the request. The passenger request specifies the origin, destination, and departure time. The departure time indicates the time when the passenger wishes to be picked up. A driver can view all requests via the platform's app, and the first driver who answers a request is matched with the corresponding passenger.

Figure 1 shows the primary interfaces. We translate the key controls to English in red. The left panel is the driver view. A driver first inputs her trip information (origin and destination of the trip; a departure time indicating the time when she wishes to start driving). She can then see a list of passengers sorted by an algorithm. The algorithm's two key inputs are similarities of routes and departure times. The app uses a compatibility score to measure route similarity. The score is calculated as the distance of the passenger trip divided by the total distance of the trip, which is the distance from the driver origin to the passenger pickup location, then to the passenger destination and finally to the driver's own destination. The score is displayed alongside the passenger's departure time, distances between driver and passenger origins, distances between their destinations and the trip fare. Passengers with similar departure times are also ranked higher. The fare is strictly based on the passenger trip distance with a slight discount on longer trips. [1] A driver can check the list of waiting passengers at any time.

The right panel is the passenger view. The top tab shows 6 different ride-sharing platforms by the same company. The first one is the company's main ride-hailing platform that uses a centralized algorithm to assign a driver to a passenger request. Similar to Uber or Lyft, most drivers on the platform are full-time. This platform is also the largest, serving 60 million riders per day in 2020. The yellow one is the carpooling platform we study. The passenger using this carpooling platform needs to fill out the origin, destination and departure time. The passenger can additionally indicate the number of people in their group, a range for the departure time as opposed to a time point, whether the passenger is willing to share a ride with another passenger, and include a tip. In our data, we find ride-sharing and tipping to be rare (<4% of all requests), and all passengers input time points for the departure time. Our empirical analysis thus focuses on one-driver-to-one-passenger-request matching, where fares are distance based and departure times are time points.

Passenger pickup and dropoff occur after a driver confirms a match with a passenger. The driver will travel to the passenger's origin and pick up the passenger by the departure time set by the passenger. The driver then follows a route set by the app to deliver the passenger to the passenger's destination. The passenger is charged the fare after the dropoff. The platform receives 10% of the fare and the driver receives the rest.

2.2 Driver Decision Rules

We conduct interviews with drivers to understand two key questions about driver choices: (1) how do drivers evaluate match quality? (2) How do they evaluate the values of waiting? We interviewed 34

[1] We fit the observed fare using a 6th order polynomial of trip distances. The resulting fit has a mean squared error of \$0.003. In comparison, the mean and standard deviations of the fares are \$4.84 and \$2.5. All units are in 2018 USD.

Figure 1: Driver and Passenger Interfaces

drivers in two waves in July 2021 (12 drivers) and in October and November 2022 (22 drivers).[2] The first wave was conducted in the city where our data were collected. The second wave was in Beijing.[3] Nine college student interviewers sent ride requests via the carpooling app. They conducted interviews with their drivers during the trips.

2.2.1 Match Quality

Regarding our first question, we find that the most important factors of match quality are the similarities of routes and departure times. In the first wave of interviews, we asked drivers to list their criteria for matching with a passenger, and 10 out of 12 drivers mentioned route similarity. The second most mentioned criterion is the similarity of departure time (7), followed by passenger rating[4] (5) and whether the passenger offers a tip (1). In the second wave, we further asked drivers to rank the criteria identified in the first wave. Among 22 drivers, 17 ranked route similarity the first, and 20 drivers listed route or time similarity as top 2 priorities. Finally, nearly all drivers were able to discuss route similarity using the compatibility score, where 32 out of 34 drivers could give us numerical thresholds (such as 90%) for whether to accept a passenger in various scenarios in the following section.

[2]The detailed descriptions of the interview process and results are available at https://econ-chenyu-yang.github.io/carpooling_interview.pdf

[3]The change of location was due to the Covid shutdowns.

[4]The rating is similar to passenger ratings on ride-hailing platforms and scored by drivers. Low ratings may reflect, for example, past disputes with drivers.

2.2.2 Driver Values of Waiting

We find some evidence that the value of waiting decreases over time, but less evidence that driver decisions are sensitive to the number of compatible passengers in a driver's choice set. Specifically, we ask the drivers the following set of questions:

1. What is the minimum compatibility score you may accept for a passenger at time t?
2. (First wave) Would you accept a passenger with a compatibility score in the first question immediately at a time $t' < t$? (Second wave) Would you choose a passenger with a lower compatibility score at time $t'' > t$?

We use the first question to help the driver frame the choice problem. In the first wave, t is 5 minutes before the driver would stop searching and leave without a match.[5] There are 4 drivers that would not accept the passenger with a compatibility score in the first question at $t' = t - 10$, and 7 such drivers at $t' = t - 25$. This pattern suggests a higher value of waiting at an earlier time. The evidence is more mixed in the second wave in Beijing. We set t to be 40 minutes before the departure time and $t'' = t + 20$. There are 5 (of 22) drivers that would require a lower compatibility score when the time approaches the departure time, while 3 would have stopped searching. We further asked the rest of the drivers why they would not relax the matching criteria. Drivers pointed to the cost of time in traffic if they chose a passenger with an incompatible route. We do note that traffic in Beijing is substantially worse than in the city of the first wave. In addition, drivers use coarse cutoffs (usually multiples of 10 percentage points) for whether to accept a passenger. It is possible that a 10 percentage point decrease in compatibility score has a much larger negative impact on drivers in Beijing than in our sample city.

We next assess how sensitive driver decisions are to the size of the choice set. Sufficiently sophisticated drivers can, for example, infer that if there are more compatible passengers at a time, the value of waiting is higher because the chance that all such compatible passengers become unavailable in the next 5 minutes is lower. Such a driver would be more likely to delay the match and wait for a more compatible passenger.

We find that most drivers in both waves are not more likely to wait when there are more than one acceptable passenger. We asked drivers whether they would wait (instead of matching immediately) when there were two or more passengers with minimally acceptable compatibility scores, following the first question above. All 12 driver in the first wave would match immediately. In the second wave, 16 out of 22 drivers would match immediately, and 5 drivers would wait. One driver was unsure about how she would adjust. These results show that the decisions of a large majority of drivers (82%) are not sensitive to the number of acceptable passengers as long as there is one.

2.3 Passenger Decision Rules

On the passenger side, we wish to understand how passengers make the decision to wait or leave. A key input to this decision is the passenger's belief about when the request is likely to be answered. A

[5] Most drivers (8 of 12) would search until their departure time. One driver would stop searching 30 minutes before the departure time. Two would wait past the departure time. One could not give a definitive answer.

survey of our interviewers shows that they can identify a time window during which matches occur. We asked interviewers to recall when and how likely they were matched. We explicitly instructed them to report their subjective belief without checking their order history. Interviewers reported that the match time depended on the departure time (regardless of when the requests were sent). The time windows of matching range from within 20 minutes to within one hour before the departure time, depending on the origins and destinations of the trips. Our interviewers did not perceive the match rate to be different within the time window. They also expected to be matched in no more than half of the times.

2.4 Data

We obtain our data from the platform operator. Our data consist of a driver sample and a passenger sample across 20 weekdays in 4 consecutive weeks in May and June of 2018 in one city of 1.8 million population. On the driver side, we observe all drivers with reported departure times between 5:00 pm and 5:20 pm. The sample contains the driver routes (origin and destination coordinates), the reported departure times and the time stamps when a driver checks the waiting passengers, which we refer to as a search. The passenger data consist of all passengers sending ride requests between 4:30 pm and 5:00 pm (regardless of departure times).[6] Throughout the paper, we use "departure times" to refer to the times that the drivers and passengers report to the platform, and we discuss how we use the times in our analysis in Section 2.4.1. The data reflect matching for late-afternoon intracity commuting on the platform. A survey of Chinese carpooling platform passengers shows that morning and afternoon commuting needs account for 64% of the rides (China Daily, 2023).

Panel (a) of Table 1 summarizes the driver search data. We define a driver trip as a driver-day combination. We observe 32,621 trips and 17,966 unique drivers. All summary statistics are based on trips, because repeat drivers may have different routes or departure times across days. The first part of the table looks at trip characteristics. On average, the trip length is over 20 km, which is about four to five times of the average taxi trips in China (Liu, Gong, Gong and Liu, 2015) or the US (Buchholz, 2022). Drivers arrive about 18 minutes before the departure time. For locations, we find that although the central business district (CBD) accounts for less than 5% of the land area of the city, the area contains around 25% of drivers' trip origins or destinations. The second part of the table provides statistics on driver search behaviors. We find that a majority of drivers (60%) do not search again after arrival and leave the market. These drivers that left after one search might have made a match or decided to leave without a match. For drivers that do wait in the market after arrival, we define a driver's search duration as the time difference between her first and last search. The average duration is 17 minutes, and a driver searches two to four times. The last search on most of the driver trips are before or very close to the departure times. About 21% of the last searches are after the departure. Within these trips, 74% exceed the departure by less than 1 minute, and 99.86% exceed the departure time by less than 5 minutes.

Due to the different time windows of the driver and passenger samples, we observe only a subset of driver trips' match outcomes. Specifically, we are able to link 12% of the driver trips to passenger

[6] We are limited by the size and the time period of the data the platform can share with us.

Table 1: Summary Statistics

	Mean	Quantile		
		25%	50%	75%
(a) Driver				
Characteristics				
Distance (km)	24.30	13.49	20.30	30.02
Arrival to Departure Time (Minutes)	18.02	5.10	17.33	29.37
% Start in CBD	26.59			
% End in CBD	24.63			
Search				
% Wait After Arrival	39.97			
Duration (Minutes) | Wait After Arrival	17.20	8.10	14.56	24.43
Number of Searches | Wait After Arrival	3.65	2	3	4
Number of Driver Trips		32,621		
(b) Passenger				
Characteristics				
Distance (km)	21.16	11.19	18.17	28.11
Fares ($)*	4.84	3.01	4.43	6.18
Arrival to Departure Time (Minutes)	20.10	14.63	17.48	29.30
% Start in CBD	31.21			
% End in CBD	27.43			
Search				
% Wait After Arrival	84.14			
Duration (Minutes) | Wait After Arrival	6.38	1.12	3.43	8.83
Duration (Minutes) | Matched	5.04	0.88	2.30	6.40
% Matched	44.24			
% Matched | Wait After Arrival	52.58			
# of Matches Per Day | Arrival Time 4:30 pm-5:00 pm**	421.70			
Revenue ($)* Per Day | Arrival Time 4:30 pm-5:00 pm**	2172.42			
Number of Passenger Requests		19,064		

Arrival times for drivers are defined as the first time they search for passengers. Arrival times for passengers are defined as the time they send a request. For those that did not send a request, the arrival time is the time they opened the main ride-hailing tab on the interface. For drivers, "Wait after arrival" means that a driver searches for passengers for at least two times. For passengers, "Wait after arrival" means that the passenger sends a request on the carpooling platform.

*: Fares are in 2018 USD.

**: Averaged across 20 days in the sample

requests in our sample. For the rest of the trips, a driver might have matched with a passenger that arrived outside the 4:30 pm-5:00 pm time window, or left the market without a match.

For each passenger request, we observe the route, the time the request is sent, and the departure time. We observe the match outcomes for all passenger requests. If a passenger is matched, we observe the time of the match and the ID of the matched driver. We can link 47% of the matched driver-passenger pairs to drivers in our driver data. We also note that the matches and cancellations may occur after 5:00 pm, and a passenger may be matched with a driver not in our driver sample (i.e. a driver with a departure time outside the 5:00 pm to 5:20 pm window). If a request is canceled (the passenger leaves the market without a match), we observe the time of the cancellation. To mirror the drivers who search only once, we additionally construct a set of potential passengers that arrive to the app but do not use the carpooling service with browsing data of the main ride-hailing platform.[7] Panel (b) of Table 1 summarizes the passenger data. We observe a total of 19,064 requests across 20 days by 14,162 passengers. Like the driver side, all statistics are based on requests. We find that the passenger and driver trip lengths are similar, with an average fare of $4.84. Passengers arrive about 20 minutes before their departure times. Over 80% of passengers decide to wait after arrival. The search duration of the passengers that decide to wait, defined as the time difference between arrival and the time of the match or cancellation, is 6.38 minutes, substantially shorter than drivers'. Most of the passenger requests are answered or canceled before the departure times (99.76%). About 974 passengers arrive at the platform and 422 matches occur per day in our passenger sample across the 20 days in our sample. In addition, passengers arrive at a roughly constant rate of 31.77 passengers/minute during the time window (Appendix A.1).

2.4.1 Departure Times

We consider the reported departure time as representing the end of an agent's planning horizon when she decides whether to continue searching or leave the platform. First, although the reported departure times are not binding,[8] most of the drivers and passengers in the data nonetheless stop searching before the departure times, as shown above. Moreover, the platform provides incentives for reporting the departure time truthfully as the time a trip should physically start. For a driver, passengers with more similar departure times are ranked higher. Our interviews with drivers additionally confirm that most drivers would leave at the reported departure times when they could not find suitable passengers. For a passenger, the driver will meet the passenger at the passenger's reported departure time for the pickup after the driver matches with the passenger. Misreporting the departure time may be undesirable for a passenger who, for example, cannot leave work early or needs to pick up children from school by a certain time.

[7] The main ride-hailing platform is similar to Uber or Lyft, and it is accessible as the first tab of "other ride sharing services" on the passenger view of the interface in Figure 1. For each of the 20 days in our sample, we define potential passengers on a day as those that (1) entered trip information on the passenger interface of the main ride-hailing service of the platform between 4:30 pm and 5:00 pm, (2) did not send a carpooling request on this day, and (3) sent at least one request on our carpooling platform on a different day. The search duration of these potential passengers are set to 0.

[8] After the departure time, an unmatched driver can continue to search and a passenger does not need to cancel her request.

2.5 Reduced Form Evidence

In this section, we first use the linked driver-passenger data to highlight empirically important determinants of matches. These findings as well as our interviews with drivers guide our specification of driver preferences. We next describe how arrival and departure times affect search durations. These variations underlie our empirical strategy to identify waiting costs.

2.5.1 Determinants of Matches

To understand the determinants of matches, we link each instance of a driver searching for passengers with the set of passengers available at that time. Despite observing only a subset of waiting passengers (only those arriving between 4:30 pm and 5:00 pm), we find robust patterns that matched driver-passenger pairs are significantly more compatible than the unmatched.

Specifically, we construct a dyadic data set given the linked data and directly compare measures of compatibility between unmatched and matched dyads. Each dyad consists of a driver who searches at a time t and a passenger waiting at t. A waiting passenger is defined as one whose arrival time is before t and whose match or cancellation time is at or after t. Table 2 shows that compatibility score is on average 0.47 for all dyads, compared with 0.83 of the dyad that corresponds with a match. These matched dyads are also more compatible on other dimensions. They have shorter pickup or dropoff distances (distances between origins and destinations) and smaller differences in departure times. The fares in matched dyads are also higher. In Appendix A.2, we use dyadic regressions to examine how being matched is related to these characteristics. We additionally find that a driver approaching her departure times is more likely to match with a passenger.

2.5.2 Arrival Time and Waiting

We next present findings on how the arrival-to-departure time affects the decisions on waiting. The arrival-to-departure time is the difference between the time of arrival and the reported departure time. This relationship sheds light on the waiting costs. For intuition, consider two agents who arrive at 4:30 pm and 4:45 pm but are otherwise identical. They both plan to depart at 5:10 pm. Conditional on not being matched, both agents should wait till 5:10 pm when the waiting cost is low, and their search durations would be 40 minutes and 25 minutes, the same as the arrival-to-departure times. On the other hand, at a high waiting cost, both might wait only 5 minutes before canceling their requests. Therefore, a high correlation between the arrival-to-departure time and the search duration points to low waiting costs. A key assumption behind this argument is that agent arrival times are independent of unobserved preferences for matches conditional on their observed characteristics and departure times. We provide more details on the identification argument in Sections 5 and 6 after introducing the model.

We find a moderate degree of correlation between arrival-to-departure time and waiting. First, we regress whether an agent waits after arrival on arrival-to-departure time and other characteristics. Second, on the subsample of agents that wait after arrival, we regress the search duration on the same covariates. Panel (a) of Table 3 reports the results for drivers. We find that the marginal effect of

Table 2: Linked Dyadic Data Summary Statistics

	Mean	Quantiles		
		25%	50%	75%
All Dyads				
Compatibility Score	0.47	0.30	0.43	0.60
Pickup Distance (km)	15.09	8.84	14.94	21.44
Dropoff Distance (km)	15.63	9.34	15.80	22.07
Fare ($)	4.42	2.93	3.98	5.41
Departure Time Difference (Minutes)	-2.88	-13	0	10
Number of Dyads		2,449,963		
Matched Dyads				
Compatibility Score	0.83	0.76	0.85	0.93
Pickup Distance (km)	2.73	0.99	1.97	3.48
Dropoff Distance (km)	3.79	1.10	2.35	4.69
Fare ($)	5.55	3.84	5.10	6.62
Departure Time Difference (Minutes)	0.63	-6	0	10
Number of Dyads		3,970		

Note: pickup and dropoff distances are distances between origins and destinations. Departure time difference is defined as the driver departure time minus the passenger departure time in a dyad. Fares in 2018 USD.

arriving 10 minutes earlier translates to up to a 20-percentage-point increase in the probability of waiting. The effect is large given that the average probability of waiting is 0.4 in Table 1. Comparing columns (1) and (2), we find that the arrival-to-departure time alone explains about 16% of the variations in the waiting decision. Including driver characteristics in the regressions decreases the estimated effects by 25%, and R^2 slightly increases. We also find that the arrival-to-departure time is positively correlated with search duration in columns (3) and (4): arriving 10 minutes earlier is associated with over 6 additional minutes of search time. Overall, the arrival-to-departure time explains 39% of the variations in the search durations. In panel (b), we use the subsample of passengers who are not matched and eventually cancel their requests. The marginal effect of arrival-to-departure time is similar to panel (a), and the effect on search duration is about half of the size.

3 Equilibrium and Market Design in an Illustrative Example

Before introducing the full model, we use an illustrate model to explain the key elements of our empirical framework. We consider a continuous-time matching market with a continuum mass of drivers and passengers. There are 2 types of drivers and 2 types of passengers. Driver and passenger preferences for matches differ across types. We use $\{a, b\}$ to index driver types and $\{1, 2\}$ to index passenger types. Agents of each type arrive to the market at a constant rate of $\frac{1}{T}$.

Table 3: Search Duration Regression

	Wait After Arrival		Search Duration | Arrival	
(a) Driver				
	(1)	(2)	(3)	(4)
Arrival to Departure Time (Minutes)	0.020	0.015	0.676	0.637
	(0.000)	(0.000)	(0.003)	(0.008)
Distance 10-30 km		0.085		-0.036
		(0.008)		(0.274)
Distance >30 km		0.074		0.266
		(0.009)		(0.299)
Start in CBD		0.022		-0.427
		(0.006)		(0.171)
End in CBD		0.029		-0.264
		(0.006)		(0.175)
Intercept		0.042		1.313
		(0.008)		(0.302)
R^2	0.16	0.18	0.39	0.39
Number of Search Instances	32,621	32,621	13,038	13,038
(b) Passenger				
	(1)	(2)	(3)	(4)
Arrival to Departure Time (Minutes)	0.030	0.019	0.310	0.292
	(0.000)	(0.000)	(0.004)	(0.013)
Distance 10-30 km		0.180		1.152
		(0.010)		(0.206)
Distance >30 km		0.257		2.059
		(0.010)		(0.249)
Start in CBD		-0.004		-0.054
		(0.008)		(0.184)
End in CBD		-0.003		-0.039
		(0.008)		(0.199)
Intercept		0.154		-0.620
		(0.012)		(0.317)
R^2	0.17	0.26	0.14	0.15
Number of Requests	10,630	10,630	7,607	7,607

Note: in columns (1) and (2), we regress the indicator of whether the agent waits after arrival on the covariates. In columns (3) and (4), on the subsample of agents that wait after arrival, we regress the search duration on the covariates. For columns (3) and (4) in the passenger panel, we use the set of passenger that were not matched and canceled their requests. We report robust standard errors in parentheses.

3.1 Driver Decision Model

Upon arrival, a driver can decide to match with a passenger, wait or leave without a match. Should the driver decide to wait, she considers these decisions again when she receives a move opportunity, which arrives at rate λ. All drivers face a departure time at T. A driver leaves the market when she reaches the departure time and is still not matched. Throughout the paper, we use "leave" to refer to the action where a driver or a passenger stops searching on the platform. The departure time in the model represents the end of an agent's planning horizon and corresponds with the reported departure time in the data.

We now specify driver preferences and waiting costs. We use $u_{k\ell}$ to denote a type k driver's value for matching with a type ℓ passenger. We also assume that drivers incur a flow waiting cost, $c^{\text{drv}}\frac{t}{T}$, at the clock time $t \in [0, T]$, where c^{drv} is a positive constant. We use this simple linear function increasing in t to capture the increasing opportunity cost of waiting when the departure time is closer.[9]

We next describe driver beliefs. We use $p_{k\ell}(t)$ to denote a type k driver's belief of observing a type ℓ passenger, and $g_{k\ell}(t)$ for the belief that, conditional on observing a type ℓ passenger, the available passenger with the highest match value is a type ℓ passenger. We use $p_k(t)$ to denote the belief that the driver choice set is not empty. Consistent with our interviews of the drivers, we assume that these beliefs do not depend on how many passengers were observed at past move opportunities, but the beliefs can vary over time and differ across types. In the equilibrium defined later, we require the beliefs to be consistent with the masses of passengers.

We now state the driver decision problem. We focus on a driver i of type k and set the value of leaving without a match to 0. At time t and for a small amount of time Δ, the driver's value function is

$$\begin{aligned} V_i(t) = \Delta\lambda \cdot \Big(& p_{k1}(t) \cdot g_{k1}(t) \cdot E \max\left\{u_{k1} + \varepsilon_{it}^1, V_i(t+\Delta) + \varepsilon_{it}^2, \varepsilon_{it}^3\right\} \\ & + p_{k2}(t) \cdot g_{k2}(t) \cdot E \max\left\{u_{k2} + \varepsilon_{it}^1, V_i(t+\Delta) + \varepsilon_{it}^2, \varepsilon_{it}^3\right\} + (1 - p_k(t)) E \max\left\{V_i(t+\Delta) + \varepsilon_{it}^2, \varepsilon_{it}^3\right\} \Big) \\ & + (1 - \Delta\lambda) V_i(t+\Delta) - \Delta \cdot c^{\text{drv}} \frac{t}{T}, \end{aligned}$$

where the expectation is taken over the i.i.d. action specific shocks $\varepsilon_{it}^{(\cdot)}$ for each action. We assume that the shocks follow the Extreme Value Type 1 (EV1) distribution. After integrating out these shocks, we note that the value function is the same for all drivers of type k. With a slight abuse of notation, we use $V_k(t)$ to denote any type k driver's value function. The formulation yields the

[9] Appendix A.3 provides evidence that the decision to leave depends on the time to departure, and not the time an agent has waited in the market.

Hamilton–Jacobi–Bellman equation,

$$0 = \lambda \cdot \Big(\Upsilon + p_{k1}(t) \cdot g_{k1}(t) \cdot \ln\left(\exp(u_{k1}) + \exp(V_k(t)) + 1\right) \tag{1}$$
$$+ p_{k2}(t) \cdot g_{k2}(t) \cdot \ln\left(\exp(u_{k2}) + \exp(V_k(t)) + 1\right) + (1 - p_k(t)) \cdot \ln\left(\exp(V_k(t)) + 1\right) \Big)$$
$$+ \frac{dV_k}{dt} - \lambda V_k(t) - c^{\text{drv}} \frac{t}{T},$$

where Υ is the Euler constant.

We can now write down the choice probabilities. We use $q_{k\ell}(t)$ to denote the probability of a type $k \in \{a, b\}$ driver matching with a type $\ell \in \{1, 2\}$ passenger conditional on a move opportunity and the driver observing a type ℓ passenger. The driver maximization problem implies that

$$q_{k1}(t) = \frac{g_{k1}(t) \cdot \exp(u_{k1})}{\exp(u_{k1}) + \exp(V_k(t)) + 1}, q_{k2}(t) = \frac{g_{k2}(t) \cdot \exp(u_{k2})}{\exp(u_{k2}) + \exp(V_k(t)) + 1}. \tag{2}$$

We use $w_k(t)$ to denote the conditional probability that a driver leaves the market without a match given a move opportunity:

$$w_k(t) = \underbrace{\frac{p_{k1}(t) g_{k1}(t)}{\exp(u_{k1}) + \exp(V_k(t)) + 1} + \frac{p_{k2}(t) g_{k2}(t)}{\exp(u_{k2}) + \exp(V_k(t)) + 1}}_{\text{When the choice set is not empty}} \tag{3}$$
$$+ \underbrace{(1 - p_k(t)) \frac{1}{\exp(V_k(t)) + 1}}_{\text{When the choice set is empty}}.$$

3.2 Passenger Decision Model

We similarly focus on a passenger j of type $\ell \in \{1, 2\}$. We model the passenger's action as choosing an optimal time $t_j^\star$ to leave the market, because passengers do not actively search for drivers. Consistent with the experience of our interviewers, we keep passenger beliefs simple. Specifically, we assume that a passenger of type ℓ believes that she is matched at a type-specific but time-invariant rate γ_ℓ. We use v_j to denote a passenger j's value for being matched and v_{0j} for the value of the outside option, which may reflect the cost of an alternative type of transport. Similar to drivers, they also incur a flow waiting cost $c^{\text{psg}} \frac{t}{T}$ at t, where c^{psg} is a positive constant.

The passenger chooses an optimal leaving time $t_j^\star$. The passenger waits until $t_j^\star$. Then she cancels her request and leaves the platform. For any $t_j^\star < T$, the marginal value of waiting over a small amount of time Δ, $\Delta\gamma_\ell v_j + (1 - \Delta\gamma_\ell) v_{0j}$, must be equal to the additional waiting cost at $t_j^\star$, $\Delta \cdot c^{\text{psg}} \frac{t_j^\star}{T}$. Therefore the optimal leaving time is

$$t_j^\star = \frac{\gamma_\ell \cdot T}{c^{\text{psg}}} (v_j - v_{0j}), \tag{4}$$

if the right hand side is less than T, and $t_j^\star = T$ otherwise.

We use (4) to find the probability that a type ℓ passenger would send a request and wait. We assume

that $v_j - v_{0j} = v_\ell + \xi_j$, where ξ_j is i.i.d. and follows the logistic distribution. For an arriving passenger at t to send a request and wait, her optimal leaving time must be no earlier than t. Otherwise, the passenger should leave immediately, because the marginal expected value of waiting would be lower than the marginal cost of waiting. We use S_ℓ to denote the probability of waiting at t for a type ℓ passenger, where

$$S_\ell(t;\gamma_\ell) \equiv \Pr\left(t_j^\star > t\right) = \frac{1}{1+\exp\left(\frac{c^{\text{psg}}\cdot t}{\gamma_\ell \cdot T} - v_\ell\right)}. \tag{5}$$

This probability also implies the leaving rate as

$$r_\ell(t) = -\frac{dS_\ell}{dt}/S_\ell. \tag{6}$$

3.3 Equilibrium

The equilibrium connects the driver and passenger beliefs and actions with how respective masses change over time. We use $n_\ell(t)$ to denote a type ℓ's mass at t. As type ℓ's passengers arrive at rate $\frac{1}{T}$, $n_\ell(t)$ should be no greater than the total arrival by t, which is $\frac{t}{T}$, and thus less than 1. We interpret this passenger mass as the probability that a driver observes a type ℓ passenger at t. More formally,

Assumption 1. *(Driver Choice Set) At time t, a driver that receives a move opportunity at t observes one passenger of type ℓ with probability $n_\ell(t)$ independently.*

Specifically, we assume that the set of passengers a driver observes is composed of at most one passenger per type. The probability that a type ℓ passenger is in this set is $n_\ell(t)$. This assumption is a key part of our equilibrium notion. An important benefit of this assumption is that consistent driver beliefs now have simple forms. As an example, suppose $n_1(t) = \frac{1}{4}$ and $n_2(t) = \frac{1}{3}$. Then the possible sets of passengers a driver searching at t are

$$\{\emptyset\}, \{\text{a type 1 passenger}\}, \{\text{a type 2 passenger}\}, \{\text{a type 1 passenger and a type 2 passenger}\}.$$

The probabilities for these outcomes are $\frac{3}{4}\cdot\frac{2}{3}$,$\frac{1}{4}\cdot\frac{2}{3}$, $\frac{3}{4}\cdot\frac{1}{3}$ and $\frac{1}{4}\cdot\frac{1}{3}$. In the following, we first explain the mechanics of the equilibrium conditions based on Assumption 1. Then in Section 3.3.1, we discuss the interpretation of our equilibrium in more detail.

Based on Assumption 1, the probabilities of observing a type ℓ passenger is just $p_{k\ell}(t) = n_\ell(t)$. The probability of observing a non-empty choice set is $p_k(t) = 1-(1-n_1(t))(1-n_2(t))$. To simplify expressions for driver beliefs (g_{k1}, g_{k2}), we assume the following:

Assumption 2. $u_{k1} > u_{k2}$.

In other words, we assume that all drivers prefer the type 1 passengers. This assumption is not necessary in our general model. Given this assumption, conditional on observing a type 1 passenger, the probability that it is the highest value passenger is $g_{k1} = 1$. Conditional on observing a type 2 passenger, the probability that it is the highest value passenger is that no type 1 is observed, and therefore $g_{k2}(t) = 1 - n_1(t)$.

For passengers, the belief about the match rate is consistent with the average match rate over $[0, T]$. Let $m_k(t)$ denote the driver mass at t. Given a small amount of time Δ, the number of matched type ℓ passengers is

$$\mathrm{dP}_\ell(t) = \Delta\lambda\left(m_a(t)\, q_{a\ell}(t) + m_b(t)\, q_{b\ell}(t)\right) \cdot n_\ell(t).$$

Therefore the conditional probability of being matched is $\mathrm{dP}_\ell(t)/n_\ell(t)$. Integrating this probability over $[0, T]$ yields the average match rate as the passenger belief:

$$\gamma_\ell = \frac{1}{T}\int_0^T \lambda\left(m_a(\tau)\, q_{a\ell}(\tau) + m_b(\tau)\, q_{b\ell}(\tau)\right) d\tau. \tag{7}$$

We now state the equilibrium definition in this setting. The equilibrium consists of three sets of conditions that discipline the quantities $(V_k, q_{k\ell}, w_k, p_k, g_{k1}, g_{k2}, \gamma_\ell, S_\ell, r_\ell, m_k, n_\ell)$, for $k \in \{a, b\}$ and $\ell \in \{1, 2\}$.

Definition 1. Equilibrium in the Illustrative Example.

1. (Optimality) The driver value functions V_k and the choice probabilities $(q_{k\ell}, w_k)$ should be consistent with (1), (2) and (3), and the passenger leaving rate r_ℓ consistent with (6).

2. (Consistent Beliefs) The driver beliefs are $p_{k\ell}(t) = n_\ell(t)$, $p_k(t) = 1 - (1 - n_1(t))(1 - n_2(t))$, $g_{k1}(t) = 1$ and $g_{k2}(t) = 1 - n_1(t)$. The passenger belief γ_ℓ is given in (7).

3. (Mass Transitions) For drivers, the mass increases when a driver arrives and decides to wait, and decreases when a waiting driver decides not to wait. Given a move opportunity, the probability that a driver leaves the market is $w_k + n_1 q_{k1} + n_2 q_{k2}$. With an arrival rate of $\frac{1}{T}$, the transition of type k's mass satisfies (omitting the t argument):

$$\frac{dm_k}{dt} = -\lambda m_k \cdot (n_1 q_{k1} + n_2 q_{k2} + w_k) + \frac{1}{T} \cdot (1 - w_k - n_1 q_{k1} - n_2 q_{k2}). \tag{8}$$

   A passenger that arrives at t would wait if its optimal leaving time is greater than t, which occurs with probability $S_\ell(t; \gamma_\ell)$. With an arrival rate of $\frac{1}{T}$, the transition of type ℓ's mass satisfies

$$\frac{dn_\ell}{dt} = -n_\ell \cdot \left(\left(\lambda m_a + \frac{1}{T}\right) q_{a\ell} + \left(\lambda m_b + \frac{1}{T}\right) q_{b\ell} + r_\ell\right) + \frac{1}{T} \cdot S_\ell(t; \gamma_\ell). \tag{9}$$

In Appendix B, we prove the existence of the equilibrium. The detailed numerical solution algorithm is given in Appendix E.

3.3.1 Interpretation of the Equilibrium

We interpret the equilibrium outcome as an approximation of a matching market with two drivers and two passengers. The agent masses and matched masses are fractional analogs of the number of agents and number of matches. Ostrovsky and Schwarz (2018) calls the resulting matches "quasi-assignments". In the empirical model, we use a large number of types, where types differ in characteristics such as routes and departure times. The equilibrium in the empirical model approximates a market with a large

number of agents with heterogeneous characteristics. We can alternatively interpret the illustrative model's equilibrium for a market with a large number of drivers and passengers, each of two types. Assumption 1 is equivalent to a search technology such that the probability for a driver to observe a type of passengers is proportional to the number of such passengers. Under this interpretation, the equilibrium approximation becomes exact with an infinite number of agents (Weintraub et al., 2008, 2010).

This equilibrium notion has a number of appealing features. First, although each individual agent receives idiosyncratic preference shocks and takes different actions, the transitions of the agent masses are still deterministic when actions of a continuum of agents are aggregated. Specifically, this aggregation results in the deterministic mass transitions (8) and (9). Agent beliefs therefore only need to condition on time, which is consistent with our interviews with drivers. We do note that the model still allows for rich heterogeneity in both value functions and choice probabilities across drivers and passengers. Second, the ordinary differential equations defining the driver value functions (1) and transitions of masses (8) and (9) are simple to solve via backward induction, and the implied driver choice probabilities (2) and (3) and passenger leaving rate (6) have closed form expressions. Third, many important statistics can be easily calculated with an equilibrium solution. For example, the number of matches is given by $\int_0^T \lambda \sum_{k,\ell} m_k(t)\, n_\ell(t)\, q_{k\ell}(t)\, dt$. In Appendix G, we show that the equilibrium predictions of these statistics are good approximations of the simulated statistics based on markets with a discrete and finite number of drivers and passengers.

We also note that the equilibrium embeds the dynamic externality central to the empirical matching market. First, the transition of masses dynamically changes match opportunities. For example, when n_a and q_{a1} are high at t, more a-1 matches would occur, reducing type 1's mass and the probabilities that type b drivers observe type 1 passengers later. Second, the decision models and the equilibrium do not predetermine whether there will be inefficiency. Inefficiency could occur when, for example, agents lack incentives to wait: passengers that arrive near $t = T$ but with high preferences for matches cannot offer high fares so that drivers that arrive near $t = 0$ would wait longer. The extent of the inefficiency in the equilibrium depends on agent preferences and waiting costs.

3.4 Market Design

Given the equilibrium model in the previous section, we use simulations to illustrate the equilibrium effects of three market designs.[10] In Section 3.4.1, we discuss the first design, which restricts drivers from leaving the platform without matching with a passenger. The second design in Section 3.4.2 limits passengers from canceling the request. The third design in Section 3.4.3 aims to improve sorting by selectively showing passengers to drivers, effectively blocking certain matches. We describe the modified matching designs, discuss practical implementation and state the modified matching equilibrium. In numerical simulations, we examine the effectiveness of the designs under different waiting costs in Section 3.4.4.

[10] Although we find multiple equilibria, the outcomes are quantitatively similar. We discuss equilibrium selection in Appendix E.

Figure 2: Market Designs under Different Waiting Costs

(a) Vary Driver Waiting Costs (b) Vary Passenger Waiting Costs

i. Number of Matches

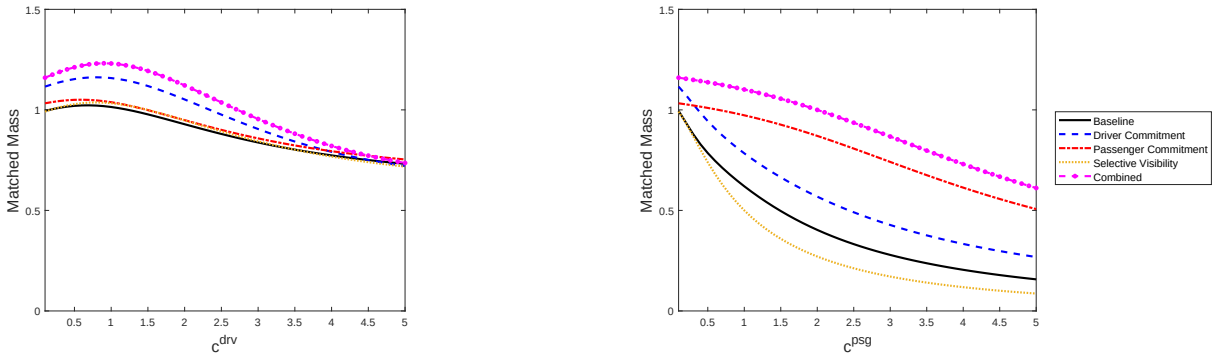

ii. Driver Surplus

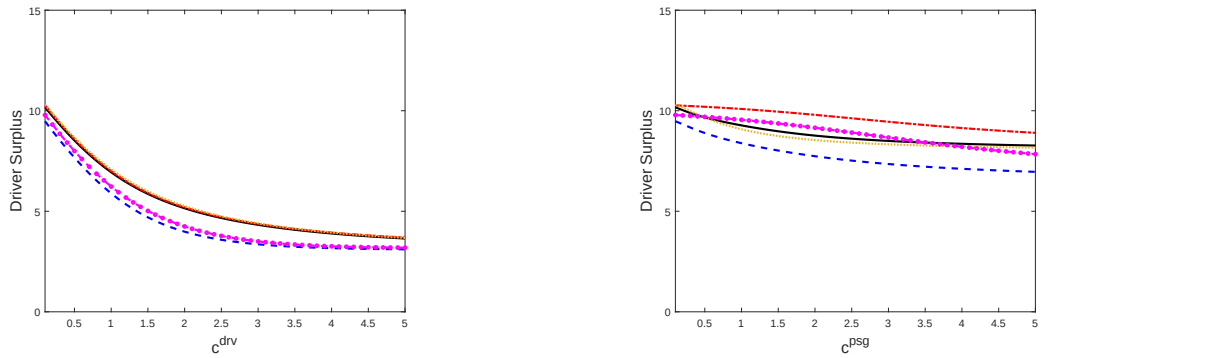

iii. Passenger Surplus

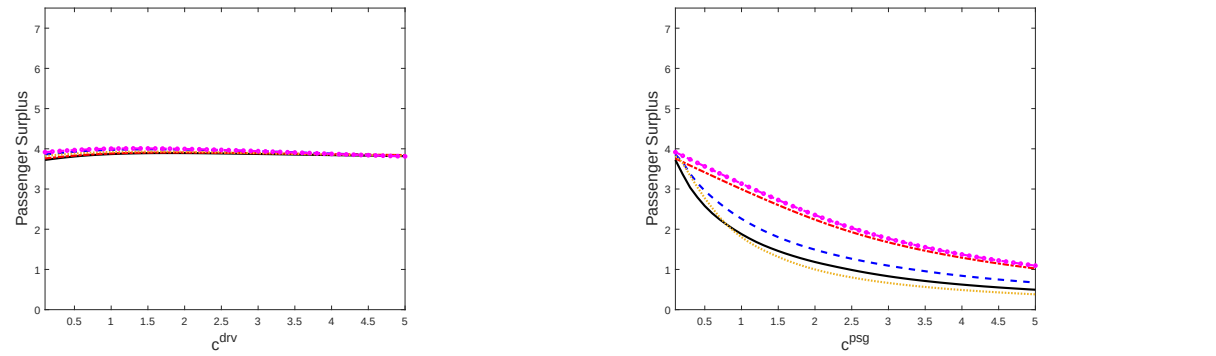

iv. Total Surplus

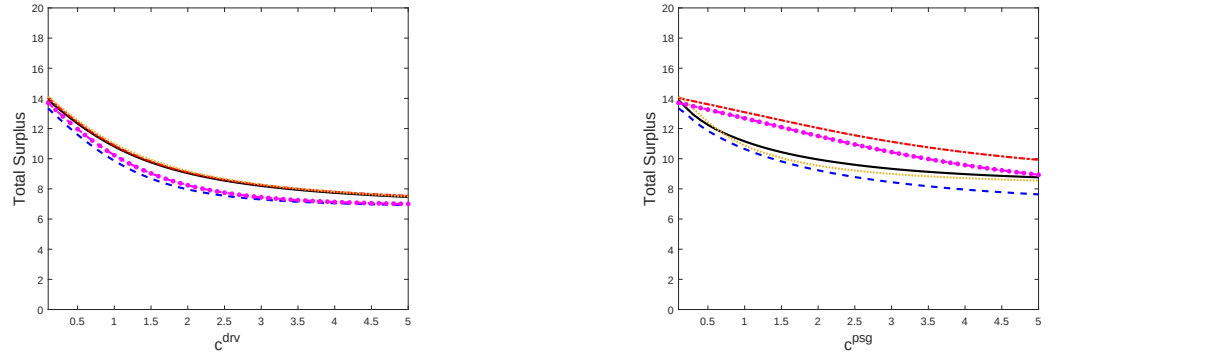

Note: We set $u_{a1} = 2, u_{a2} = 1.5, u_{b1} = 4, u_{b2} = -4$, $v_1 = v_2 = 2$, $T = 10$. Drivers and passengers arrive between 0 and T with a departure time of T. Drivers move at frequency $\lambda = 1$. In Figure (a), we set $c^{psg} = 0.1$ and vary c^{drv} from 0.1 to 5. In Figure (b), we set $c^{drv} = 0.1$ and vary c^{psg} from 0.1 to 5.

3.4.1 Redesign I: Driver Commitment

We first consider a matching design that directly prevents a waiting driver from leaving without a match. Specifically, when a driver arrives at the platform, she can choose a passenger, continue to wait or leave the platform. Should she choose to continue to wait, the driver's choice is more limited: at every move opportunity, she can choose from the observed passengers or wait. The driver cannot leave the market without a match until reaching her departure time. The number of matches may increase through a direct effect: matching with a passenger now becomes a relatively more attractive option, because the driver has fewer actions available (leaving without a match is no longer an option), and the value of waiting may be lower because the driver also has fewer actions available in the future. There is also an indirect effect that operates through the equilibrium: when facing undesirable passengers, drivers now must wait instead of leaving, increasing the total number of waiting drivers and hence the passengers' value of waiting. This equilibrium force in turn increases passenger waiting, leading to a thicker passenger market and more choices for drivers. We also note that the equilibrium effect could also reduce the number of matches, because few drivers may decide to wait in the market after arrival when the value of waiting is low. Fewer drivers may decrease passenger values of waiting, which in turn reduces the number of waiting passengers and driver choices.

Practical Implementation Given the truthfully reported departure times, the design is simple to implement: when a driver opens the app, the platform shows her three choices: choose a passenger, leave the platform or agree to the commitment. If the driver agrees to the commitment, she can check the list of passengers periodically until when she matches with a passenger or her departure time. We discuss several implementation challenges and potential solutions. First, a driver may self-report an early departure time so that she is "locked in" for less time. We note that the departure time difference between most matched driver-passenger pairs is within 10 minutes. To incentivize truthful reporting, the platform can limit the set of passengers a driver sees to those whose departures times are within 10 minutes from the driver's. The platform can also stop the driver from accessing the list of passengers after the self-reported departure time.[11] Second, a driver may participate in the matching nominally. Namely, after agreeing to wait but deciding to leave anyway, a driver may still keep the app open but just start her trip. To address this issue, the platform can geo-locate a driver's phone to ensure that the driver remains in the same location. We note that geo-location is an essential and uncontroversial part of almost all ride-hailing apps. In addition, the app can send periodic reminders to prompt the drivers to view the set of waiting passengers. The platform can also require a driver to view the list at least once per, for example, 5 or 10 minutes as part of the commitment. Third, a driver may simply decide to close the app and stop the search even after agreeing to wait after arrival. A direct solution is to temporarily suspend the driver from using the platform for violations. In general, limiting usage is a common way for ride-hailing platforms to enforce control.[12] On the other hand,

[11] Similarly, a driver may start the search closer to her departure time, but doing so means that the driver would lose some opportunities to match and may be undesirable.

[12] A nontrivial share of drivers routinely use this carpooling platform, and limiting usage could be a sufficient deterrence. In our 20-day sample, 34% of drivers search for passengers the platform on at least two different days. On Lyft, for example, a driver may lose "driving priority", the priority for receiving orders, if a driver declines requests too many

it is also common for ride-hailing platforms to reward more active drivers, such as the Uber Pro and Lyft Rewards programs. The carpooling platform can similarly offer additional (fixed-sum) pay to drivers for complying with the market design. Finally, drivers may decide not to open the app for fear of accidentally agreeing to wait. User-interface designs, such as requiring multiple confirmations before the waiting starts, can reduce chance errors.

Equilibrium We now define the new matching equilibrium under this design. The new equilibrium modifies the equations underlying the driver decisions and mass transitions. We group the modifications in the same order as in Definition 1.

1. (Optimality) For a type k driver, the value function is modified as

$$\begin{aligned} 0 = \lambda \cdot \Big(& \Upsilon + p_{k1}(t) \cdot g_{k1}(t) \cdot \ln\left(\exp(u_{k1}) + \exp V_k(t)\right) \\ & + p_{k2}(t) \cdot g_{k2}(t) \cdot \ln\left(\exp(u_{k2}) + \exp V_k(t)\right) + (1 - p_k(t)) \cdot V_k(t) \Big) \\ & + \frac{dV_k}{dt} - \lambda V_k(t) - c^{\text{drv}} \frac{t}{T}, \end{aligned}$$

   For the equivalent of choice probability functions (2) and (3), we first distinguish choices of arriving drivers from those of waiting drivers. Upon arrival, the conditional choice probabilities at t are

$$q^0_{k1}(t) = \frac{g_{k1}(t)\exp(u_{k1})}{\exp(u_{k1}) + \exp(V_k(t)) + 1}, q^0_{k2}(t) = \frac{g_{k2}(t)\exp(u_{k2})}{\exp(u_{k2}) + \exp(V_k(t)) + 1}.$$

   The leaving probability upon arrival is

$$\begin{aligned} w^0_k(t) = & \frac{p_{k1}(t) \cdot g_{k1}(t)}{\exp(u_{k1}) + \exp(V_k(t)) + 1} + \frac{p_{k2}(t) \cdot g_{k2}(t)}{\exp(u_{k2}) + \exp(V_k(t)) + 1} \\ & + \frac{1 - p_k(t)}{\exp(V_k(t)) + 1}. \end{aligned}$$

   A waiting driver no longer has the option to leave the platform unless she matches with a passenger or reaches the departure time T. The conditional choice probabilities at t for a driver that receives a move opportunity at t but arrives before t are

$$q_{k1}(t) = \frac{g_{k1}(t)\exp(u_{k1})}{\exp(u_{k1}) + \exp(V_k(t))}, q_{k2}(t) = \frac{g_{k2}(t)\exp(u_{k2})}{\exp(u_{k2}) + \exp(V_k(t))}.$$

2. (Consistent Belief) Driver beliefs are the same as in Definition 1. The passenger beliefs are modified as (omitting t argument)

$$\gamma_\ell = \frac{1}{T}\int_0^T \left(\lambda m_a q_{a\ell} + \frac{1}{T} q^0_{a\ell} + \lambda m_b q_{b\ell} + \frac{1}{T} q^0_{b\ell}\right) d\tau.$$

times (Lyft (2019, 2023)). Uber sends out fewer requests to drivers who declines rides (Marshall (2020)).

3. (Mass Transitions) The transition of driver mass (8) is modified as

$$\frac{dm_k}{dt} = -\lambda m_k \cdot (n_1 q_{k1} + n_2 q_{k2}) + \frac{1 - w_k^0 - n_1 q_{k1}^0 - n_2 q_{k2}^0}{T}.$$

The passenger mass transition is

$$\frac{dn_\ell}{dt} = -n_\ell \cdot \left(\lambda m_a q_{a\ell} + \frac{1}{T} q_{a\ell}^0 + \lambda m_b q_{b\ell} + \frac{1}{T} q_{b\ell}^0 + r_\ell \right) + \frac{1}{T} \cdot S_\ell \left(t; \gamma_\ell \right). \tag{10}$$

3.4.2 Redesign II: Passenger Commitment

We can implement a similar design for passengers. Specifically, the platform can ask an arriving passenger to either leave the platform or wait till T. The design modifies the probability $S_\ell \left(t; \gamma_\ell \right)$ in (5), which is the probability that an arriving passenger decides to wait, and the mass transition condition in (10). We provide the equilibrium conditions under this design in Appendix C.1.

Practical Implementation Implementing this design faces similar challenges as on the driver side. We note that usage limits, geo-location and user interface designs can still be effective in ensuring compliance with the platform rules without discouraging the use of the app. Passengers may have an incentive to report an earlier departure time than the truth and save on waiting costs. We note that most of the passengers in our context commute from work to home. Therefore reporting an early departure time could mean that the passenger has to leave work early to receive the ride when a driver accepts the passenger's request, which may be undesirable for these passengers.

3.4.3 Redesign III: Selective Visibility

The last design aims to improve sorting. As an example, we assume that, although all drivers prefer type 1 passengers, the two types of passengers are similarly compatible for type a drivers (e.g., $u_{a1} = 2, u_{a2} = 1.5$), but a type b driver prefers the type 1 passenger relatively more ($u_{b1} = 4, u_{b2} = -4$). To improve sorting, the platform can hide a type 1 passenger from a type a driver to free up the passenger for a type b driver, leaving the type a driver to match with a type 2 passenger. This strategy can also increase the total surplus, because type b drivers and type 2 passengers may be unmatched when type a drivers match with type 1 passengers. Blocking a-1 matches can potentially reduce unmatched agents. We provide the equilibrium conditions under this design in Appendix C.2.

Practical Implementation The platform can directly change the set of passengers a driver sees on the app. However, knowing which passengers to show requires knowledge of driver and passenger preferences. These preferences can be estimated following our approach in Sections 5 and 6.[13]

[13] Our approach recovers the mean preferences and a distribution of unobserved heterogeneity. Alternatively, the platform can use a longer panel of data than in this paper that involves multiple observations of a same driver or passenger to estimate an individual agent's unobserved heterogeneity.

3.4.4 Simulated Effects of Market Designs

In Figure 2, we plot the market outcomes for the baseline, driver commitment, passenger commitment, selective visibility, and the combination of all three market designs. For driver preferences for matches, we set $u_{a1} = 2, u_{a2} = 1.5$, $u_{b1} = 4, u_{b2} = -4$. We set passenger match values at $v_1 = v_2 = 2$. The time horizon is $T = 10$. The action frequency is $\lambda = 1$. We vary the marginal waiting costs c^{drv} and c^{psg}. In column (a), we vary c^{drv} from 0.1 to 5 while fixing c^{psg} at 0.1, and in panel (b), we vary c^{psg} from 0.1 to 5 while setting c^{drv} at 0.1. Across rows, we plot the following market outcomes: the matched mass, driver surplus, passenger surplus and total surplus. We summarize our findings below:

1. Driver waiting costs have a non-linear effect on the number of matches. At low costs, drivers wait to match with more compatible passengers, risking passengers leaving the market without a match. At a higher cost, drivers' willingness to wait decrease. Therefore the options of matching and leaving both become relatively more attractive, and the number of matches increases. At an even higher cost, waiting becomes more costly, and any driver that does not meet a desirable passenger is more likely to leave than to wait. This market-thinning effect eventually dominates, reducing the total number of matches. In contrast, passenger waiting costs tend to always reduce the number of matches.

2. Market Designs

   (a) All three market designs can increase the number of matches. The effect of selective visibility is more sensitive to waiting costs, compared with the commitment designs.

   (b) Driver commitment reduces driver surplus and increase passenger surplus. The net effect on total surplus tends to be negative. However, in additional numerical simulations, we find that, when the passenger surplus is sufficiently high (say when $v_1 = v_2 > 10$), the increase in passenger surplus can overcome the decrease in driver surplus and the total surplus increases.

   (c) Passenger commitment improves both driver and passenger surpluses. This result is robust under various match preference and waiting cost parameters in addition to the results we show here, but may change when the passenger waiting cost function has a different shape. For example, if the waiting cost increases rapidly near T, passenger commitment can potentially decrease passenger entry sufficiently that the passenger surplus may fall.

   (d) Selective visibility increases total surplus above the baseline at low passenger waiting costs. At higher costs, blocking matches reduces the values of waiting, and more drivers and passengers leave the market without a match.

4 Empirical Model

We now extend the decision models and the equilibrium notion so that they can be applied to our data. The full model generalizes the illustrative model in three ways:

1. We consider a potentially large number of types with different arrival and departure times. They also differ in preferences for matches and waiting costs.

2. We enrich driver preferences for matches with additional driver-passenger specific shocks.

3. We generalize the waiting costs.

In this model, there are K types of drivers and L types of passengers. We assume that a mass $m_k^0 \leq 1$ of type k drivers arrives to the market at t_k^0, and their departure time is $T_k > t_k^0$.[14] Similarly, a mass $n_\ell^0 \leq 1$ of type ℓ passengers arrives at t_ℓ^0 with a departure time $T_\ell > t_\ell^0$. In the model, the arrival and departure times are fixed.

4.1 Model Primitives and Beliefs

Drivers We focus on a driver i of type k. Move opportunities randomly arrive to the driver at rate $\lambda_k(t)$. Given a move opportunity at t, the driver observes a set of passengers and decides whether to match with one, continue to wait or leave the market without a match. As in the illustrative example, each of the three option is associated with an independent EV1 shock. We assume that driver i's value for matching with passenger j of type ℓ is $u_{ij} = u_{k\ell} + \sigma\nu_{ij}$, where $u_{k\ell}$ represents the compatibility of observed characteristics such as routes and departure times, and ν_{ij} is an i.i.d. idiosyncratic driver preference shock for a passenger with the standard normal density ϕ. The parameter σ captures the magnitude of this preference shock. This shock reflects other driver preferences not in our data, such as the traffic condition near the passenger. The value of leaving the market without a match is normalized to be 0. The driver also incurs a flow waiting cost $c_k(t)$. For driver beliefs, we use $p_k(t)$ to denote the probability that the observed set of passengers $\mathfrak{S}_t$ is non-empty at t. The driver also forms a belief about the highest passenger value $\max_{j\in\mathfrak{S}_t} u_{ij}$. We use $G_k(u;t)$ to denote, conditional on $\mathfrak{S}_t \neq \emptyset$, the distribution of the highest match value u at time t. We also use $g_{k\ell}(u;t)$ to denote the probability that a type ℓ passenger with match value u is the highest value passenger conditional on $\mathfrak{S}_t \neq \emptyset$.

Passengers As in the illustrative model, we use v_j to denote a passenger j's value for being matched and v_{0j} for the value of the outside option. We assume that, for a type ℓ passenger j, $v_j - v_{0j} = v_\ell + \xi_j$, where ξ_j is i.i.d. and follows the logistic distribution. A type ℓ passenger incurs a waiting cost $o_\ell(t)$ at t, and the function increases in t. Type ℓ passengers form beliefs about the average match rate γ_ℓ.

4.2 Matching Designs

4.2.1 Designs

For the driver commitment design corresponding with Section 3.4.1, we introduce K binary parameters $d_k \in \{0,1\}$, where $d_k = 1$ indicates that type k drivers are subject to the commitment and $d_k = 0$

[14] We can interpret the mass m_k^0 as the probability of arrival. Alternatively, we can also assume that type k drivers arrive between t_k^0 and a time t_k^1 at some continuous rate $\eta_k(t)$. The mass transition functions are slightly different, but agent decision problems are the same.

otherwise. A driver upon arrival can take one of three actions: (1) choose a passenger, (2) wait and (3) leave without a match. At any subsequent move opportunity, if the type k drivers are not subject to the commitment, all three actions are available. If they are subject to the commitment, they can only take actions (1) or (2) until reaching their departure times.

The passenger commitment design corresponds with L binary parameters $d_\ell \in \{0,1\}$, where $d_\ell = 1$ indicates that type ℓ passengers are subject to the commitment and $d_\ell = 0$ otherwise. If a passenger is not subject to the commitment, she chooses a time to leave the market if she still remains unmatched at that time. If the passenger is subject to the commitment, she is given a choice when she arrives at the platform. The passenger must either leave immediately, or wait till her departure time unless she is matched while waiting.

For the selective visibility design, we use $K \cdot L$ functions $h_{k\ell}(t) \in [0,1]$ to modify driver choice sets. With probability $h_{k\ell}(t) \cdot n_\ell(t)$, a type k driver observes a type ℓ passenger at t. As in the illustrative example, a platform can suppress certain less compatible matches to increase match compatibility and potentially increase the number of matches.

In the baseline, the platform does not restrict drivers or passengers from leaving the platform or alter driver choice sets. This case corresponds with $d_k = d_\ell = 0, h_{k\ell}(t) = 1$.

4.2.2 Information Assumption

In the two commitment designs, the platform only needs to know agent departure times. The third design requires more information. For each driver type k and passenger type ℓ, the platform knows the arrival times (t_k^0, t_ℓ^0), departure times (T_k, T_ℓ), arrival rates of move opportunity $\lambda_k(t)$, routes, type-level preferences $u_{k\ell}$ and v_ℓ, waiting costs and distributions of agent-specific shocks (driver-passenger specific shocks ν_{ij}, driver action-specific EV1 shocks, and passenger preferences for matches ξ_j), but does not know the exact values of the shocks or driver move opportunity arrival times.

4.3 Driver Decisions

The BJH equation for type k drivers in (1) of the illustrative example becomes

$$\begin{aligned} 0 = \lambda_k(t) \cdot \Bigg(& \Upsilon + p_k(t)(1-d_k) \int \ln\left(\exp(u) + \exp(V_k(t)) + 1\right) dG_k(u;t) \\ & + p_k(t)\, d_k \int \ln\left(\exp(u) + \exp(V_k(t))\right) dG_k(u;t) \\ & + (1 - p_k(t))(1-d_k) \ln\left(\exp(V_k(t)) + 1\right) + (1-p_k(t))\, d_k V_k(t) \Bigg) \\ & + \frac{dV_k}{dt} - \lambda_k(t) V_k(t) - c_k(t). \end{aligned} \tag{11}$$

For driver choice probabilities, we first consider drivers who decide to wait upon arrival. Conditional on a move opportunity at t, the probability $q_{k\ell}(t)$ that a type k driver matches with a type ℓ

passenger when this passenger is observed is

$$q_{k\ell}(t) = p_k(t) \int \left((1-d_k) \cdot \frac{\exp(u)}{\exp(u) + \exp(V_k(t)) + 1} + d_k \frac{\exp(u)}{\exp(u) + \exp(V_k(t))} \right) g_{k\ell}(u;t)\, \phi\left(\frac{u - u_{k\ell}}{\sigma} \right) / \sigma du. \tag{12}$$

The probability of a driver leaving the market without a match is:

$$w_k(t) = (1 - d_k(t)) \left(p_k(t) \int \frac{1}{\exp(u) + \exp(V_k(t)) + 1} dG_k(u;t) + (1 - p_k(t)) \frac{1}{\exp(V_k(t)) + 1} \right). \tag{13}$$

For drivers that just arrive, the conditional choice probability is

$$q^0_{k\ell}\left(t^0_k\right) = p_k\left(t^0_k\right) \int \frac{\exp(u)\, g_{k\ell}\left(u; t^0_k\right) \phi\left(\frac{u - u_{k\ell}}{\sigma} \right) / \sigma}{\exp(u) + \exp\left(V_k\left(t^0_k\right)\right) + 1} du \tag{14}$$

and the probability of leaving is

$$w^0_k\left(t^0_k\right) = p_k\left(t^0_k\right) \int \frac{1}{\exp(u) + \exp(V_k(t)) + 1} dG_k\left(u; t^0_k\right) + \left(1 - p_k\left(t^0_k\right)\right) \frac{1}{\exp\left(V_k\left(t^0_k\right)\right) + 1}. \tag{15}$$

4.4 Passenger Decisions

For a type ℓ passenger j not subject to the commitment, the value of waiting upon arrival at t^0_j normalized with respect to the outside option is

$$W^0_j = \max\left\{ 0, \max_{t^\star \le T_\ell} \int_{t^0_j}^{t^\star} \gamma_\ell \left(v_\ell + \xi_j - o_\ell(\tau) \right) \exp\left(-\gamma_\ell \left(\tau - t^0_j \right) \right) d\tau \right\}. \tag{16}$$

Similar to the illustrative model, the probability that a type ℓ passenger waits at t is

$$S_\ell(t; \gamma_\ell) \equiv \Pr\left(t^\star_j > t \right) = \frac{1}{1 + \exp\left(o_\ell(t) / \gamma_\ell - v_\ell \right)}. \tag{17}$$

The leaving rate at t, $r_\ell(t)$, is given by (6). For passengers subject to the commitment, as in (SC.2), the normalized value function upon arrival is

$$\overline{W}^0_j = \max\left\{ 0, \int_{t^0_j}^{T_\ell} \gamma_\ell \left(v_\ell + \xi_j - o_\ell(\tau) \right) \exp\left(-\gamma_\ell \left(\tau - t^0_j \right) \right) d\tau \right\}. \tag{18}$$

The implied probability that a type ℓ passenger arriving at t^0_j will send a request and wait is $\overline{S}_\ell\left(t^0_j; \gamma_\ell\right)$,

$$\overline{S}_\ell\left(t^0_j; \gamma_\ell\right) = \exp\left(v_\ell - \overline{v}_\ell\left(t^0_j\right) \right) / \left(1 + \exp\left(v_\ell - \overline{v}_\ell\left(t^0_j\right) \right) \right), \tag{19}$$

where

$$\overline{v}_\ell\left(t_j^0\right) = \frac{\int_{t_j^0}^{T_\ell} \gamma_\ell o_\ell(\tau) \exp\left(-\gamma_\ell\left(\tau - t_j^0\right)\right) d\tau}{1 - \exp\left(-\gamma_\ell\left(T_\ell - t_j^0\right)\right)}.$$

4.5 Matching Equilibrium

The equilibrium consists of driver choice probabilities and passenger leaving rates given in equations (11) through (19), driver and passenger beliefs linked to their masses and a set of mass transition equations based on Assumption 1. We detail the latter two sets of conditions in Appendix D.

5 Driver Parameters Estimation

The structural parameters on the driver side are match preferences $u_{k\ell}$ and waiting costs $c_k(t)$. Our identification and estimation proceed in two steps. The first step directly identifies the match utility $u_{k\ell}$ as a function of type k's and ℓ's routes and departure times, the magnitude of the unobservable σ and the value function $V_k(t)$ from driver choices in a mixed multinomial logit model. The second step recovers the waiting costs $c_k(t)$ using the identified value functions and the structure of the driver's decision problem in Section 4.1.

5.1 First Step

Given a set of passengers $\mathfrak{S}_t$ at the clock time t and a move opportunity for driver i, the driver model in Section 4 shows that the probability of a driver i choosing a passenger j is

$$p_{ij}(t) = \int \prod_{\substack{j' \neq j \\ j' \in \mathfrak{S}_t}} \Phi\left(\frac{u_{k(i)\ell(j)} - u_{k(i)\ell(j')}}{\sigma} + \nu_{ij}\right) \frac{\exp\left(u_{k(i)\ell(j)} + \sigma\nu_{ij}\right)}{1 + \exp\left(u_{k(i)\ell(j)} + \sigma\nu_{ij}\right) + \exp\left(V_{k(i)}(t)\right)} \phi(\nu_{ij})\, d\nu_{ij}, \tag{20}$$

where $k(i)$ and $\ell(j)$ denote i's and j's types. This probability is the basis of our identification and estimation.

We specify the match utility as

$$u_{k\ell} = \beta_z z_{k\ell} + \beta_x x_k + \beta_f f_\ell + \beta_k. \tag{21}$$

In the above, $z_{k\ell}$ captures the compatibility between the driver and passenger types and includes the compatibility score used by the platform, the pickup and dropoff distances, whether departure time differences are less than 5 minutes, whether the differences are less than 15 minutes, and whether the passenger has a later departure time than the driver. The vector of variables x_k is a vector of characteristics of the driver type's route, including indicators for whether the driver route's distance is between 10 to 30 km, whether the distance is above 30 km, whether the trip starts in the CBD, and whether the trip ends in CBD. We use f_ℓ for a type ℓ passenger's fare.

In estimation, we treat the characteristics of each observed driver as representing a driver type. Therefore $x_{k(i)}$ corresponds with the trip characteristics of driver i. We also treat the characteristics of each observed passenger as representing a passenger type, and $z_{k(i)\ell(j)}$ measures the compatibility of trip characteristics between i and j.

The parameter β_k captures the unobserved heterogeneity across types. Specifically, we assume that drivers with similar origins and destinations have similar willingness to carpool. We divide the city into 2 km-by-2 km square regions. The unobserved heterogeneity β_k differs across pairs of regions that contain a type's starting and ending locations.[15] The heterogeneity captures the similarity of driver preferences based on workplace or home similarity. For example, drivers leaving from CBD to a residential area with expensive housing are likely to have higher incomes and weaker preferences for matches. We assume that the heterogeneity has a discrete distribution. We estimate the support and the associated probabilities.

We next flexibly specify a driver's value function. The value function is a solution to the driver's maximization problem in Section 4.1. Estimating a flexibly specified value function is akin to the first-step policy function estimation of two-step estimations of dynamic models (Hotz and Miller, 1993; Bajari et al., 2007). However, a unique aspect of our first step is that we can separately estimate both the preference parameters underlying $u_{k\ell}$ and the value function directly due to the variations in driver choice sets.

Specifically, we specify the value function as a piece-wise linear function in t:

$$\begin{aligned} V_k(t) = \theta_x x_k &+ \theta_{10}\mathbb{1}(T_k - t < 10)\left(1 + \frac{t - T_k}{10}\right) + \theta_{20}\mathbb{1}(T_k - t < 20)\left(1 + \frac{t - T_k}{20}\right) \\ &+ \theta_{30}\mathbb{1}(T_k - t < 30)\left(1 + \frac{t - T_k}{30}\right) + \theta_{60,x}\mathbb{1}(T_k - t < 60)\left(1 + \frac{t - T_k}{60}\right) x_k \\ &+ \theta_{60,k}\mathbb{1}(T_k - t < 60)\left(1 + \frac{t - T_k}{60}\right) + \theta_k. \end{aligned} \tag{22}$$

We note several features of this specification. First, this specification gives us a continuous function of time that flexibly depends on time-to-departure. Specifically, the slope can change when the driver is 30, 20 and 10 minutes from the departure time and differs across the driver characteristics.[16] The flexibility is important because the value function is a nonlinear equilibrium object. Second, the value function depends on the time between t and departure, but not the time between arrival and t. We show in Appendix A.3 that the latter does not explain driver or passenger decisions to leave the market at t. Third, the value function accounts for observed and unobserved heterogeneities in preference for matches and waiting costs, which affect the value function through the driver decision problem. We use a parsimonious specification where we include parameters $\theta_{60,x}$ and $\theta_{60,k}$ that allow the marginal value of waiting to differ across observed and unobserved driver characteristics. We also allow the driver characteristics to affect the intercept and include a heterogeneous intercept θ_k. We use the same set of driver characteristics x_k as in the specification of the utility function. Like β_k, the

[15] Among these pairs of regions, 17% have at least 2 driver trips, and 7% have at least three trips. Pairs of regions with 2 or more trips account for 46% of driver trips, and those with at least 3 trips account for 29% of all driver trips.

[16] All observed drivers arrive within one hour from their departure times. We therefore specify the value function to change when t is within 60 minutes from the departure time.

heterogeneity parameters $(\theta_{60,k}, \theta_k)$ differ across trips whose origins and destinations are in different pairs of 2km-by-2km square regions. We do not restrict β_k to be independent of $\theta_{60,k}$ or θ_k, and we jointly estimate the distribution of $(\beta_k, \theta_{60,k}, \theta_k)$.

5.1.1 Identification

We assume that the arrival times of drivers are independent of unobservables, and the arrival rates of driver move opportunities depend on observed characteristics (routes and departure times).

Assumption 3. *Identification of Driver Parameters*

1. *Driver arrival times are independent of unobserved shocks* $(\nu_{ij}, \varepsilon_{it})$ *and unobserved heterogeneity* $(\beta_k, \theta_{60,k}, \theta_k)$.
2. $\lambda_k(t) = \lambda(t; route_k, T_k)$.

The assumptions rule out that the timing of driver actions is correlated with unobservables, and we can thus use the variations in driver characteristics, choice sets, and arrival timing to identify the driver choice problem.

Driver Preferences for Match-Specific Parameters β_z, β_f The variation of passenger characteristics in the choice set $\mathfrak{S}_t$ identifies β_z. For example, if z is the compatibility score, we can compare the match decisions of drivers when they face passengers that have different compatibility scores but are otherwise observably identical. The differences in the match probabilities identify β_z. Similar arguments apply to other match specific regressors. The formal identification argument is similar to the idea of special regressors (Manski, 1988; Lewbel, 2014, 2019), because the variation in the choice set, thus z, is excluded from the choices of waiting and leaving. The match compatibility covariates z do not enter the value function in our model. This formulation is consistent with the equilibrium defined in Section 4.[17]

Heterogeneity of Driver Preferences for Passengers σ To identify σ, we use the variations in the size of $\mathfrak{S}_t$. Specifically, we compare two drivers with the same characteristics but facing different choice sets. A larger σ corresponds with a higher probability that a driver matches with any passenger when $\mathfrak{S}_t$ is larger. For intuition, suppose one driver's choice set has 1 passenger. We use $q(1;\sigma)$ to denote the probability that driver finds a match. The other driver's choice set has 2 passengers with routes and departure times similar to the first driver's. We use $q(2;\sigma)$ to denote this driver's match probability. The match probabilities depends on driver preferences for passenger characteristics and the shocks ν_{ij}. We argue that σ increases the difference of the match probabilities $q(2;\sigma) - q(1;\sigma)$. In the extreme case where $\sigma = 0$, the match probability difference should be close to 0. In the case where σ is extremely large, a match occurs whenever the normally distributed ν_{ij} is positive. If, for example, the match value and waiting value are both 0 and σ is large, the probability of a match would be 50%

[17] Our model differs from models of oligopolistic dynamic games (e.g. Ericson and Pakes 1995), where an agent tracks the states of all other agents.

with a single passenger (50% probability that ν_{ij} is positive), but 75% with two passengers. Therefore the choice probability difference $q(2;\sigma) - q(1;\sigma)$ would be 25% in this case. This intuition is similar to the identification of multinomial choice demand models based on variations in consumer choice sets (Berry and Haile, 2014).

Driver Specific Preference Parameters $\beta_x, \theta_x, \theta_{10}, \theta_{20}, \theta_{30}, \theta_{60,x}$ Separately identifying β_x in the match preference and $(\theta_x, \theta_{10}, \theta_{20}, \theta_{30}, \theta_{60,x})$ in the value function relies on two sources of variations. The first source is the variation of driver characteristics. The different driver characteristics (such as whether the starting point is in a key region or trip distance) vary both the value for matching with a passenger and the value of waiting relative to the option of leaving. If x is whether the driver trip distance is greater than 30 km, a high preference for this characteristic in the match value leads to more matches for this type of drivers, and a high θ_x parameter leads to more waiting, relative to other drivers. An additional source of variation is the time to departure $T_k - t$. Specifically, we can compare two drivers' decisions upon arrival, where one driver arrives within 20 minutes to her departure time and the other driver arrives more than 20 minutes to the departure time. The two drivers are otherwise observably identical and face the same choice sets. For example, if θ_{20} is negative and large, the driver closer to the departure time is more likely to choose a passenger or leave upon arrival than the other driver. The key assumption here is that the arrival-to-departure times are independent of their preferences for matches or waiting costs, conditional on driver characteristics. Suppose an agent with a lower waiting cost is more likely to arrive early relative to her departure time. Then we expect the probability of leaving in a given minute to be negatively correlated with the amount of time the agent has waited in the market. Conversely, if arrival-to-departure times are independent of unobserved driver preferences, we expect this correlation to be small. In Appendix A.3, we find that this correlation is indeed small for most drivers and passengers. We see this result as suggestive evidence supporting our assumption.

Unobserved Driver Heterogeneity $\beta_k, \theta_{60,k}, \theta_k$ To identify the unobserved heterogeneity, we group drivers by their origins and destinations and use the panel structure of the data. Specifically, we divide the city into 2 km-by-2 km square regions, and we define route groups based on whether a route starts and ends in a pair of squares. We assume that $(\beta_k, \theta_{60,k}, \theta_k)$ are the same for the drivers whose origins and destinations are in the same pair of 2 km-by-2 km square regions, and the heterogeneity is distributed independently across these pairs. The formal identification argument follows from the literature on the finite-mixture dynamic discrete choice models with panel data (Kasahara and Shimotsu, 2009), which applies when at least three drivers are observed for each pair of 2 km-by-2 km squares. For intuition, consider the case where we observe many drivers for each pair of regions. Within a pair $\mathfrak{r}$, the variations of choice sets and driver arrival times identify the heterogeneity corresponding to that pair, $(\beta_{\mathfrak{r}}, \theta_{60,\mathfrak{r}}, \theta_{\mathfrak{r}})$. Then the distribution of $(\beta_{\mathfrak{r}}, \theta_{60,\mathfrak{r}}, \theta_{\mathfrak{r}})$ across pairs of regions identifies the distribution of the heterogeneity.

Discussion: Direction Estimation of Structural Parameters in $u_{k\ell}$ Notably, the estimation of structural parameters in the driver preference function does not require directly solving the driver

decision problem. This result differs from most conditional choice estimators of dynamic models (e.g., Hotz and Miller 1993; Bajari et al. 2007). In our model, drivers do not use current choice sets to form beliefs about future choices. This modeling assumption is based on our interviews with the drivers and our equilibrium model. Therefore the characteristics associated with the current choice sets do not enter the value of waiting. These variations identify the match preference parameters separately from the value of waiting. However, we emphasize that, although the estimated driver match preference parameters are structural parameters, the estimated value function parameters are not. We use the estimated value functions and the dynamic driver decisions to invert the structural waiting costs in the following section. When we simulate the counterfactual market equilibrium, the value functions are re-computed under the new matching designs.

5.1.2 Estimation

The estimation based on (20) would be straightforward if we observe the full set of $\mathfrak{S}_t$. However, we observe only passengers that arrive between 4:30 pm and 5:00 pm and are still unmatched and active at time t, which are a subset of $\mathfrak{S}_t$. We discuss how we simulate the "missing" passengers in Appendix A.5. The procedure first computes the mass transitions of passengers arriving outside the data time window and then simulates whether a passenger is in a driver's choice set using the probabilistic interpretation of the passenger mass in Assumption 1.

We account for these missing passengers, preference shocks ν_{ij} and unobserved heterogeneity in a simulated maximum likelihood estimator. Drivers can choose a passenger from the choice set, wait, or leave the market. The choice set is a combination of actual passengers in the data and the simulated passengers. To form the likelihood function, we first specify the choice probabilities in (20) for each moment a driver searches. Then we integrate the probabilities over simulated sets of passengers and unobserved preferences ν_{ij} for passengers to form the likelihood corresponding with a driver and a move opportunity (the instance a driver checks her phone). Finally, we integrate over the joint likelihood of drivers traveling to and from the same pairs of 2 km-by-2 km squares over the distribution of $(\beta_k, \theta_{60,k}, \theta_k)$. Our baseline estimates are based on a 2-component finite mixture model. We also report estimates with 3 unobserved components.

Estimation Results Table 4 reports the estimates of preference parameters for matches in (21). We find that drivers have strong preferences for route compatibility. Ten percentage points in compatibility scores are worth $(10\% \times 2.94/0.12 =)2.45$ dollars. Other estimates are also reasonable: drivers dislike longer pickup or dropoff distances or large differences between departure times. We also find that drivers starting or ending in CBD regions have weaker preferences for matches. In addition, there is substantial match level heterogeneity, where the standard deviation σ of match specific preferences ν is nearly \$8. The support difference in driver heterogeneity (β_k) has a similar magnitude. Overall, the estimates are similar across the 2- and 3-component mixture models.

We report the estimates of the value function in (22) in Table 5. The value of waiting is higher for drivers on longer trips and those starting or ending in CBD. We also find significant unobserved heterogeneity in the value of waiting. These driver types differ in the intercept as well as the marginal

Table 4: Driver Preferences for Matches

	2-Component	3-Component		2-Component	3-Component
Match Specific			Fares β_f	0.12	0.12
Characteristics β_z				(0.01)	(0.01)
Compatibility Score	2.94	2.98			
	(0.12)	(0.12)			
Pickup Distance	-0.29	-0.29	Unobserved Preference		
	(0.01)	(0.00)	For Passengers σ	0.86	0.86
Dropoff Distance	-0.18	-0.19		(0.02)	(0.02)
	(0.00)	(0.00)			
Dptr. Time Difference	0.07	0.07			
$\leq$ 5 Minutes	(0.03)	(0.03)	Unobserved Heterogeneity		
Dptr. Time Difference	0.32	0.32	Component 1		
$\leq$ 15 Minutes	(0.03)	(0.03)	β_k	-2.76	-2.54
				(0.13)	(0.14)
Passenger Dptr. Time	-0.50	-0.51	Prob	0.48	0.24
Later Than Driver's	(0.03)	(0.03)		(0.02)	(0.02)
Driver Specific			Component 2		
Characteristics β_x			β_k	-3.20	-3.14
Distance 10-30 km	0.13	0.13		(0.13)	(0.14)
	(0.07)	(0.07)	Prob	0.52	0.52
Distance>30 km	-0.11	-0.11		(0.01)	(0.02)
	(0.10)	(0.10)	Component 3		
Start in CBD	-0.41	-0.42	β_k		-3.20
	(0.04)	(0.04)			(0.15)
End in CBD	-0.15	-0.14	Prob		0.24
	(0.04)	(0.04)			(0.02)

Note: we report standard errors in parentheses.

Table 5: Driver Value Function Estimates

	2-Component	3-Component			2-Component	3-Component
Characteristics θ_x			Unobserved Heterogeneity			
Distance 10-30 km	0.85	0.85	Component 1			
	(0.15)	(0.16)		θ_k	2.14	2.81
Distance>30 km	0.93	1.00			(0.20)	(0.24)
	(0.16)	(0.17)		$\theta_{60,k}$	-2.52	-2.92
Start in CBD	0.30	0.21			(0.37)	(0.41)
	(0.10)	(0.10)		Prob	0.48	0.24
End in CBD	0.34	0.37			(0.02)	(0.02)
	(0.10)	(0.11)				
Marginal Value of Waiting						
			Component 2			
θ_{10}	-3.25	-3.27		θ_k	-0.23	1.00
	(0.09)	(0.09)			(0.20)	(0.22)
θ_{20}	1.30	1.29		$\theta_{60,k}$	-1.43	-1.98
	(0.16)	(0.16)			(0.36)	(0.39)
θ_{30}	-0.10	-0.09		Prob	0.52	0.52
	(0.24)	(0.25)			(0.01)	(0.02)
Interaction with Characteristics						
$\theta_{60,\text{Start in CBD}}$	-0.20	-0.13				
	(0.13)	(0.14)	Component 3			
$\theta_{60,\text{End in CBD}}$	-0.25	-0.27		θ_k		-1.10
	(0.14)	(0.14)				(0.30)
$\theta_{60,\text{Distance 10-30km}}$	-0.39	-0.39		$\theta_{60,k}$		-1.59
	(0.20)	(0.21)				(0.50)
$\theta_{60,\text{Distance >30km}}$	-0.59	-0.67		Prob		0.24
	(0.22)	(0.23)				(0.02)

Note: we report standard errors in parentheses.

value of waiting, although we still consistently find that the value of waiting decreases when it is closer to the departure time. The decrease slows down within 20-30 minutes from the departure time and becomes larger again when the departure time is within 10 minutes.

5.2 Second Step

Given the driver value function in (11), the waiting cost can be inverted as

$$c_k(t) = \lambda_{kt} \cdot \left(\Upsilon + p_k(t) \int \ln\left(\exp(u) + \exp\left(V_k(t)\right) + 1\right) dG_k(u;t) \right. \tag{23}$$
$$\left. + \left(1 - p_k(t)\right) \ln\left(\exp\left(V_k(t)\right) + 1\right) \right) + \frac{dV_k}{dt} - \lambda_{kt} V_k(t).$$

The above identifies the waiting cost because the right hand side consists entirely of known quantities. The first step in Section 5.1 identifies $u_{k\ell}$ and V_{kt} directly from driver choice problems. The passenger masses $n_{\ell t}$ is recovered based on the same procedure in Appendix A.5, which we use to simulate missing passengers. The masses in turn imply the probabilities that the driver choice is non-empty, $p_k(t)$, and the distribution of the most compatible passenger $G_k(u;t)$ based on (SD.1) and (SD.3).

The identification of the waiting cost is related to the literature on identifying discount factors in dynamic models (e.g., Rust 1994; Magnac and Thesmar 2002; Abbring and Daljord 2020). The typical approach of identification relies on instruments that vary the expected future values but not the instantaneous payoffs. In our setting, the time to departure is such a variable. Specifically, we assume that the arrival time is independent of unobserved heterogeneity $(\beta_k, \theta_{60,k}, \theta_k)$ and random shocks (ν_{ij} and ε_{it}) conditional on a driver's observed characteristics. Furthermore, time-to-departure is excluded from the match utility. Therefore, when waiting costs are high, drivers behave differently at the time of their arrival. For example, drivers that arrive closer to the departure time and make choices for the first time are more impatient and more likely to choose a passenger or leave than drivers further away from the departure time but facing the same choice set. This observation is the foundation for identifying the value function from other model parameters. The identified value function in turn allows us to identify waiting costs through a transformation of the driver value function in (23).

The inversion of waiting costs can be done for every driver type and for each component of unobserved heterogeneity.[18] We visualize the waiting costs in panel (a) of Figure 3. Specifically, we compute the distribution of the waiting costs across drivers for every 5-minute interval within one hour from the departure time, and we plot the median and the 25%-75% quantiles of the waiting costs. The waiting costs remain fairly stable at about \$5 per 5 minutes until between 10 to 20 minutes till departure, after which the waiting costs start to increase sharply. The estimates are consistent with the data patterns that fewer drivers continue to search closer to the departure time. These waiting costs are high compared with local income, which was about 103,000 RMB per capita in 2018 (or about \$8 per hour per capita). We note that a car owner likely has a higher income, and the waiting cost embeds both the opportunity costs of search and the efforts of search.

5.3 Other Components of the Driver Model

In addition to preferences for matches and waiting costs, the number of types, routes, arrival times, departure times and arrival rates of move opportunities are also inputs to the simulation of the full equilibrium model in Section 4.

Driver Types In the simulation procedure described in Appendix F.1, we explain how we construct types. We assume that the arrival times approximate a Poisson process, and we find that an aggregate arrival rate of 77.6 drivers/minute allows us to match the number of drivers with departure times between 5:00 pm and 5:20 pm (1631 drivers per day) with our data. We also simulate the routes and arrival-to-departure times for the types according to their empirical distributions.

Arrivals of Move Opportunities Consistent with Assumption 3, we estimate the move opportunity arrival rate based on driver characteristics and time-to-departure in Appendix A.6. The estimates show that drivers search more frequently closer to the departure time.

[18] We approximate the driver value function with a piecewise linear function in (22) for flexibility and interpretability, but the function is not differentiable, and technically dV/dt is undefined at certain points. Nonetheless, non-differentiability does not pose a problem in estimation or simulation, because we discretize time and use numerical derivatives.

Figure 3: Waiting Cost Estimates

(a) Driver

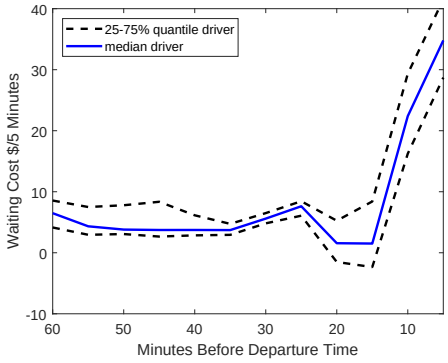

(b) Passenger

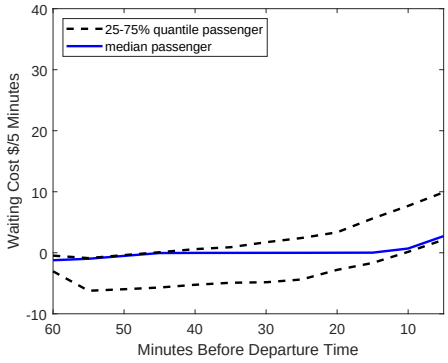

Note: The waiting costs are in units of $/5 minute in 2018 USD. For a given 5-minute interval, points on the black broken lines represent the 25% and 75% quantiles of waiting costs across drivers or passengers. The blue line represents the median costs. The standard errors are approximately one to two orders of magnitudes smaller than the dispersion across agents.

6 Passenger Parameter Estimation

We estimate the passenger utility v_ℓ and waiting cost $o_\ell(t)$. We assume $v_\ell = \zeta_x x_\ell - \zeta_f f_\ell + \zeta_\ell$, where x_ℓ consists of whether a passenger's trip starts in CBD and whether it ends in CBD, f_ℓ is the fare and ζ_ℓ captures the passenger unobserved heterogeneity. We specify a flexible passenger cost function $o_\ell(t)$:

$$\begin{aligned} o_\ell(t) = {} & \vartheta_{10}\mathbb{1}(T_\ell - t < 10)\left(1 + \frac{t - T_\ell}{10}\right) + \vartheta_{20}\mathbb{1}(T_\ell - t < 20)\left(1 + \frac{t - T_\ell}{20}\right) \\ & + \vartheta_{30}\mathbb{1}(T_\ell - t < 30)\left(1 + \frac{t - T_\ell}{30}\right) + \vartheta_{60,x}\mathbb{1}(T_\ell - t < 60)\left(1 + \frac{t - T_\ell}{60}\right) x_\ell \\ & + \vartheta_{60,\ell}\mathbb{1}(T_\ell - t < 60)\left(1 + \frac{t - T_\ell}{60}\right) + \vartheta_\ell. \end{aligned}$$

This waiting cost function shares similar features with the driver value function: the function is continuous and flexible in how it changes over time; the function depends on the time from t to the departure time, not the time the passenger has waited since arrival; the unobserved heterogeneity $(\zeta_\ell, \vartheta_{60,\ell}, \vartheta_\ell)$ has finite support and is the same for all passengers whose origins and destinations are in the same pairs of 2 km-by-2 km square regions.[19] We also emphasize that ζ_ℓ is not required to be independent of $\vartheta_{60,\ell}$ or ϑ_ℓ, but the joint distribution is independent across pairs of square regions. An additional restriction we require here is that the flow waiting cost is increasing in t, consistent with the passenger model in Section 4.4.

As in the driver side estimation, we treat the characteristics of each observed passenger as representing a type. A passenger's route, arrival time and departure time are treated as the type's. We also estimate a belief for each observed passenger in Appendix A.4.

[19] Among these pairs of regions, 36% have at least 2 passenger trips, and 15% have at least 3 trips. Pairs of regions with 2 or more trips account for 63% of all passenger trips, and those with at least 3 account for 39% of all passenger trips.

Given a passenger's belief of the match rate, we can specify the likelihood for each passenger based on her outcome. Consider three passengers j, j' and j'' with beliefs γ_j, γ'_j and γ''_j. The passenger j is matched at time t_j, and therefore its optimal leaving time is greater than t_j. The resulting likelihood is $S_\ell(t_j;\gamma_j) = \dfrac{1}{1+\exp\left(o_\ell(t_j)/\gamma_j - v_\ell\right)}$. For passenger j' that leaves at $t_{j'}$, the likelihood corresponds with the hazard rate of leaving, $\dfrac{S_\ell\left(t_{j'};\gamma'_j\right) - S_\ell\left(t_{j'}+\Delta^{\text{psg}};\gamma'_j\right)}{\Delta^{\text{psg}} \cdot S_\ell\left(t_{j'};\gamma'_j\right)}$,[20] where $\Delta^{\text{psg}} = 30$ seconds. Finally, for j'' that arrives at $t_{j''}$ but does not send a request,t the likelihood is $1 - S_\ell\left(t_{j''};\gamma''_j\right)$. These likelihoods are the basis of identification and estimation.

6.1 Identification

Passenger Belief γ_ℓ To identify the passenger belief, we require the following assumption:

Assumption 4. *1. Passenger arrival times are independent of unobserved shocks ξ_j and unobserved heterogeneity $(\zeta_\ell, \vartheta_\ell, \vartheta_{60,\ell})$.*

2. $z_{k\ell} = z\left(route_k, T_k, route_\ell, T_\ell\right)$.

The second assumption states that, in the driver choice function, measures of compatibility are based on route characteristics and departure times observable to the econometrician. We rule out that preferences are based on the unobserved passenger preference for matches ξ_j, ζ_ℓ, $\vartheta_{60,\ell}$ or ϑ_ℓ. Combined with the first assumption, the decision to leave is not correlated with matching, conditional on a passenger's observed characteristics. We can thus separately identify the rates of leaving and matching (Cox, 1962), and then integrate over the instantaneous match rates to identify the passenger belief of the average rate in (SD.4). We emphasize that the passenger belief is an equilibrium object and is re-computed for different market designs.

Passenger Specific Preference for Match ζ_x and ζ_f For ζ parameters in v_ℓ, the variations in passenger characteristics lead to different leaving times. For example, if x_ℓ is whether the starting location is in CBD, and ζ_x is positive, then passengers with origins in CBD but facing the same match rate γ_ℓ are more likely to wait longer, if their other characteristics are the same. Similarly, the fare coefficient ζ_f is identified when we compare how long passengers are willing to wait between passengers that face high and low fares but have similar γ_ℓ and other characteristics.

Passenger Waiting Costs $o_\ell(t)$ To identify the waiting cost parameters in $o_\ell(t)$, we use the variations in the arrival times. As an example, consider the identification of ϑ_{20}. Suppose that two passengers arrive before and after $T_\ell - 20$, and that they have the same departure time and face similar γ_ℓ. We compare the probabilities that each passenger does not leave within a small amount of time Δ. If ϑ_{20} is large, we then expect the probabilities of waiting Δ minutes to be higher for the passenger

[20] We use the numerical derivative because $o_\ell(t)$, while flexible, is not differentiable everywhere. In data, no passenger leaves at exactly 10, 20 or 30 minutes before departure.

that arrives before 20 minutes.[21] In Section 5.1.1, we have argued that the arrival times are unlikely to be correlated with unobserved passenger characteristics.

Passenger Unobserved Heterogeneity $\zeta_\ell, \vartheta_\ell, \vartheta_{60,\ell}$ The identification of the unobserved heterogeneity follows a similar approach to Section 5.1.1. We rely on the correlation of passenger decisions to wait across passengers whose origins and destinations are in the same pair of 2 km-by-2 km square regions. To separately identify ζ_ℓ from ϑ_ℓ and $\vartheta_{60,\ell}$, we rely on the variations of beliefs γ_ℓ across passengers that are in the same region but have different arrival-to-departure times.

6.2 Estimation

We use a two-step maximum likelihood estimator to estimate v_ℓ and $o_\ell(t)$. The first step estimates the belief γ_ℓ as the average of a passenger's instantaneous match rates, which in turn are estimated as a flexible function of passenger characteristics (Appendix A.4). The second step uses the estimates of γ_ℓ to form the simulated likelihood of passenger outcomes, where we integrate the joint likelihood of passengers traveling to and from the same pairs of 2 km-by-2 km square regions over the distribution of $(\zeta_\ell, \vartheta_\ell, \vartheta_{60,\ell})$.

Table 6 reports the estimates. We find that passengers traveling from the CBD have a lower preference for the match. We also find substantial unobserved heterogeneity in both preferences for the match and the waiting costs. The two-component mixture specification suggests that one type of passengers has both weaker preference for the match (low ζ_ℓ) but also lower marginal cost of waiting (low $\vartheta_{60,\ell}$).

We visualize the marginal cost of waiting in panel (b) of Figure 3. We compute the distribution of waiting costs for every 5-minute interval within one hour from the departure time across passengers and plot the median and 25%-75% quantiles of the waiting costs. The waiting costs are close to 0 or even negative until about 10 minutes from the departure times. We note that both positive and negative waiting costs are plausible. In particular, the negative cost could reflect saved opportunity costs of planning alternative transports. It is also not surprising that the cost is much lower than drivers', consistent with the app design where passengers do not need to actively choose drivers.

Passenger Types As on the driver side, the number of types and their characteristics are inputs to the simulation of the full equilibrium model in Section 4. We similarly assume that arrival times approximate a Poisson process, which is consistent with our finding in Appendix A.1. We estimate the aggregate arrival rate directly from data as the average number of arriving passengers per minute. This rate is 31.77 passengers/minute. For each type, we simulate a route and a departure time based on the empirical distribution of these characteristics. We explain how we construct types in the simulation procedure in Appendix F.1.

[21] We also note that we do not include passenger specific characteristics x_ℓ in $o_\ell(t)$. In principle, variations in the match rate γ_ℓ can help to identify the effects of x_ℓ on the waiting costs. In practice, we find the estimated effects to be close to 0.

Table 6: Passenger Preference Estimates

	2-Component	3-Component			2-Component	3-Component
Match Preference			Unobserved Heterogeneity			
Characteristics ζ_x			Component 1			
Start in CBD	-0.30	-0.18		ζ_ℓ	0.45	-1.16
	(0.07)	(0.07)			(0.09)	(0.19)
End in CBD	0.19	0.13		ϑ_ℓ	-0.32	-1.21
	(0.07)	(0.08)			(0.03)	(0.16)
				$\vartheta_{60,\ell}$	0.07	0.80
					(0.03)	(0.17)
Fare ζ_f	-0.12	-0.12		Prob	0.27	0.17
	(0.00)	(0.01)			(0.01)	(0.01)
Waiting Cost						
			Component 2			
Marginal Cost of Waiting				ζ_ℓ	2.10	1.62
ϑ_{10}	0.14	0.18			(0.06)	(0.12)
	(0.02)	(0.02)		ϑ_ℓ	-0.09	0.03
ϑ_{20}	0.50	0.47			(0.01)	(0.02)
	(0.02)	(0.02)		$\vartheta_{60,\ell}$	0.62	0.13
ϑ_{30}	0.14	0.10			(0.02)	(0.03)
	(0.02)	(0.02)		Prob	0.73	0.28
					(0.01)	(0.02)
Interaction with						
Characteristics			Component 3			
				ζ_ℓ		2.34
$\theta_{60,\text{Start in CBD}}$	0.01	0.04				(0.09)
	(0.02)	(0.03)		ϑ_ℓ		-0.21
$\theta_{60,\text{End in CBD}}$	-0.05	-0.02				(0.02)
	(0.02)	(0.03)		$\vartheta_{60,\ell}$		0.93
						(0.05)
				Prob		0.55
						(0.02)

Note: we report standard errors in parentheses.

7 Comparing Market Designs

7.1 Matching Designs

Using the matching equilibrium in Section 4 and the driver and passenger estimates in Sections 5 and 6, we compare the effects of different matching designs. Specifically, we choose values for the design parameters $\{d_k, d_\ell, h_{k\ell}(t)\}$ and compute the corresponding equilibrium outcomes after allowing drivers and passengers to adjust their strategies. The design parameters are chosen to maximize one of the three objectives: (1) total surplus, (2) total number of matches and (3) platform revenue. Appendices F.1 and F.2 describe how we compute the equilibrium in detail and provide the expressions for these objectives.[22] We use a large number of types in the simulation (8,880 for drivers and 4,000 for passengers) to approximate the market between 4:00 pm and 6:00 pm, and optimizing over all design parameters is not feasible. We thus compare the following market designs:

1. Baseline. This market represents the status quo, where $d_k = d_\ell = 0$ (no commitment to waiting) and $h_{k\ell}(t) = 1$ (no selective visibility).

2. Driver commitment. We set $d_k = 1, d_\ell = 0$, and search for $h_{k\ell}(t)$ to maximize each of the objectives.[23]

3. Passenger commitment. We set $d_k = 0, d_\ell = 1$, and search for $h_{k\ell}(t)$ to maximize the objectives.

4. Selective visibility. We set $d_k = d_\ell = 0$, and search for $h_{k\ell}(t)$ to maximize the objectives.

5. Driver & passenger commitment. We set $d_k = d_\ell = 1$, and search for $h_{k\ell}(t)$ to maximize the objectives.

Appendix F.3 describes how we choose $h_{k\ell}(t)$. To reduce the dimensionality of the maximization problem, we group drivers, passengers and the times of driver actions by observable characteristics and assign a common h parameter to each group. We use estimates based on the estimated 2-component mixture models for the results. The results based on the 3-component model are similar. We discuss the multiplicity of equilibria and equilibrium selection in Appendix F.4.

7.2 Results

First, in designs 2, 3, 4 and 5, we find that setting $h_{k\ell}(t) = 1$ maximizes total surplus, number of matches and total revenue given the choices of d_k and d_ℓ. This result is not surprising, because our numerical simulations suggest that we are unlikely to improve welfare by blocking certain matches when waiting costs are high. We indeed find that these estimated costs are substantial (relative to the fares or local income levels), especially for drivers close to their departure times. In Table 7, we

[22] We note a limitation of our exercise. While we allow counterfactual market designs to change the decisions to wait after agent arrivals, we take the arrivals as given. Potentially, when a design increases (decrease) the surplus on one side of the market, we may also expect more (fewer) arrivals.

[23] We maximize the social surplus of agents that arrive between 4:30 pm and 5:00 pm as in our data. Maximizing the surplus over a longer time window (4:00 pm to 6:00 pm) yields the same result that $h_{k\ell}(t) = 1$ maximizes these objectives.

describe the equilibrium effects of the designs of 2, 3 and 5, setting $h_{k\ell}(t) = 1$. To be comparable with our data, we report the statistics for drivers with departure times between 5:00 pm and 5:20 pm and passengers that arrive between 4:30 pm and 5:00 pm. Changes across market designs based on alternative arrival or departure times are qualitatively similar.

We also find that our model fits the data well. The simulated baseline model predicts the number of matches and total revenue close to those in the data summary statistics in Table 1. The equilibrium shares of drivers and passengers that wait after arrival are also similar. Average search durations in the model are slightly longer. In the following, we compare the simulated baseline model with the counterfactual designs.

Under the driver commitment design, we find a large increase in the number of matches and revenue. The number of matches increases by 52%. We note that this result is consistent with the numerical simulations in Section 3, which also predict a large increase in the number of matches under the driver commitment design when the driver waiting cost is moderately high and passenger waiting cost is low (panel (a)(i) of Figure 2). The percentage of drivers who wait after arrival (as opposed to leaving or choosing a passenger) decreases by more than 65.46% from 42.9% to 14.81%. The vast majority of drivers that decide not to wait after arrival choose to leave immediately (87%) as opposed to matching with a passenger. The remaining drivers spend 84.4% more time searching. Overall, the driver surplus decreases. In equilibrium, the design reduces the waiting time of passengers and improves their values of waiting. More passengers decide to wait upon arrival, and their surplus increases by nearly \$5 on average, which is approximately the difference between taxi and carpooling fares for a median-distance (21 km) passenger trip. However, because there are more drivers than passengers, the total surplus still falls.

We further note that this design in fact reduces market thickness. On the driver side, with the share of waiting drivers down by over 65% and the search duration up by 84%, the average number of waiting drivers still fall by 36%. On the passenger side, the number of waiting passenger decreases less, by 6%. Therefore the additional matches are not the result of a thicker market, but a result of stronger driver willingness to match. We note two mechanisms in the driver commitment design contributing to this result. First, waiting drivers can no longer leave the market without a match. This loss of an option increases the attractiveness of the remaining options, including matching. There is also a selection effect, where drivers with stronger preferences for matches and lower waiting costs remain in the market. The selection effect reallocates passengers across drivers. In Appendix A.7, we decompose the matched drivers and passengers by their characteristics. We find that most of the added matches are between drivers that arrive early (>20 minutes before the departure time) and the passengers that arrive late ($\leq$20 minutes before the departure time). Consequently, we also find the smallest decrease in driver surplus and greatest increase in passenger surplus in these two groups.

Next, we find that the passenger commitment increases driver surplus but decreases passenger surplus. As discussed in Section 3.4.4, this result may occur when the passenger waiting cost increases quickly near the departure time. The number of matches increases slightly (5.33%), but the share of passengers that wait in the market decreases from 80.18% in the baseline to just 58.64%. As a result, the average number of waiting passengers at a given moment decreases slightly by 6%. The equilibrium

effect of this decrease is a slightly lower share of drivers that wait after arrival. Interestingly, the driver surplus still improves despite a slightly thinner passenger market. We note that this result is primarily a change in the composition of waiting and matched passengers. The decomposition exercise in Appendix A.7 shows that most of the added matches are between drivers and passengers on shorter trips (<30 km) and between those traveling on routes outside the CBD. These two groups represent the majority of drivers and passengers. These drivers make more matches when similar passengers stay in the market longer.

Imposing both commitments achieves the highest number of matches and revenue. The shares of drivers and passengers that wait in the market after arrival fall below the baseline levels. Drivers' search durations increase and passengers' fall. The passenger surplus also increases, but the decrease in driver surplus is similar in magnitude, and the average surplus falls.

8 Conclusion

In this paper, we study dynamic matching on a carpooling platform. The platform primarily connects commuting drivers with passengers as an information intermediary by setting low fares based on trip distances. We analyze the matching through a tractable equilibrium model and quantify the effects of committing agents to delay unmatched exits from the market. We also explore whether changing the set of passengers a driver observes can improve sorting. We show that the effects of these designs critically depend on agent preferences for matches and their waiting costs. In our empirical model, we find that the commitment designs, especially when imposed on drivers, can significantly increase the number of matches and revenues. Designs that modify driver choice sets do not increase the number of matches or revenue. None of the designs can improve social surplus.

References

Abbring, Jaap H and Øystein Daljord, "Identifying the discount factor in dynamic discrete choice models," *Quantitative Economics*, 2020, *11* (2), 471–501.

Agarwal, Nikhil and Eric Budish, "Market design," *Handbook of Industrial Organization*, 2021, *5* (1), 1–79.

_ , Itai Ashlagi, Michael A Rees, Paulo Somaini, and Daniel Waldinger, "Equilibrium allocations under alternative waitlist designs: Evidence from deceased donor kidneys," *Econometrica*, 2021, *89* (1), 37–76.

Akbarpour, Mohammad, Shengwu Li, and Shayan Oveis Gharan, "Thickness and information in dynamic matching markets," *Journal of Political Economy*, 2020, *128* (3), 783–815.

Ashlagi, Itai, Maximilien Burq, Patrick Jaillet, and Vahideh Manshadi, "On matching and thickness in heterogeneous dynamic markets," *Operations Research*, 2019, *67* (4), 927–949.

Table 7: Counterfactual Simulation

	Baseline	Driver Commitment		Passenger Commitment		Driver and Passenger Commitment	
			Change From Baseline				Change From Baseline
Number of Matches*	421.87	641.52	52.07%	444.34	5.33%	653.30	54.86%
Total Revenue ($)*	2019.85	3043.47	50.68%	2152.68	6.58%	3119.08	54.42%
Δ of Average Surplus ($)**	-	-1.41	-	-0.34	-	-1.52	-
Driver***							
% Wait After Arrival	42.90	14.81	-65.46%	42.85	-0.11%	14.94	-65.16%
Search Duration (Minutes) | Wait After Arrival	20.66	38.10	84.40%	20.68	0.06%	37.91	83.49%
Search Duration (Minutes) | Matched	4.87	8.82	80.86%	4.90	0.45%	8.69	78.21%
Δ of Surplus ($)	-	-4.15	-	0.12	-	-4.06	-
Passenger*							
% Wait After Arrival	80.18	84.77	5.72%	58.64	-26.86%	76.28	-4.87%
Search Duration (Minutes) | Wait After Arrival	6.67	5.90	-11.60%	8.54	28.06%	6.37	-4.47%
Search Duration (Minutes) | Matched	5.52	4.78	-13.30%	7.25	31.41%	5.46	-0.95%
Δ of Surplus ($)	-	4.96	-	-1.43	-	4.40	-

*: Calculated based on passengers arriving between 4:30 pm and 5:00 pm. **: Weighted by the respective driver and passenger arrival rates. The driver arrival rate is 77.60 drivers/minute. The passenger arrival rate is 31.77 passengers/minute. ***: Calculated based on drivers with departure times between 5:00 pm and 5:20 pm.

Baccara, Mariagiovanna, SangMok Lee, and Leeat Yariv, "Optimal dynamic matching," *Theoretical Economics*, 2020, *15* (3), 1221–1278.

Bajari, Patrick, C Lanier Benkard, and Jonathan Levin, "Estimating dynamic models of imperfect competition," *Econometrica*, 2007, *75* (5), 1331–1370.

Barnes, Stuart J, Yue Guo, and Rita Borgo, "Sharing the air: Transient impacts of ride-hailing introduction on pollution in China," *Transportation Research Part D: Transport and Environment*, 2020, *86*, 102434.

Berry, Steven T and Philip A Haile, "Identification in differentiated products markets using market level data," *Econometrica*, 2014, *82* (5), 1749–1797.

Bian, Bo, "Search frictions, network effects and spatial competition: taxis versus Uber," Technical Report, mimeo, Penn State University 2020.

Bimpikis, Kostas, Wedad J Elmaghraby, Ken Moon, and Wenchang Zhang, "Managing market thickness in online business-to-business markets," *Management Science*, 2020, *66* (12), 5783–5822.

Brancaccio, Giulia, Myrto Kalouptsidi, and Theodore Papageorgiou, "Geography, transportation, and endogenous trade costs," *Econometrica*, 2020, *88* (2), 657–691.

_ , _ , _ , and Nicola Rosaia, "Search frictions and efficiency in decentralized transport markets," *Quarterly Journal of Economics*, 2023, *138* (4), 2451–2503.

Buchholz, Nicholas, "Spatial equilibrium, search frictions, and dynamic efficiency in the taxi industry," *Review of Economic Studies*, 2022, *89* (2), 556–591.

Castillo, Juan Camilo, "Who Benefits from Surge Pricing?," *Available at SSRN 3245533*, 2020.

Chen, M Keith, Peter E Rossi, Judith A Chevalier, and Emily Oehlsen, "The value of flexible work: Evidence from uber drivers," *Journal of Political Economy*, 2019, *127* (6), 2735–2794.

Chen, Yan, "Matching market experiments," in Federico Echenique, Nicole Immorlica, and Vijay V. Vazirani, eds., *Online and Matching-Based Market Design*, Cambridge University Press, 2023.

_ , Peter Cramton, John A List, and Axel Ockenfels, "Market design, human behavior, and management," *Management Science*, 2021, *67* (9), 5317–5348.

China Daily, "2023 social value report of the ridesharing industry," 2023.

Cox, David Roxbee, "Renewal theory," *Chapman and Hall*, 1962.

Cullen, Zoë and Chiara Farronato, "Outsourcing tasks online: Matching supply and demand on peer-to-peer internet platforms," *Management Science*, 2020.

Diao, Mi, Hui Kong, and Jinhua Zhao, "Impacts of transportation network companies on urban mobility," *Nature Sustainability*, 2021, *4* (6), 494–500.

Doval, Laura, "Dynamically stable matching," *Theoretical Economics*, 2022, *17* (2), 687–724.

Einav, Liran, Chiara Farronato, and Jonathan Levin, "Peer-to-peer markets," *Annual Review of Economics*, 2016, *8*, 615–635.

Ericson, Richard and Ariel Pakes, "Markov-perfect industry dynamics: A framework for empirical work," *Review of Economic Studies*, 1995, *62* (1), 53–82.

Farronato, Chiara and Andrey Fradkin, "The welfare effects of peer entry: the case of Airbnb and the accommodation industry," *American Economic Review*, 2022, *112* (6), 1782–1817.

Fong, Jessica, "Effects of market size and competition in two-sided markets: Evidence from online dating," *Marketing Science*, 2024.

Frechette, Guillaume R, Alessandro Lizzeri, and Tobias Salz, "Frictions in a competitive, regulated market: evidence from taxis," *American Economic Review*, 2019, *109* (8), 2954–92.

Gaineddenova, Renata, "Pricing and efficiency in a decentralized ride-hailing platform," 2022.

Hitsch, Gunter J, Ali Hortaçsu, and Dan Ariely, "Matching and sorting in online dating," *American Economic Review*, 2010, *100* (1), 130–63.

Hopenhayn, Hugo A, "Entry, exit, and firm dynamics in long run equilibrium," *Econometrica*, 1992, pp. 1127–1150.

Hotz, V Joseph and Robert A Miller, "Conditional choice probabilities and the estimation of dynamic models," *Review of Economic Studies*, 1993, *60* (3), 497–529.

Jovanovic, Boyan, "Selection and the evolution of industry," *Econometrica*, 1982, pp. 649–670.

Jullien, Bruno, Alessandro Pavan, and Marc Rysman, "Two-sided markets, pricing, and network effects," in "Handbook of Industrial Organization," Vol. 4, Elsevier, 2021, pp. 485–592.

Kasahara, Hiroyuki and Katsumi Shimotsu, "Nonparametric identification of finite mixture models of dynamic discrete choices," *Econometrica*, 2009, *77* (1), 135–175.

Lagos, Ricardo, "An analysis of the market for taxicab rides in New York City," *International Economic Review*, 2003, *44* (2), 423–434.

Lewbel, Arthur, "An overview of the special regressor method," 2014.

_ , "The identification zoo: Meanings of identification in econometrics," *Journal of Economic Literature*, 2019, *57* (4), 835–903.

Li, Jun and Serguei Netessine, "Higher market thickness reduces matching rate in online platforms: Evidence from a quasiexperiment," *Management Science*, 2020, *66* (1), 271–289.

Liu, Xi, Li Gong, Yongxi Gong, and Yu Liu, "Revealing travel patterns and city structure with taxi trip data," *Journal of Transport Geography*, 2015, *43*, 78–90.

Loertscher, Simon, Ellen V Muir, and Peter G Taylor, "Optimal market thickness," *Journal of Economic Theory*, 2022, *200*, 105383.

Lyft, "What the New TLC Rules Mean for You," https://www.lyft.com/hub/posts/what-the-new-tlc-rules-mean-for-you 2019.

_ , "Acceptance rate," https://help.lyft.com/hc/lt/all/articles/115013077708-Acceptance-rate 2023.

Magnac, Thierry and David Thesmar, "Identifying dynamic discrete decision processes," *Econometrica*, 2002, *70* (2), 801–816.

Manski, Charles F, "Identification of binary response models," *Journal of the American statistical Association*, 1988, *83* (403), 729–738.

Marshall, Aarian, "Uber Changes Its Rules, and Drivers Adjust Their Strategies," *WIRED*, Feb 2020.

Ostrovsky, Michael and Michael Schwarz, "Carpooling and the Economics of Self-Driving Cars," 2018.

Reeling, Carson and Valentin Verdier, "Welfare effects of dynamic matching: An empirical analysis," *Review of Economic Studies*, 2021.

Rosaia, Nicola, "Competing platforms and transport equilibrium: evidence from New York City," Technical Report, mimeo, Harvard University 2020.

Roth, Alvin E, "Experiments in market design," *Handbook of Experimental Economics*, 2016, *2*, 290–346.

Rust, John, "Structural estimation of Markov decision processes," *Handbook of Econometrics*, 1994, *4*, 3081–3143.

Rysman, Marc, "The economics of two-sided markets," *Journal of Economic Perspectives*, 2009, *23* (3), 125–143.

Schäfer, Uwe, *From Sperner's Lemma to Differential Equations in Banach Spaces: An Introduction to Fixed Point Theorems and Their Applications*, KIT Scientific Publishing, 2014.

Shapiro, Matthew H, "Density of demand and the benefit of Uber," 2018.

Tarduno, Matthew, "The congestion costs of Uber and Lyft," *Journal of Urban Economics*, 2021, *122*, 103318.

Waldinger, Daniel, "Targeting in-kind transfers through market design: A revealed preference analysis of public housing allocation," *American Economic Review*, 2021, *111* (8), 2660–96.

Weintraub, Gabriel Y, C Lanier Benkard, and Benjamin Van Roy, "Markov perfect industry dynamics with many firms," *Econometrica*, 2008, *76* (6), 1375–1411.

_ , _ , Przemysław Jeziorski, and Benjamin Van Roy, "Nonstationary oblivious equilibrium," Technical Report, working paper 2010.

Figure SA.1. Number of Passenger Arrivals Per Minute

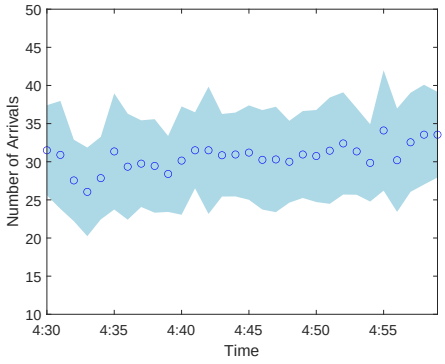

Note: the color fill indicates 95% confidence intervals based on the number of arrivals in each minute across 20 days in the data.

A Additional Estimates

A.1 Passenger Arrival Rate

In Figure SA.1, we plot the average number of passenger arrivals per minute from 4:30 pm to 5:00 pm averaged across the 20 days in our data. The arrival rate is 31.77 passengers / minute.

A.2 Dyadic Regressions

We estimate the effects of compatibility measures and time-to-departure on matching using dyadic regressions. For each dyad, we regress the indicator of whether the driver matches with the passenger on measures of compatibility, driver characteristics and driver waiting time. Specifically, we use $y_{ijt} = 1$ to denote a match between driver i and passenger j at time t. The linear probability model we estimate is

$$\begin{aligned} y_{ijt} = {} & \alpha_z z_{ij} + \alpha_f f_j + \alpha_x x_i + \alpha_{30} \mathbb{1}\left(T_i - t < 30\right) + \alpha_{20} \mathbb{1}\left(T_i - t < 20\right) \\ & + \alpha_{10} \mathbb{1}\left(T_i - t < 10\right) + \alpha_0 + \text{unobservables}, \end{aligned}$$

where z_{ij} is a vector of the compatibility measures, including the compatibility score, pickup and dropoff distances and differences in departure times, f_j is the fare of the request and x_i consists of driver characteristics, including trip lengths and whether it starts or ends in CBD. The parameters $\alpha_{30}, \alpha_{20}, \alpha_{10}$ measure the change in the probability of matching when the driver is within 30, 20, and 10 minutes from the departure time. The regression results are presented in Table SA.1. The estimates are in percentage point terms (multiplied by 100). We find that a 10 percentage-point increase in compatibility scores is associated with up to 0.177 percentage point increase in match probability. This effect is large, given that the mean probability of matching with a passenger in the dyadic sample is 0.16%. The estimates of other covariates on measures of compatibility are also

intuitive. Furthermore, the regression shows that a driver closer to the departure time is more likely to match with a passenger. These findings are consistent with our interviews of drivers.

A.3 Leaving Probability and Waiting Time

We estimate the effects of the time an agent has waited on the probability of leaving in the next 5 minutes separately for drivers and passengers. Specifically, let $\tilde{t}$ denote the number of minutes before the departure time. We define $y_{i\tilde{t}} = 1$ if a driver i is still in the market $\tilde{t}$ minutes before the departure time but matches with a passenger or leaves in the next 5 minutes (driver's last search is after $\tilde{t}$ but before $\tilde{t} - 5$ minutes from the departure time), and $y_{i\tilde{t}} = 0$ otherwise. We regress $y_{i\tilde{t}}$ on the time the driver has waited, controlling for whether the trip distance is between 10 and 30 km, whether the trip length is greater than 30 km, whether the trip starts in CBD and whether the trip ends in CBD. The key variable is the time a driver has waited, where the variation at a given $\tilde{t}$ is a result of different arrival times across passengers conditional on a departure time. We estimate the effect of the time waited for $\tilde{t} = 45, 40, \ldots, 5$ minutes before the departure time. For each regression, the sample consists of drivers that are still in the market $\tilde{t}$ minutes before the departure time. In panel (a) of Figure SA.2, we plot the marginal effect of having waited an additional 5 minutes on the probability of leaving at $\tilde{t}$ (5 times the coefficient of time waited) and the average leaving probability at $\tilde{t}$. This estimated marginal effect measures the average difference in probabilities of leaving between drivers that arrive early and that arrive late. For example, consider the probabilities of leaving between 15 minutes and 20 minutes from the departure time. For a given $t \geq 20$ minutes, one group of drivers arrives at t minutes before the departure, and another group arrives at $t + 5$ minutes before the departure. The marginal effect measures the difference in the probabilities of leaving at some point between 15 and 20 minutes before the departure across these two groups of drivers, averaged across all $t \geq 20$ minutes. We find that the marginal effect is nearly 0 with a tight 95% confidence interval for drivers whose arrival time is within 40 minutes of departure time, compared with the mean leaving probability. These drivers account for more than 91% of all drivers. We repeat this exercise in panel (b) for passengers, where $y_{j\tilde{t}} = 1$ if passenger j has not canceled the request when the passenger is $\tilde{t}$ minutes before the departure time but cancels the request between $\tilde{t}$ and $\tilde{t} - 5$ minutes before the departure. We find an even smaller effect of the time a passenger has waited on the probability of leaving.

A.4 Estimated Passenger Match Probabilities

To flexibly estimate the match probabilities, we discretize time into 30-second intervals and specify the probability that the passenger is matched in the next period as a logit function of a vector of covariates that include a constant, fare, fare's square, whether the trip starts in CBD, whether the trip ends in CBD, whether the distance is between 10 to 30 km, whether the distance is greater than 30 km, whether the stated departure time is between 20 to 30 minutes later after arrival, and whether the departure time is more than 30 minutes after arrival. We allow the coefficients to vary across each 30-second interval by separately estimating this logit probability function for each period after arrival via maximum likelihood. The sample for each period consists of all passengers who are in the market

Table SA.1. Dyadic Regression: Effects of Compatibility Measures and Time to Departure on Match

α_z		
	Compatibility Score	1.774
		(0.035)
	Pickup Distance (km)	-0.022
		(0.000)
	Dropoff Distance (km)	-0.019
		(0.000)
	Departure Time	0.024
	Difference $\leq$5 minutes	(0.007)
	Departure Time	0.050
	Difference $\leq$15 minutes	(0.006)
	Passenger Departure	-0.099
	Later Than Driver's	(0.007)
α_f, Fare ($)		0.098
		(0.002)
α_{30}		0.015
		(0.008)
α_{20}		0.040
		(0.007)
α_{10}		0.049
		(0.007)
α_x		
	Distance 10-30 km	-0.335
		(0.011)
	Distance >30 km	-0.779
		(0.022)
	Start in CBD	-0.130
		(0.006)
	End in CBD	-0.085
		(0.006)
Intercept		-0.087
		(0.015)
R^2		0.01
Number of Dyads		2,449,963

Note: The dependent variable is 1 if the dyad is a match and 0 otherwise. All estimates are in percentage point terms (multiplied by 100). We report robust standard errors in parentheses.

Figure SA.2. Leaving Probability and Waiting Time

(a) Driver

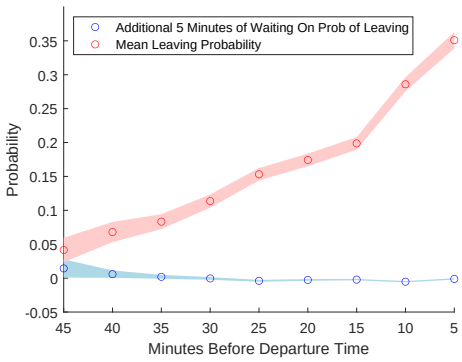

(b) Passenger

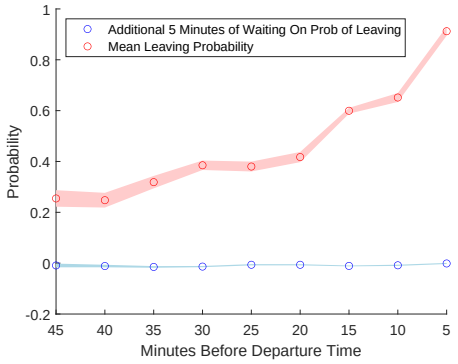

Note: the color fill indicates the 95% confidence intervals based on robust standard errors.

at the beginning of the period. Let j denote a passenger and $\mathfrak{t}$ index a period, which is $\Delta^{\text{psg}} = 0.5$ minutes long. Given the arrival time t_j^0 and departure time T_j, the total number of periods for the passenger is $\mathfrak{T}_j = \left\lceil \frac{T_j - t_j^0}{\Delta^{\text{psg}}} \right\rceil$, where $\lceil \cdot \rceil$ denotes the function to round up to the nearest integer. Let $\mathfrak{p}_{j\mathfrak{t}}$ denote the estimated match probability. Figure SA.3.(a) shows the estimated match probabilities as time approaches the departure time. The black lines represent the 25% and 75% quantiles across passengers and reflect the dispersion of this probability for different passengers, and the blue line represents the median.[24] Panel (b) plots the histogram of the passenger beliefs, which is the average probability of match in every 30 seconds:

$$\gamma_j = \frac{1}{\mathfrak{T}_j} \sum_{\mathfrak{t}=1}^{\mathfrak{T}_j} \mathfrak{p}_{j\mathfrak{t}}. \tag{SA.1}$$

A.5 Simulate Passengers That Arrive Before 4:30 pm or After 5:00 pm

We assume that the arrival times of passengers approximate a Poisson process at the estimated rate of 31.77 passengers/minute from 4:00 pm to 6:00 pm. We also assume that routes and departure times are independently distributed conditional on the arrival time. We therefore simulate the routes and departure times using the respective empirical distributions. We then simulate the unobserved passenger types based on passenger routes from the estimated distributions in Section 6. For each simulated passenger, we compute the belief of the average match rate in (SA.1) using estimates of the match probability based on passenger characteristics in Appendix A.4. We then compute the discretized passenger mass transition following Appendix F.1.2. We use $\mathfrak{t}$ to index a period and $n_{j\mathfrak{t}}$ to denote the mass of a passenger in a period $\mathfrak{t}$. For each driver that searches at the clock time t, the set of passengers that the driver sees includes

[24] Standard errors are about one to two orders of magnitudes smaller than the dispersion across passengers.

Figure SA.3. Passenger Match Probabilities

(a) Match Probability Over Time

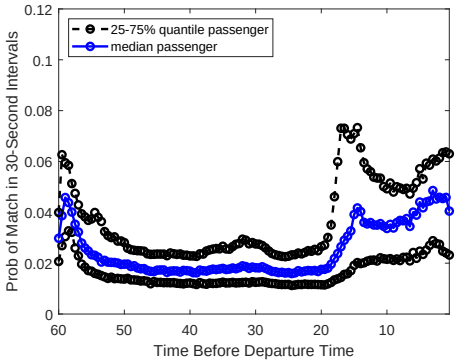

(b) Beliefs Across Passengers

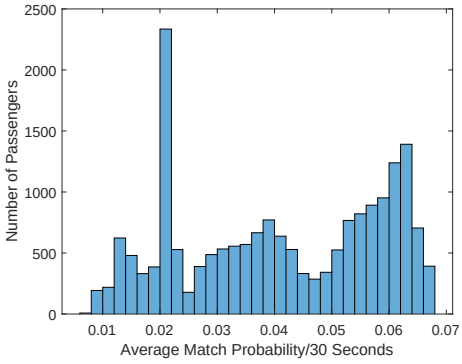

Note: (a) plots the estimated match probabilities as time approaches the departure time. The black lines represent the 25% and 75% quantiles of the match probabilities across passengers and reflect the dispersion of this probability for different passengers, and the blue line represents the median. The differences represent dispersions across passengers. Standard errors are one to two orders of magnitudes smaller than the cross-passenger differences. Panel (b) plots the distribution of the constructed passenger beliefs based on the match probability over time.

1. the waiting passengers that arrive between 4:30 pm and 5:00 pm in data, and

2. a set of simulated passengers that arrive outside this time window.

For each simulated j that arrives outside our data window (i.e., $t_j^0 \notin$ [4:30 pm, 5:00 pm]), we find the period $\mathfrak{t}_j(t)$ that includes t, and then linearly interpolate the mass n_{jt} at t from $n_{j,\mathfrak{t}_j(t)}$ and $n_{j,\mathfrak{t}_j(t)+1}$. Then we randomly and independently include j in the driver's choice set at t with probability n_{jt}. In the simulated likelihood function, we simulate 50 passenger sets for each instance of a driver search, and for each set we independently simulate a set of ν_{ij} for each driver-passenger pair.

A.6 Driver Move Opportunity

We assume that a driver receives a move opportunity at most once every 5 minutes, which corresponds with a search during that interval in the data. For each 5-minute interval after arrival, we estimate the probability of a search as a logit function of driver characteristics. Covariates include driver distances (whether the driver distance is less than 10 km, whether it is between 10-30 km) and locations (whether the driver starts in CBD, whether the driver ends in CBD) and a constant. We estimate the move probability separately for each 5-minute intervals up to the last 5 minutes before departure, allowing the probability of search to vary flexibly over time. Each regression's sample consists of drivers that are still in the market at the corresponding time. We set the move probability to be 1 in the last five minutes till departure. Similar to Figure SA.3, we plot the the median estimated probability and 25-75% quantiles across drivers in Figure SA.4. In general, the probability increases as time approaches the departure time.

Figure SA.4. Move Opportunity Arrival Probability

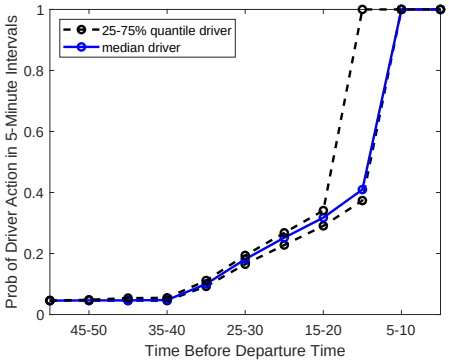

A.7 Decomposition of Counterfactual Results

Table SA.2 reports the changes of surplus and the number of matches across groups of agent characteristics under the driver commitments counterfactual. The CF column reports the results from the driver commitment counterfactual. Table SA.3 reports the changes of surplus and the number of matches across groups of agent characteristics under the passenger commitments counterfactual. The CF column reports the results from the passenger commitment counterfactual.

Table SA.2. Distributional Impact of the Driver Commitment

	Number of Arrivals	ΔSurplus ($)	# Matches Baseline	# Matches CF	Change in # Matches
(a) Driver*					
Distance					
Distance < 10 km	440	-4.15	133	193	44.82%
Distance 10-30 km	808	-4.19	242	371	53.31%
Distance ≥ 30 km	182	-4.13	51	79	55.88%
Arrival Time					
Arrival Time < Departure -20Min	851	-4.48	248	335	35.03%
Arrival Time ≥ Departure - 20 Min	579	-3.72	177	307	73.28%
Location					
Start & End in CBD	163	-4.26	51	79	55.96%
Start in CBD, End outside CBD	293	-4.25	85	126	48.90%
Start outside CBD, End in CBD	234	-4.07	75	111	48.66%
Start in CBD, End outside CBD	740	-4.16	216	327	51.38%
(b) Passenger**					
Distance					
Distance < 10 km	304	4.32	131	199	51.90%
Distance 10-30 km	527	5.15	234	364	55.09%
Distance ≥ 30 km	129	5.70	56	79	39.87%
Arrival Time					
Arrival Time < Departure -20Min	617	5.31	223	382	71.74%
Arrival Time ≥ Departure - 20 Min	343	4.34	199	259	30.08%
Location					
Start & End in CBD	101	4.90	42	69	62.91%
Start in CBD, End outside CBD	183	5.24	88	130	48.20%
Start outside CBD, End in CBD	166	5.97	85	124	45.35%
Start in CBD, End outside CBD	510	4.55	207	319	54.25%

*: based on drivers with departure times between 5:00 pm to 5:20 pm.
**: based on passengers with arrival times between 4:30 pm to 5:30 pm.
The CF column reports the results from the driver commitment counterfactual.

Table SA.3. Distributional Impact of the Passenger Commitment

	Number of Arrivals	ΔSurplus ($)	# Matches Baseline	# Matches CF	Change in # Matches
(a) Driver*					
Distance					
Distance < 10 km	440	0.15	133	141	5.61%
Distance 10-30 km	808	0.11	242	253	4.68%
Distance ≥ 30 km	182	0.12	51	53	5.10%
Arrival Time					
Arrival Time < Departure -20Min	851	0.12	248	261	5.05%
Arrival Time ≥ Departure - 20 Min	579	0.13	177	186	4.98%
Location					
Start & End in CBD	163	0.13	51	53	4.62%
Start in CBD, End outside CBD	293	0.12	85	89	4.78%
Start outside CBD, End in CBD	234	0.10	75	77	3.89%
Start in CBD, End outside CBD	740	0.14	216	228	5.60%
(b) Passenger**					
Distance					
Distance < 10 km	304	-1.12	131	136	3.33%
Distance 10-30 km	527	-1.47	234	248	5.59%
Distance ≥ 30 km	129	-1.94	56	61	8.87%
Arrival Time					
Arrival Time < Departure -20Min	617	-1.36	223	237	6.28%
Arrival Time ≥ Departure - 20 Min	343	-1.55	199	208	4.26%
Location					
Start & End in CBD	101	-1.21	42	44	4.55%
Start in CBD, End outside CBD	183	-1.39	88	92	5.44%
Start outside CBD, End in CBD	166	-1.46	85	90	5.42%
Start in CBD, End outside CBD	510	-1.47	207	218	5.40%

*: based on drivers with departure times between 5:00 pm to 5:20 pm.
**: based on passengers with arrival times between 4:30 pm to 5:30 pm.
The CF column reports the results from the passenger commitment counterfactual.

B Equilibrium Existence in the Illustrative Model

B.1 Preliminaries

We first note that the driver value function can be rewritten in the following integral form, with the boundary condition of $V_k(T) = 0$:

$$\begin{aligned} V_k(t) = \int_t^T \exp(-\lambda(\tau - t)) \cdot \Big(& \lambda \cdot (\Upsilon + n_1(\tau) \ln(\exp(u_{k1}) + \exp(V_k(\tau)) + 1) \\ & + (1 - n_1(\tau)) n_2(\tau) \ln(\exp(u_{k2}) + \exp(V_k(\tau)) + 1) \\ & + (1 - n_1(\tau))(1 - n_2(\tau)) \ln(\exp(V_k(\tau)) + 1)) - c^{\text{drv}} \frac{\tau}{T} \Big) d\tau. \end{aligned} \tag{SB.1}$$

Similarly, we can write the mass transitions in integral forms. For driver masses m_k, let $\tilde{w}_k = n_1 q_{k1} + n_2 q_{k2} + w_k$, then

$$m_k(t) = \int_0^t \frac{1 - \tilde{w}_k(\tau)}{T} \exp\left(-\lambda \int_\tau^t \tilde{w}_k(\tau_1)\, d\tau_1\right) d\tau \tag{SB.2}$$

Similarly, let $\tilde{r}_\ell = \left(\lambda m_a + \frac{1}{T}\right) q_{a\ell} + \left(\lambda m_b + \frac{1}{T}\right) q_{b\ell} + r_\ell$ and $S_\ell = \dfrac{1}{1 + \exp\left(\dfrac{c^{\text{psg}}}{T}\dfrac{t}{\gamma_\ell} - v_\ell\right)}$, then

$$n_\ell(t) = \int_0^t \frac{S_\ell(\tau)}{T} \exp\left(-\int_\tau^t \tilde{r}_\ell(\tau_1)\, d\tau_1\right) d\tau \tag{SB.3}$$

B.2 Equilibrium Existence

B.2.1 Equilibrium Definition

The equilibrium existence amounts to finding functions

$$V_k, q_{k1}, q_{k2}, \tilde{w}_k, m_k, \tilde{r}_\ell, S_\ell, n_\ell$$

defined on $t \in [0, T]$ and scalars γ_ℓ, for $k \in \{a, b\}$ and $\ell \in \{1, 2\}$ that satisfy the following set of equations.

1. Driver value function (SB.1).

2. Driver choice probabilities conditional on observing a type ℓ passenger.

$$q_{k1}(t) = \frac{\exp(u_{k1})}{\exp(u_{k1}) + \exp(V_k(t)) + 1} \tag{SB.4}$$

$$q_{k2}(t) = \frac{(1 - n_1(t)) \exp(u_{k2})}{\exp(u_{k2}) + \exp(V_k(t)) + 1} \tag{SB.5}$$

3. We also define the combined driver exit rates (rates of matching and leaving without a match):

$$\tilde{w}_k(t) = \frac{n_1(t)(\exp(u_{k1}) + 1)}{\exp(u_{k1}) + \exp(V_k(t)) + 1} + \frac{(1 - n_1(t))\, n_2(t)(\exp(u_{k2}) + 1)}{\exp(u_{k2}) + \exp(V_k(t)) + 1} + \frac{(1 - n_1(t))(1 - n_2(t))}{\exp(V_k(t)) + 1} \tag{SB.6}$$

4. Driver mass transition functions in integral forms (SB.2).

5. Passenger belief

$$\gamma_\ell = \frac{1}{T} \int_0^T \left(\left(\lambda m_a(t) + \frac{1}{T}\right) q_{a\ell}(t) + \left(\lambda m_b(t) + \frac{1}{T}\right) q_{b\ell}(t)\right) dt. \tag{SB.7}$$

6. Passenger leaving rate

$$r_\ell(t) = \frac{c^{\text{psg}}}{T\gamma_\ell} \frac{\exp\left(\frac{c^{\text{psg}}}{T}\frac{t}{\gamma_\ell} - v_\ell\right)}{1+\exp\left(\frac{c^{\text{psg}}}{T}\frac{t}{\gamma_\ell} - v_\ell\right)} \tag{SB.8}$$

7. We also define the combined passenger exit rates (rates of matching and leaving without a match):

$$\tilde{r}_\ell = \left(\lambda m_a + \frac{1}{T}\right) q_{a\ell} + \left(\lambda m_b + \frac{1}{T}\right) q_{b\ell} + r_\ell \tag{SB.9}$$

8. Passenger probability of leaving after arrival

$$S_\ell = \left(1+\exp\left(\frac{c^{\text{psg}}}{T}\frac{t}{\gamma_\ell} - v_\ell\right)\right)^{-1} \tag{SB.10}$$

9. Passenger mass transition function in integral form (SB.3).

B.2.2 Proof Overview

We use Schauder Fixed Point Theorem to prove the equilibrium existence. The proof strategy is as follows. We define a mapping A whose fixed point is a solution to the 9 sets of equations above. Therefore the existence of equilibrium is equivalent to the existence of the fixed point of mapping A. The proof has two parts. First, we find a set $\mathcal{M}$ where $A(\mathcal{M}) \subset \mathcal{M}$, and $\mathcal{M}$ is closed, bounded, convex and non-empty. Second, we show that A is equicontinuous. Therefore the Arzela-Ascoli Theorem shows that an equicontinuous A would also be a compact operator, which implies that A has a fixed point following the Schauder Fixed Point Theorem (Schäfer, 2014).

B.2.3 Proof Step 1: Define $\mathcal{M}$

We first specify the mapping's domain. Let $C[a,b]$ denote the set of continuous functions on the interval $[a,b]$. We collect the functions and scalars corresponding with the equilibrium in the vector

$$\begin{aligned} X = (&V_a, V_b, m_a, m_b, n_1, n_2, \\ &q_{a1}, q_{a2}, q_{b1}, q_{b2}, \tilde{w}_a, \tilde{w}_b, \\ &r_1, r_2, \tilde{r}_1, \tilde{r}_2, S_1, S_2, \gamma_1, \gamma_2). \end{aligned} \tag{SB.11}$$

We then define the Banach space

$$\mathcal{X} = C[0,T]^{18} \times [0,\infty)^2,$$

with the following norm $\|X\|$: for an element $X = (X_1(t), \cdots, X_{18}(t), X_{19}, X_{20}) \in \mathcal{X}$,

$$\|X\|_\infty = \sup_{\tau\in[0,T]} |X_1(\tau)| + \cdots + \sup_{\tau\in[0,T]} |X_{18}(\tau)| + |X_{19}| + |X_{20}|.$$

We use $\mathcal{M}$ to denote the domain of our mapping, which is a subset of $\mathcal{X}$. The set $\mathcal{M}$ is defined as

$$\begin{aligned}\mathcal{M} = &\left\{X \in C[0,t], X(t) \geq \underline{V}_a(t), X(t) \leq \overline{V}_a(t)\right\} \times \left\{X \in C[0,t], X(t) \geq \underline{V}_b(t), X(t) \leq \overline{V}_b(t)\right\} \\ &\times \{X \in C[0,t], X(t) \geq \underline{m}_a(t), X(t) \leq \overline{m}_a(t)\} \times \{X \in C[0,t], X(t) \geq \underline{m}_b(t), X(t) \leq \overline{m}_b(t)\} \\ &\ldots \\ &\times \{X \in C[0,t], X(t) \geq \underline{r}_1(t), X(t) \leq \overline{r}_1(t)\} \times \{X \in C[0,t], X(t) \geq \underline{r}_2(t), X(t) \leq \overline{r}_2(t)\} \\ &\times \left[\underline{\gamma}_1, \overline{\gamma}_1\right] \times \left[\underline{\gamma}_2, \overline{\gamma}_2\right].\end{aligned}$$

Below, we define the terms in the Cartesian product above.

For $k \in \{a, b\}$,we define $\overline{V}_k(t)$ to be the solution of the following ODE:

$$0 = \lambda \cdot \left(\Upsilon + \ln\left(\exp(u_{k1}) + \exp\left(\overline{V}_k(t)\right) + 1\right)\right) + \frac{d\overline{V}_k}{dt} - \lambda \overline{V}_k(t) - c^{\text{drv}}\frac{t}{T},$$

and $\underline{V}_k(t)$ solves

$$0 = \lambda \cdot \left(\Upsilon + \ln\left(\exp\left(\overline{V}_k(t)\right) + 1\right)\right) + \frac{d\overline{V}_k}{dt} - \lambda \overline{V}_k(t) - c^{\text{drv}}\frac{t}{T}, \tag{SB.12}$$

with the boundary conditions $\overline{V}_k(T) = \underline{V}_k(T) = 0$. One can show that the functions $\overline{V}_k$ and $\underline{V}_k(T)$ exist and are unique. We detail these steps in Appendix B.3. For any finite u_{k1}, we also have $\underline{V}_k \leq \overline{V}_k$. Given that $\overline{V}_k$ and $\underline{V}_k$ are both continuous functions on a closed interval, they are also finite. We use U_V to denote $\sup_{t,k}|V_k|$.

We next define bounds $\overline{\tilde{w}}_k$ and $\underline{\tilde{w}}_k$. Let

$$\overline{\tilde{w}}_k = \max\left\{\frac{1+\exp(u_{k1})}{1+\exp(u_{k1})+\exp(\underline{V}_k)}, \frac{1}{1+\exp(\underline{V}_k)}\right\}.$$

We use this quantity to define $\underline{m}_k$.

$$\underline{m}_k = \int_0^t \frac{1-\overline{\tilde{w}}_k}{T}\exp\left(-\lambda\int_\tau^t \overline{\tilde{w}}_k(\tau_1)\,d\tau_1\right)d\tau.$$

We set $\underline{\tilde{w}}_k = 0$ and $\overline{m}_k = 1$.[25]

We next define bounds $\overline{q}_{k1}$ and $\underline{q}_{k1}$:

$$\overline{q}_{k1} = \frac{\exp(u_{k1})}{\exp(u_{k1})+\exp(\underline{V}_k)+1}, \underline{q}_{k1} = \frac{\exp(u_{k1})}{\exp(u_{k1})+\exp\left(\overline{V}_k\right)+1}.$$

[25] These bounds suffice for this proof, but can be tightened.

We use these probabilities to define $\left(\overline{\gamma}_1, \underline{\gamma}_1\right)$:

$$\overline{\gamma}_1 = \frac{1}{T}\int_0^T \left(\left(\lambda \overline{m}_a(t) + \frac{1}{T}\right)\overline{q}_{a1}(t) + \left(\lambda \overline{m}_b(t) + \frac{1}{T}\right)\overline{q}_{b1}(t)\right) dt$$
$$\underline{\gamma}_1 = \frac{1}{T}\int_0^T \left(\left(\lambda \underline{m}_a(t) + \frac{1}{T}\right)\underline{q}_{a1}(t) + \left(\lambda \underline{m}_b(t) + \frac{1}{T}\right)\underline{q}_{b1}(t)\right) dt$$

We note $\underline{\gamma}_1 > 0$. These probabilities help to define bounds $\overline{r}_1$ and $\underline{r}_1$, by replacing γ_ℓ in (SB.8) with $\overline{\gamma}_\ell$ and $\underline{\gamma}_\ell$.

We now define bounds associated with the type 1 leaving rate and mass. Let

$$\overline{\tilde{r}}_1 = \left(\lambda \overline{m}_a + \frac{1}{T}\right)\overline{q}_{a1} + \left(\lambda \overline{m}_b + \frac{1}{T}\right)\overline{q}_{b1} + \overline{r}_\ell, \underline{\tilde{r}}_1 = \left(\lambda \underline{m}_a + \frac{1}{T}\right)\underline{q}_{a1} + \left(\lambda \underline{m}_b + \frac{1}{T}\right)\underline{q}_{b1} + \underline{r}_\ell$$

and

$$\overline{S}_1 = \left(1 + \exp\left(\frac{c^{\text{psg}}}{T}\frac{t}{\overline{\gamma}_1} - v_1\right)\right)^{-1}, \underline{S}_1 = \left(1 + \exp\left(\frac{c^{\text{psg}}}{T}\frac{t}{\underline{\gamma}_1} - v_1\right)\right)^{-1},$$

then

$$\overline{n}_1(t) = \int_0^t \frac{\overline{S}_1(\tau)}{T}\exp\left(-\int_\tau^t \underline{\tilde{r}}_1(\tau_1)\, d\tau_1\right) d\tau, \underline{n}_1(t) = \int_0^t \frac{\underline{S}_1(\tau)}{T}\exp\left(-\int_\tau^t \overline{\tilde{r}}_1(\tau_1)\, d\tau_1\right) d\tau.$$

These probabilities in turn help us to define bounds corresponding with q_{k2}, γ_2, $\tilde{r}_2$, S_2 and n_2 in analogous manners. Given the discussion above, the set $\mathcal{M}$ is closed, bounded, convex and non-empty.

B.2.4 Proof Step 2: Define Mapping A

Now we define the mapping A from $\mathcal{M}$ to $\mathcal{M}$, and the fixed point of A corresponds with the solution to the system of equations. For $X \in \mathcal{M}$ in (SB.11), the mapping is

$$A(X) = \left(A\{V_a\}, A\{V_b\} \ldots, A\{\gamma_2\}\right),$$

where $A\{V_k\}$ is given by the right hand sides of (SB.1), $A\{m_k\}$ the right hand sides of (SB.2), $A\{n_\ell\}$ the right hand side of (SB.3), $A\{q_{k\ell}\}$ the right hand sides of (SB.4) and (SB.5), $A\{\tilde{w}_k\}$ the right hand sides of (SB.6), $A\{r_\ell\}$ the right hand sides of (SB.8), $A\{\tilde{r}_\ell\}$ the right hand sides of (SB.9), $A\{S_\ell\}$ the right hand sides of (SB.10), and $A\{\gamma_\ell\}$ the right hand sides of (SB.7).

B.2.5 Proof Step 3: Show $A(\mathcal{M}) \subset \mathcal{M}$

To show that the fixed point exists, we need to show (1) $A(\mathcal{M}) \subset \mathcal{M}$ and (2) A is equicontinuous before applying the Arzela-Ascoli Theorem. For $A(\mathcal{M}) \subset \mathcal{M}$, we first note that the right hand side of (SB.1) implies $\underline{V}_k \leq A\{V_k\} \leq \overline{V}_k$ given that n_1 and n_2 are strictly bounded above 0 and below 1

and that $u_{k2} < u_{k1}$. For the same reasons, $A\{\tilde{w}_k\} \geq 0$. To verify the upper bound, we have

$$\begin{aligned}
A\{\tilde{w}_k\} =& \frac{n_1(\exp(u_{k1})+1)}{\exp(u_{k1})+\exp(V_k)+1} + \frac{(1-n_1)n_2(\exp(u_{k2})+1)}{\exp(u_{k2})+\exp(V_k)+1} + \frac{(1-n_1)(1-n_2)}{\exp(V_k)+1} \\
\leq& (n_1 + (1-n_1)n_2 + (1-n_1)(1-n_2)) \\
& \cdot \max\left\{\frac{\exp(u_{k1})+1}{\exp(u_{k1})+\exp(V_k)+1}, \frac{\exp(u_{k2})+1}{\exp(u_{k2})+\exp(V_k)+1}, \frac{1}{\exp(V_k)+1}\right\} \\
\leq& \max\left\{\frac{\exp(u_{k1})+1}{\exp(u_{k1})+\exp(V_k)+1}, \frac{1}{\exp(V_k)+1}\right\} \leq \bar{\tilde{w}}_k,
\end{aligned}$$

One can similarly verify that each of the rest of the components of A falls in $\mathcal{M}$.

B.2.6 Proof Step 4: Show A is Equicontinuous

We next argue that A is equicontinuous. We note that A is uniformly bounded on $\mathcal{M}$. To show that A is equicontinuous, it suffices to verify that each of A's output is Lipshitz continuous. Given two functions $X_1, X_2 \in \mathcal{M}$, we use $V_a\langle X_1\rangle, V_b\langle X_1\rangle, \cdots$ to denote each component of X. Then

$$\begin{aligned}
A\{V_k\}(X_1) - A\{V_k\}(X_2) = \int_t^T & \exp(-\lambda(\tau-t)) \cdot \lambda \cdot (n_1\langle X_1\rangle(\tau) \ln(\exp(u_{k1}) + \exp(V_k\langle X_1\rangle(\tau)) + 1) \\
& - n_1\langle X_2\rangle(\tau) \ln(\exp(u_{k1}) + \exp(V_k\langle X_2\rangle(\tau)) + 1) \\
& + (1 - n_1\langle X_1\rangle(\tau)) n_2\langle X_1\rangle(\tau) \ln(\exp(u_{k2}) + \exp(V_k\langle X_1\rangle(\tau)) + 1) \\
& - (1 - n_1\langle X_2\rangle(\tau)) n_2\langle X_2\rangle(\tau) \ln(\exp(u_{k2}) + \exp(V_k\langle X_2\rangle(\tau)) + 1) \\
& + (1 - n_1\langle X_1\rangle(\tau))(1 - n_2\langle X_1\rangle(\tau)) \ln(\exp(V_k\langle X_1\rangle(\tau)) + 1) \\
& - (1 - n_1\langle X_2\rangle(\tau))(1 - n_2\langle X_2\rangle(\tau)) \ln(\exp(V_k\langle X_2\rangle(\tau)) + 1))\, d\tau.
\end{aligned} \tag{SB.13}$$

Inside the integral, there are three differences. We consider the first difference as an example. By the mean value theorem, there exists $\varpi(\tau)$ between $V_k\langle X_1\rangle(\tau)$ and $V_k\langle X_2\rangle(\tau)$ such that

$$\begin{aligned}
& \ln(\exp(u_{k1}) + \exp(V_k\langle X_1\rangle(\tau)) + 1) - \ln(\exp(u_{k1}) + \exp(V_k\langle X_2\rangle(\tau)) + 1) \\
=& \frac{\exp(\varpi)}{1 + \exp(\varpi) + \exp(u_{k1})} \cdot (V_k\langle X_1\rangle(\tau) - V_k\langle X_2\rangle(\tau)) \\
\equiv& \delta(\tau)(V_k\langle X_1\rangle(\tau) - V_k\langle X_2\rangle(\tau)),
\end{aligned}$$

where $\delta \in (0,1)$. The absolute value of the integral of the first difference in (SB.13) is

$$\begin{aligned}
&\left| \int_t^T \exp\left(-\lambda\left(\tau - t\right)\right) \cdot \lambda \cdot \left(n_1\left\langle X_1 \right\rangle\left(\tau\right) \ln\left(\exp\left(u_{k1}\right) + \exp\left(V_k\left\langle X_1 \right\rangle\left(\tau\right)\right) + 1\right)\right.\right. \\
&\left.\left. - n_1\left\langle X_2 \right\rangle\left(\tau\right) \ln\left(\exp\left(u_{k1}\right) + \exp\left(V_k\left\langle X_2 \right\rangle\left(\tau\right)\right) + 1\right)\right) d\tau \right| \\
=&\left| \int_t^T \exp\left(-\lambda\left(\tau - t\right)\right) \cdot \lambda \left(n_1\left\langle X_1 \right\rangle\left(\tau\right) \cdot \delta\left(\tau\right) \cdot \left(V_k\left\langle X_1 \right\rangle\left(\tau\right) - V_k\left\langle X_2 \right\rangle\left(\tau\right)\right)\right.\right. \\
&\left.\left. + \left(n_1\left\langle X_1 \right\rangle\left(\tau\right) - n_1\left\langle X_2 \right\rangle\left(\tau\right)\right) V_k\left\langle X_2 \right\rangle\left(\tau\right)\right) d\tau \right| \\
\leq& \left(1 - \exp\left(-\lambda\left(T - t\right)\right)\right) \left(\sup_{\tau \in [t,T]} \left| V_k\left\langle X_1 \right\rangle - V_k\left\langle X_2 \right\rangle \right| + U_V \sup_{\tau \in [t,T]} \left| n_1\left\langle X_1 \right\rangle - n_2\left\langle X_2 \right\rangle \right| \right) \\
\leq& C_1 \left\| X_1 - X_2 \right\|
\end{aligned}$$

for some finite constant C_1 that does not depend on X_1 or X_2. Similar applications of triangular inequalities and mean value theorems can be used to verify the Lipshitz continuity of other differences in (SB.13) and other outputs of A. This completes the proof.

B.3 Existence and Uniqueness of $\overline{V}_k$ and $\underline{V}_k$

Without loss of generality, we show the existence and uniqueness of $\underline{V}_k$. In the space of continuous functions on $[0,T]$, denoted as $C\left[0,T\right]$, we define the mapping B, such that for a function $V\left(t\right) \in C\left[0,T\right]$,

$$B\left(V\right) = \int_t^T \exp\left(-\lambda\left(\tau - t\right)\right) \cdot \lambda\left(\Upsilon + \ln\left(\exp\left(\underline{V}_k\left(\tau\right)\right) + 1\right)\right) d\tau + \frac{c^{\text{drv}}}{2T}\left(t^2 - T^2\right).$$

A fixed point of B is a solution to (SB.12). We show that B is a contraction mapping using the norm $\left\|V\right\| = \sup_t \left|V\right|$. Specifically, for any two elements $V_1, V_2 \in C\left[0,T\right]$,

$$\begin{aligned}
\left\| B\left(V_1\right) - B\left(V_2\right) \right\| &= \sup_t \left| \int_t^T \exp\left(-\lambda\left(\tau - t\right)\right) \lambda\left(\ln\left(\exp\left(V_1\left(\tau\right)\right) + 1\right) - \ln\left(\exp\left(V_2\left(\tau\right)\right) + 1\right)\right) d\tau \right| \\
&= \sup_t \left| \int_t^T \exp\left(-\lambda\left(\tau - t\right)\right) \lambda \frac{\exp\left(\tilde{V}\left(\tau\right)\right)}{1 + \exp\left(\tilde{V}\left(\tau\right)\right)} \left(V_1\left(\tau\right) - V_2\left(\tau\right)\right) d\tau \right|,
\end{aligned}$$

where by the mean value theorem, there exists a $\tilde{V}\left(\tau\right) \in \left[V_1\left(\tau\right), V_2\left(\tau\right)\right]$ such that

$$\ln\left(\exp\left(V_1\left(\tau\right)\right) + 1\right) - \ln\left(\exp\left(V_2\left(\tau\right)\right) + 1\right) = \frac{\exp\left(\tilde{V}\left(\tau\right)\right)}{1 + \exp\left(\tilde{V}\left(\tau\right)\right)} \left(V_1\left(\tau\right) - V_2\left(\tau\right)\right).$$

Therefore,

$$\begin{aligned}
&\sup_t \left| \int_t^T \exp\left(-\lambda\left(\tau - t\right)\right) \lambda \frac{\exp\left(\tilde{V}\left(\tau\right)\right)}{1+\exp\left(\tilde{V}\left(\tau\right)\right)} \left(V_1\left(\tau\right) - V_2\left(\tau\right)\right) d\tau \right|, \\
\leq &\sup_t \left(\left| \int_t^T \exp\left(-\lambda\left(\tau - t\right)\right) \lambda d\tau \right| \cdot \sup_{\tau \in [t,T]} \left|V_1\left(\tau\right) - V_2\left(\tau\right)\right| \right) \\
= &\sup_t \left(1 - \exp\left(-\lambda\left(T - t\right)\right)\right) \left\|V_1 - V_2\right\| \leq \left(1 - \exp\left(-\lambda T\right)\right) \left\|V_1 - V_2\right\|.
\end{aligned}$$

Therefore B is a contraction mapping with a Lipshitz constant no greater than $1 - \exp\left(-\lambda T\right) < 1$ on $C\left[0, T\right]$, and thus the solution to (SB.12) with a boundary condition of $\underline{V}_k\left(T\right) = 0$ exists and is unique by the Banach's fixed point theorem (Schäfer, 2014).

C Additional Market Designs in the Illustrative Model

C.1 Passenger Commitment

For a passenger j of type ℓ that arrives at t_j^0, she agrees to wait if the expected payoff for waiting until T exceeds the value of leaving immediately:

$$\int_{t_j^0}^T \gamma_\ell \left(v_j - c^{\text{psg}} \frac{\tau}{T}\right) \exp\left(-\gamma_\ell \left(\tau - t_j^0\right)\right) d\tau + \exp\left(-\gamma_\ell \left(T - t_j^0\right)\right) v_{0j} > v_{0j}.$$

Therefore the passenger waits if

$$v_j - v_{0j} > \frac{\int_{t_j^0}^T \gamma_\ell c^{\text{psg}} \frac{\tau}{T} \exp\left(-\gamma_\ell \left(\tau - t_j^0\right)\right) d\tau}{1 - \exp\left(-\gamma_\ell \left(T - t_j^0\right)\right)} \equiv \overline{v}_\ell\left(t_j^0\right). \tag{SC.1}$$

The probability that a type ℓ passenger who arrives at t would send a request and wait is

$$\overline{S}_\ell\left(t; \gamma_\ell\right) = \exp\left(v_\ell - \overline{v}_\ell\left(t\right)\right) / \left(1 + \exp\left(v_\ell - \overline{v}_\ell\left(t\right)\right)\right). \tag{SC.2}$$

In the equilibrium under this market design, driver decision problems and mass transitions are the same as in Definition 1. The passengers choose whether to participate in the matching based on (SC.1), and the passenger mass transition is modified as:

$$\frac{dn_\ell}{dt} = -n_\ell \cdot \left(\lambda m_a q_{a\ell} + \frac{1}{T} q_{a\ell} + \lambda m_b q_{b\ell} + \frac{1}{T} q_{b\ell}\right) + \frac{1}{T} \cdot \overline{S}_\ell\left(t; \gamma_\ell\right).$$

C.2 Selective Visibility

We list the modifications by groups in Definition 1.

1. (Optimality) The Bellman equations and choice probabilities remain the same as in Definition 1.

2. (Consistent Beliefs) A type a driver either observes a type 2 passenger or no one. The beliefs of observing each type of passengers are $p_{a1}(t) = 0$, $p_{a2}(t) = n_2(t)$. The belief of observing a non-empty set of choices is $p_a(t) = n_2(t)$. We still set $g_{a1} = 1$ for convenience (even though the driver would not see any type 1 passengers under this design). Conditional on observing a type 2 passenger, the belief of type a drivers that it is the highest value passenger is $g_{a2} = 1$. For type b drivers, the beliefs are the same as in Definition 1.
   Type 1 passengers adjust their belief to reflect the design that no type a drivers match with them, and the modified (7) for type 1 is

$$\gamma_1 = \frac{1}{T}\int_0^T \left(\lambda m_b(\tau) q_{b1}(\tau) + \frac{1}{T} q_{b1}\right) d\tau. \tag{SC.3}$$

   Type b drivers' and type 2 passengers' beliefs are the same as in Def. 1.

3. (Mass Transitions) For type a drivers, the decrease in driver mass is now due to matching with type 2 passengers or leaving. Therefore (8) is modified as

$$\frac{dm_a}{dt} = -\lambda m_a (n_2 q_{a2} + w_a) + \frac{1}{T}(1 - n_2 q_{a2} - w_a).$$

   The type 1's new mass transition is

$$\frac{dn_1}{dt} = -n_1 \cdot \left(\left(\lambda m_b + \frac{1}{T}\right) q_{b1} + r_1\right) + \frac{1}{T} \cdot S_1(t; \gamma_1).$$

   Type b drivers' and type 2 passengers' mass transitions are the same as in Def. 1.

D Matching Equilibrium of the Empirical Model

We first define driver beliefs. Based on Assumption 1, the probability of observing a non-empty set for a type k driver is

$$p_k(t) = 1 - \prod_\ell (1 - h_{k\ell}(t) n_\ell(t)). \tag{SD.1}$$

For $g_{k\ell}$, if the driver value for matching with a type ℓ passenger is u, then the probability that the driver prefers this passenger to another type ℓ' passenger is $\Phi\left(\frac{u - u_{k\ell'}}{\sigma}\right)$. Therefore the probability that the driver prefers this passenger to any other passenger is

$$g_{k\ell}(u;t) = h_{k\ell}(t) \cdot n_\ell(t) \cdot \prod_{\ell' \neq \ell} \left(h_{k\ell'}(t) n_{\ell'}(t) \cdot \Phi\left(\frac{u - u_{k\ell'}}{\sigma}\right) + 1 - h_{k\ell'}(t) n_{\ell'}(t)\right), \tag{SD.2}$$

where $1 - h_{k\ell'}(t) n_{\ell'}(t)$ is the probability that the type ℓ' passenger is not in the choice set. Hence the density function $g_k(u;t)$ of $G_k(u;t)$ is

$$g_k(u;t) = \frac{\sum_\ell g_{k\ell}(u;t) \phi\left(\frac{u - u_{k\ell}}{\sigma}\right)/\sigma}{p_k(t)}, \tag{SD.3}$$

where ϕ is the standard normal density.

For passengers, analogous to (7), we define the passenger belief as the average type ℓ match rate (omitting the t argument):

$$\gamma_\ell = \frac{1}{T_\ell - t_\ell^0} \int_{t_\ell^0}^{T_\ell} \sum_{k=1}^{K} \left(\lambda_k m_k h_{k\ell} q_{k\ell} + h_{k\ell} \eta_k q_{k\ell}^0 \right) dt. \tag{SD.4}$$

The equilibrium places three sets of restrictions on $\{V_k, q_{k\ell}, w_k, S_\ell, r_\ell, p_k, g_{k\ell}, G_k, \gamma_\ell, m_k, n_\ell\}$.

1. (Optimality conditions) The driver value functions and choice probabilities are given in (11), (12) and (13). The passenger leaving rate is given by (6).

2. (Consistent beliefs) The driver beliefs $(p_k, g_{k\ell}, G_k)$ are consistent with (SD.1), (SD.2) and (SD.3); the passenger belief of the average match rate is consistent with (SD.4).

3. (Mass transitions) The driver mass $m_k(t)$ is 0 for $t \notin [t_k^0, T_k]$. For $t \in [t_k^0, T_k]$,(omitting the argument of t)
$$\frac{dm_k}{dt} = -\lambda_k m_k \cdot \left(\sum_\ell h_{k\ell} n_\ell q_{k\ell} + (1 - d_k) w_k \right), \tag{SD.5}$$
with the boundary condition $m_k(t_k^0) = m_k^0 \left(1 - \sum_\ell h_{k\ell}(t_k^0) n_\ell(t_k^0) q_{k\ell}^0(t_k^0) - w_k^0(t_k^0)\right)$. For passengers, the mass $n_\ell(t) = 0$ for $t \notin [t_\ell^0, T_\ell]$. For $t \in [t_\ell^0, T_\ell]$,
$$\frac{dn_\ell}{dt} = -n_\ell \left(\sum_k \lambda_k h_{k\ell} m_k q_{k\ell} + \sum_k h_{k\ell} \eta_k q_{k\ell}^0 + (1 - d_\ell) r_\ell \right), \tag{SD.6}$$
with the boundary condition $n_\ell(t_\ell^0) = n_\ell^0 \left((1 - d_\ell) S_\ell(t_\ell^0; \gamma_\ell) + d_\ell \overline{S}_\ell(t_\ell^0; \gamma_\ell) \right)$.

To establish equilibrium existence, we assume that, for any type ℓ passenger, there exists at least one driver type k such that $[t_\ell^0, T_\ell]$ and $[t_k^0, T_k]$ overlap. The overlap condition ensures that the passenger belief γ_ℓ is bounded strictly above 0 so that the passenger type has a positive mass. Then we can apply the proof strategy for the illustrative example in Appendix B.

E Numerical Solution of the Equilibrium in the Illustrative Model

We set $T = 10$ and discretize the time into $\mathfrak{T} = 100$ periods. The length of each period is $\Delta = \frac{T}{\mathfrak{T}}$. We set the arrival rate of move opportunities to be $\lambda = 1$. Given a vector of passenger masses $n_{\ell \mathfrak{t}}$ for each

type ℓ in period $\mathfrak{t}$, the discretized driver value function is

$$\begin{aligned} V_{k\mathfrak{t}} = \Delta\lambda \big(\Upsilon &+ (1-d_k)\left(n_{1\mathfrak{t}}h_{k1}\ln\left(1+\exp\left(u_{k1}\right)+\exp\left(V_{k\mathfrak{t}+1}\right)\right)\right. \\ &+ \left(1-n_{1\mathfrak{t}}h_{k1}\right)n_{2\mathfrak{t}}\ln\left(1+\exp\left(u_{k2}\right)+\exp\left(V_{k\mathfrak{t}+1}\right)\right) \\ &+ \left.\left(1-n_{1\mathfrak{t}}h_{k1}\right)\left(1-n_{2\mathfrak{t}}\right)\ln\left(1+\exp\left(V_{k\mathfrak{t}+1}\right)\right)\right) \\ &+ d_k\left(n_{1\mathfrak{t}}h_{k1}\ln\left(\exp\left(u_{k1}\right)+\exp\left(V_{k\mathfrak{t}+1}\right)\right)\right. \\ &+ \left.\left(1-n_{1\mathfrak{t}}h_{k1}\right)n_{2\mathfrak{t}}\ln\left(\exp\left(u_{k2}\right)+\exp\left(V_{k\mathfrak{t}+1}\right)\right)+\left(1-n_{1\mathfrak{t}}h_{k1}\right)\left(1-n_{2\mathfrak{t}}\right)V_{k\mathfrak{t}+1}\right) \\ &+ \left(1-\Delta\lambda\right)V_{k\mathfrak{t}+1}-\Delta c^{\mathrm{drv}}\mathfrak{t}\Delta/T, \end{aligned} \tag{SE.1}$$

where $d_k = 1$ means the driver commits to waiting till T and $d_k = 0$ otherwise, and $h_{k1} = 0$ means that the type 1 passengers are not shown to type k drivers and $h_{k1} = 1$ otherwise. We set $V_{k\mathfrak{T}} = 0$.

Next, we define driver choice probabilities. We use $q_{k\ell\mathfrak{t}}$ to denote the probability of choosing a type ℓ passenger in period $\mathfrak{t}$ conditional on observing a type ℓ passenger,

$$\begin{aligned} q_{k1\mathfrak{t}} &= \frac{\left(1-d_k\right)\exp\left(u_{k1}\right)}{1+\exp\left(u_{k1}\right)+\exp\left(V_{k\mathfrak{t}+1}\right)}+\frac{d_k\exp\left(u_{k1}\right)}{\exp\left(u_{k1}\right)+\exp\left(V_{k\mathfrak{t}+1}\right)} \\ q_{k2\mathfrak{t}} &= \left(1-n_{1\mathfrak{t}}h_{k1}\right)\left(\frac{\left(1-d_k\right)\exp\left(u_{k2}\right)}{1+\exp\left(u_{k2}\right)+\exp\left(V_{k\mathfrak{t}+1}\right)}+\frac{d_k\exp\left(u_{k2}\right)}{\exp\left(u_{k2}\right)+\exp\left(V_{k\mathfrak{t}+1}\right)}\right). \end{aligned} \tag{SE.2}$$

The probability that a driver arriving in period $\mathfrak{t}$ chooses a type ℓ passenger upon arrival, conditional on observing the type ℓ, is

$$q^0_{k1\mathfrak{t}} = \frac{\exp\left(u_{k1}\right)}{1+\exp\left(u_{k1}\right)+\exp\left(V_{k\mathfrak{t}+1}\right)}, q^0_{k2\mathfrak{t}} = \frac{\left(1-n_{1\mathfrak{t}}h_{k1}\right)\cdot\exp\left(u_{k2}\right)}{1+\exp\left(u_{k2}\right)+\exp\left(V_{k\mathfrak{t}+1}\right)}. \tag{SE.3}$$

The probability of leaving upon arrival is

$$\begin{aligned} w^0_{k\mathfrak{t}} = &\frac{n_{1\mathfrak{t}}h_{k1}}{1+\exp\left(u_{k1}\right)+\exp\left(V_{k\mathfrak{t}+1}\right)}+\frac{\left(1-n_{1\mathfrak{t}}h_{k1}\right)n_{2\mathfrak{t}}}{1+\exp\left(u_{k2}\right)+\exp\left(V_{k\mathfrak{t}+1}\right)} \\ &+\frac{\left(1-n_{1\mathfrak{t}}h_{k1}\right)\left(1-n_{2\mathfrak{t}}\right)}{1+\exp\left(V_{k\mathfrak{t}+1}\right)}. \end{aligned}$$

For a waiting driver, the probability of leaving is

$$w_{k\mathfrak{t}} = \left(1-d_k\right)w^0_{k\mathfrak{t}}. \tag{SE.4}$$

These probabilities allow us to compute the driver masses:

$$m_{k\mathfrak{t}+1} = \frac{\Delta}{T}\left(1-n_{1\mathfrak{t}}h_{k1}q^0_{k1\mathfrak{t}}-n_{2\mathfrak{t}}q^0_{k2\mathfrak{t}}-w^0_{k\mathfrak{t}}\right)+m_{k\mathfrak{t}}\left(1-\lambda\Delta\times\left(n_{1\mathfrak{t}}h_{k1}q_{k1\mathfrak{t}}+n_{2\mathfrak{t}}q_{k2\mathfrak{t}}+w_{k\mathfrak{t}}\right)\right), \tag{SE.5}$$

where $m_{k1} = 0$.

On the passenger side, we first compute the average match rate as a type ℓ passenger's belief,

$$\gamma_\ell = \frac{1}{\mathfrak{T}} \sum_{\mathfrak{t}=1}^{\mathfrak{T}} \left(\sum_{k \in \{a,b\}} \left(\lambda \Delta m_{k\mathfrak{t}} q_{k\ell\mathfrak{t}} + \frac{1}{\mathfrak{T}} q^0_{k\ell\mathfrak{t}} \right) \cdot \left(h_{k1} \cdot \mathbb{1}\left(\ell = 1\right) + \mathbb{1}\left(\ell = 2\right) \right) \right). \tag{SE.6}$$

When the passenger is not committed to waiting till T, the probability that the optimal leaving time is greater than $\mathfrak{t}$ is

$$S_{\ell\mathfrak{t}} = \left(1 + \exp\left(\mathfrak{t} \cdot \frac{c^{\text{psg}}}{\mathfrak{T}} / \gamma_\ell - v_\ell \right) \right)^{-1}. \tag{SE.7}$$

The cancellation probability in period $\mathfrak{t}$ is

$$r_{\ell\mathfrak{t}} = \frac{S_{\ell\mathfrak{t}} - S_{\ell\mathfrak{t}+1}}{S_{\ell\mathfrak{t}}}. \tag{SE.8}$$

When the passenger is subject to the commitment, the probability that the passenger would wait upon arriving at $\mathfrak{t}$ is

$$\bar{S}_{\ell\mathfrak{t}} = \frac{\exp\left(v_\ell - \overline{v}_{\ell\mathfrak{t}}\right)}{1 + \exp\left(v_\ell - \overline{v}_{\ell\mathfrak{t}}\right)}, \tag{SE.9}$$

where

$$\overline{v}_{\ell\mathfrak{t}} = \frac{\sum_{\mathfrak{t}_1=\mathfrak{t}}^{\mathfrak{T}} \gamma_\ell \mathfrak{t}_1 \frac{c^{\text{psg}}}{\mathfrak{T}} \exp\left(-\gamma_\ell \left(\mathfrak{t}_1 - \mathfrak{t}\right)\right)}{1 - \exp\left(-\gamma_\ell \left(\mathfrak{T} - \mathfrak{t}\right)\right)}.$$

We next compute the passenger mass using

$$\begin{aligned} n_{\ell\mathfrak{t}+1} = {} & \frac{1}{\mathfrak{T}} \left(\left(1 - d_\ell\right) S_{\ell\mathfrak{t}} + d_\ell \overline{S}_{\ell\mathfrak{t}} \right) \\ & + n_{\ell\mathfrak{t}} \left(1 - \sum_{k \in \{a,b\}} \left(\lambda \Delta m_{k\mathfrak{t}} q_{k\ell\mathfrak{t}} + \frac{1}{\mathfrak{T}} q^0_{k\ell\mathfrak{t}} \right) \cdot \left(h_{k1} \cdot \mathbb{1}\left(\ell = 1\right) + \mathbb{1}\left(\ell = 2\right) \right) - \left(1 - d_\ell\right) r_{\ell\mathfrak{t}} \right), \end{aligned} \tag{SE.10}$$

with the initial condition $n_{\ell 1} = 0$, where $d_\ell = 1$ means that the passenger commits to waiting till T and $d_\ell = 0$ otherwise. The following algorithm summarizes the procedure.

1. Start with initial values of $n_{\ell\mathfrak{t}}$, which are two vectors of length $\mathfrak{T}$ with values between 0 and 1.
2. Use (SE.1) and (SE.5) to compute driver choice probabilities and mass functions.
3. Use the probabilities computed in Step 2 and (SE.6) through (SE.10) to update the passenger mass functions.
4. Repeat steps 2 and 3 until convergence.

By varying the initial passenger mass functions, we can explore the multiplicity of the equilibria. The equilibria found through varying $n_{\ell\mathfrak{t}}$ are quantitatively similar. Our reported results are based on initial values of $n_{\ell\mathfrak{t}} = 0.5$.

F Numerical Solution of the Equilibrium in the Empirical Model

We first discuss how we solve the equilibrium in Section F.1, extending the procedure in Appendix E. We then describe how we use the equilibrium solution to compute the several market level statistics in Appendix F.2. We discuss how to choose the selective visibility parameters h in Appendix F.3. Appendix F.4 adapts the method to find multiple equilibria.

F.1 Solution Procedure

We extend the procedure in Section E to include heterogeneous driver preferences for passengers ν_{ij} with a large number of types and time-varying rates of move opportunities.

We first simulate driver and passenger types. We assume that matching starts at 4:00 pm, 30 minutes before the start of our sample. We also assume that driver arrival times approximate a Poisson process. We simulate the driver arrival times from 4:00 pm to 6:00 pm, where the inter-arrival time is exponentially distributed with the estimated rate of 77.6 drivers/minute. For each arrival time, we simulate the respective driver's route and departure time based on their empirical distribution. For each simulated route, we then simulate driver heterogeneity parameter β_k and waiting costs based on the estimated distribution. We repeat this procedure for passengers, where the arrival times approximate a Poisson process with a rate of 31.77 passengers/minute. We simulate passengers' unobserved heterogeneity $\zeta_\ell, \vartheta_\ell$ and $\vartheta_{60,\ell}$.

Next, for each arrival time, route, departure time and preference parameter combination, we solve for driver and passenger choice probabilities and the transitions of the mass. We use $\imath$ and $\jmath$ to index this combination for drivers and passengers to emphasize that we condition on the arrival time. The simulation uses 8,880 $\imath$s and $4,000$ different $\jmath$s. We use $t^0_\imath, T_\imath, t^0_\jmath$ and $T_\jmath$ to denote the arrival and departure times of drivers and passengers. We discretize the driver time, and we set each period to be $\Delta^{\text{drv}} = 5$ minutes. Time is discretized more finely on the passenger side and we set each period to be $\Delta^{\text{psg}} = 0.05$ minutes. By choosing $\Delta^{\text{psg}} \ll \Delta^{\text{drv}}$, we allow the passenger mass to evolve more "continuously" so that if multiple drivers' simulated move opportunities arrive close to each other, those that move later would find a lower passenger mass because of matches with earlier-moving drivers. To keep the notation simple, we still use the Δ^{psg} notation, although Δ^{psg} has a different value from that in Section A.4. We use $m_{\imath\mathfrak{t}}$ and $n_{\jmath\mathfrak{t}}$ to denote driver combination $\imath$'s and passenger combination $\jmath$'s masses $\mathfrak{t}$ periods after arrival. The maximum number of periods for $\imath$ and $\jmath$ are denoted as $\mathfrak{T}_\imath = \left\lceil \frac{T_\imath - t^0_i}{\Delta^{\text{drv}}} \right\rceil$ and $\mathfrak{T}_\jmath = \left\lceil \frac{T_\jmath - t^0_\jmath}{\Delta^{\text{psg}}} \right\rceil$. Therefore for $\imath$, $\mathfrak{t}$ varies from 1 to $\mathfrak{T}_\imath$, where each $\mathfrak{t}$ represents the $\mathfrak{t}$th 5-minute interval after the arrival. Similarly for each $\jmath$, $\mathfrak{t}$ varies from 1 to $\mathfrak{T}_\jmath$, where each $\mathfrak{t}$ represents the $\mathfrak{t}$th 0.05-minute interval after the arrival.

F.1.1 Driver

For each $\imath$ and $\mathfrak{t}$, we uniformly randomly select a time point $t(\imath, \mathfrak{t})$ in the 5-minute period $\mathfrak{t}$ as the move time if a move opportunity arrives. The move opportunity arrives with probability $\Lambda_{\imath\mathfrak{t}}$, estimated in Section A.6. We set $\Lambda_{\imath 1} = 1$, i.e., all arriving drivers can choose an action upon arrival. We construct

$\imath'$s choice set as the set of $\jmath$ where $t(\imath,\mathfrak{t}) \in \left[t^0_\jmath, T_\jmath\right]$, i.e., any passenger that overlaps with the move time. We use $\mathfrak{S}_{\imath\mathfrak{t}}$ to denote this set of passengers and $|\mathfrak{S}_{\imath\mathfrak{t}}|$ for the number of passengers in this set. We use $n_\jmath(\imath,\mathfrak{t})$ to denote the passenger $\jmath$'s mass in the period that coincides with $t(\imath,\mathfrak{t})$. Given a move opportunity, the probability that the driver observes a non-empty set of passengers is

$$p_{\imath\mathfrak{t}} = 1 - \prod_{\jmath\in\mathfrak{S}_{\imath,\mathfrak{t}}} \left(1 - h_{\imath\jmath\mathfrak{t}} n_\jmath(\imath,\mathfrak{t})\right),$$

where $h_{\imath\jmath\mathfrak{t}} \in [0,1]$ denotes the probability that a passenger $\jmath$ is visible to the driver $\imath$ in the $\mathfrak{t}$th period after $\imath$'s arrival. We take h values as given when solving for an equilibrium. To solve for driver vale functions, we first simulate a $NS \times |\mathfrak{S}_{\imath\mathfrak{t}}|$ matrix of standard normal draws of driver preference for passengers $\nu^{(ns)}_{\imath\jmath}, ns = 1 \ldots NS$. We set $NS = 50$ in our simulation. For each $1 \times |\mathfrak{S}_{\imath\mathfrak{t}}|$ row vector of νs corresponding with the draw ns, we find the highest match value $\overline{u}^{ns}_{\imath\mathfrak{t}}$ among passengers in the set $\mathfrak{S}_{\imath\mathfrak{t}}$. Let $\jmath^{ns}_{\imath\mathfrak{t}}$ be the corresponding passenger index. The driver's Bellman equation is

$$\begin{aligned} V_{\imath\mathfrak{t}} = \Lambda_{\imath\mathfrak{t}} \Bigg(& \Upsilon + (1-d_\imath) \Bigg(\frac{1}{NS} \sum_{ns=1}^{NS} h_{\imath\jmath^{ns}_{\imath\mathfrak{t}}\mathfrak{t}} n_{\jmath^{ns}_{\imath\mathfrak{t}}}(\imath,\mathfrak{t}) \ln\left(1 + \exp\left(\overline{u}^{ns}_{\imath\mathfrak{t}}\right) + \exp\left(V_{\imath\mathfrak{t}+1}\right)\right) \\ & + (1-p_{\imath\mathfrak{t}}) \ln\left(1 + \exp\left(V_{\imath\mathfrak{t}+1}\right)\right) \Bigg) \\ & + d_\imath \Bigg(\frac{1}{NS} \sum_{ns=1}^{NS} h_{\imath\jmath^{ns}_{\imath\mathfrak{t}}\mathfrak{t}} n_{\jmath^{ns}_{\imath\mathfrak{t}}}(\imath,\mathfrak{t}) \ln\left(\exp\left(\overline{u}^{ns}_{\imath\mathfrak{t}}\right) + \exp\left(V_{\imath\mathfrak{t}+1}\right)\right) \\ & + (1-p_{\imath\mathfrak{t}}) V_{\imath\mathfrak{t}+1} \Bigg) \Bigg) + (1-\Lambda_{\imath\mathfrak{t}}) V_{\imath\mathfrak{t}+1} - c_{\imath\mathfrak{t}}, \end{aligned} \tag{SF.11}$$

where $d_\imath = 1$ indicates that $\imath$ commits to waiting till departure time $T_\imath$ and $d_\imath = 0$ otherwise. The waiting cost $c_{\imath,\mathfrak{t}}$ corresponds with the waiting cost over Δ^{drv} in $\imath$'s period $\mathfrak{t}$. We set $V_{\imath\mathfrak{T}_\imath} = 0$.

We use the value function to define the choice probabilities. The probability of choosing $\jmath$ in $\mathfrak{t} > 1$ conditional on a move opportunity and observing $\jmath$ is

$$q_{\imath\jmath\mathfrak{t}} = \frac{1}{NS} \sum_{ns=1}^{NS} \mathbb{1}\left(\jmath = \jmath^{ns}_{\imath\mathfrak{t}}\right) \left(\frac{(1-d_\imath)\exp\left(\overline{u}^{ns}_{\imath\mathfrak{t}}\right)}{1 + \exp\left(\overline{u}^{ns}_{\imath\mathfrak{t}}\right) + \exp\left(V_{\imath\mathfrak{t}+1}\right)} + \frac{d_\imath \exp\left(\overline{u}^{ns}_{\imath\mathfrak{t}}\right)}{\exp\left(\overline{u}^{ns}_{\imath\mathfrak{t}}\right) + \exp\left(V_{\imath\mathfrak{t}+1}\right)} \right). \tag{SF.12}$$

The leave probability is

$$w_{\imath\mathfrak{t}} = (1-d_\imath) \left(\frac{1}{NS} \sum_{ns=1}^{NS} \frac{h_{\imath\jmath^{ns}_{\imath\mathfrak{t}}\mathfrak{t}} n_{\jmath^{ns}_{\imath\mathfrak{t}}}(\imath,\mathfrak{t})}{1 + \exp\left(\overline{u}^{ns}_{\imath\mathfrak{t}}\right) + \exp\left(V_{\imath\mathfrak{t}+1}\right)} + \frac{1-p_{\imath\mathfrak{t}}}{1 + \exp\left(V_{\imath\mathfrak{t}+1}\right)} \right). \tag{SF.13}$$

For these probabilities upon arrival ($q_{\imath\jmath 1}$ and $w_{\imath 1}$), we set $d_\imath = 0$ in the above.

The mass function is given by

$$m_{\imath\mathfrak{t}+1} = m_{\imath\mathfrak{t}} \left(1 - \Lambda_{\imath\mathfrak{t}} \left(\sum_{\jmath\in\mathfrak{S}_{i\mathfrak{t}}} q_{\imath\jmath\mathfrak{t}} h_{\imath\jmath\mathfrak{t}} n_\jmath(\imath,\mathfrak{t}) + w_{\imath\mathfrak{t}} \right) \right), \tag{SF.14}$$

where

$$m_{\imath 1} = \exp\left(V_{\imath 2}\right)\left(\frac{1}{NS}\sum_{ns=1}^{NS}\frac{h_{\imath \jmath_{\imath 1}^{ns}1} n_{\jmath_{\imath 1}^{ns}}\left(\imath,1\right)}{1+\exp\left(\overline{u}_{\imath 1}^{ns}\right)+\exp\left(V_{\imath 2}\right)}+\frac{1-p_{\imath 1}}{1+\exp\left(V_{\imath 2}\right)}\right). \tag{SF.15}$$

which is the probability of continuing to wait upon arrival.

F.1.2 Passenger

We first compute the match rate. For each $\jmath$ and $\mathfrak{t}$, we first find the total mass matched with drivers. Let $m_\imath\left(\jmath,\mathfrak{t}\right)$ denote the mass of driver $\imath$ when its move time falls in the period $\mathfrak{t}$ of the passenger $\jmath$. We set $m_\imath\left(\jmath,\mathfrak{t}\right)=0$ if no such time exists for $\imath$. We denote the corresponding driver period as $\tilde{\mathfrak{t}}\left(\jmath,\mathfrak{t}\right)$. The belief is computed as

$$\gamma_\jmath = \frac{1}{\mathfrak{T}_\jmath}\sum_{\mathfrak{t}=1}^{\mathfrak{T}_\jmath}\sum_{\imath}\Lambda_{\imath\tilde{\mathfrak{t}}(\jmath,\mathfrak{t})} m_\imath\left(\jmath,\mathfrak{t}\right) h_{\imath\jmath\tilde{\mathfrak{t}}(\jmath,\mathfrak{t})} q_{\imath\jmath\tilde{\mathfrak{t}}(\jmath,\mathfrak{t})}.$$

When we construct the passenger masses for driver estimation, the belief $\gamma_\jmath$ is replaced with the estimated belief in Appendix A.4.

We next compute the leaving rate. When the passenger does not commit to waiting till her departure time, we first compute the survival probability

$$S_{\jmath\mathfrak{t}} = \frac{1}{1+\exp\left(o_{\jmath\mathfrak{t}}/\gamma_\jmath - v_\jmath\right)}, \tag{SF.16}$$

where $o_{\jmath\mathfrak{t}}$ and $v_\jmath$ are the estimated waiting costs and passenger match value. The waiting cost $o_{\jmath\mathfrak{t}}$ corresponds with the flow waiting cost over Δ^{psg}. The leaving probability is then

$$r_{\jmath\mathfrak{t}} = \frac{S_{\jmath\mathfrak{t}} - S_{\jmath\mathfrak{t}+1}}{S_{\jmath\mathfrak{t}}}. \tag{SF.17}$$

If the passenger commits to waiting till $T_\jmath$, then we compute

$$\overline{S}_{\jmath 1} = \frac{\exp\left(v_\jmath - \overline{v}_\jmath\right)}{1+\exp\left(v_\jmath-\overline{v}_\jmath\right)}, \tag{SF.18}$$

where

$$\overline{v}_\jmath = \frac{\sum_{\mathfrak{t}_1=1}^{\mathfrak{T}_\jmath}\gamma_\ell o_{\jmath\mathfrak{t}_1}\exp\left(-\gamma_\jmath \mathfrak{t}_1\right)}{1-\exp\left(-\gamma_\jmath\mathfrak{T}_\jmath\right)}.$$

The conditional mass function is then given by

$$n_{\jmath\mathfrak{t}} = n_{\jmath\mathfrak{t}}\cdot\max\left\{0, 1-\sum_{\mathfrak{t}=1}^{\mathfrak{T}_\jmath}\sum_{\imath}\Lambda_{\imath\tilde{\mathfrak{t}}(\jmath,\mathfrak{t})} m_\imath\left(\jmath,\mathfrak{t}\right) h_{\imath\jmath\tilde{\mathfrak{t}}(\jmath,\mathfrak{t})} q_{\imath\jmath\tilde{\mathfrak{t}}(\jmath,\mathfrak{t})} - \left(1-d_\jmath\right) r_{\jmath\mathfrak{t}}\right\}, \tag{SF.19}$$

with $n_{\jmath 1} = \left(1-d_\jmath\right) S_{\jmath 1} + d_\jmath \overline{S}_{\jmath 1}$. The indicator $d_\jmath = 1$ indicates that $\jmath$ commits to waiting till departure time $T_\jmath$ and $d_\jmath = 0$ otherwise.

The solution algorithms iterates over SF.11 through SF.19 till convergence. The input to the

algorithm is the initial passenger mass, $n_{\jmath \mathfrak{t}}, \mathfrak{t} = 1, \ldots, \mathfrak{T}_\jmath$ for each simulated $\jmath$. We compute these initial masses using mass transition functions with estimated passenger exit rates. These exit rates are estimated using the same logit functions in Section A.4 but with exits (by matching or leaving without a match) as the outcome. We can also change these initial masses to explore the multiplicity of equilibria. We discuss our approach in Section F.4.

F.2 Equilibrium Quantities

We provide expressions for aggregate equilibrium outcomes below. Let

$$\begin{aligned}
\mathcal{I}_\imath &= \mathbb{1}\left(\text{4:30 pm} \leq t_\imath^0 < \text{5:00 pm}\right) \\
\mathcal{I}_\jmath &= \mathbb{1}\left(\text{4:30 pm} \leq t_\jmath^0 < \text{5:00 pm}\right) \\
\widetilde{\mathcal{I}}_\imath &= \mathbb{1}\left(\text{5:00 pm} \leq T_\imath < \text{5:20 pm}\right)
\end{aligned}$$

1. Number of matches among passengers that arrive between 4:30 pm and 5:00 pm,

$$\sum_\jmath \sum_{\mathfrak{t}=1}^{\mathfrak{T}_\jmath} \sum_\imath \Lambda_{\imath \tilde{\mathfrak{t}}(\jmath,\mathfrak{t})} m_\imath\left(\jmath, \mathfrak{t}\right) h_{\imath\jmath\tilde{\mathfrak{t}}(\jmath,\mathfrak{t})} q_{\imath\jmath\tilde{\mathfrak{t}}(\jmath,\mathfrak{t})} n_{\jmath\mathfrak{t}} \mathcal{I}_\jmath.$$

2. Total revenue from passengers that arrive between 4:30 pm and 5:00 pm,

$$\sum_\jmath \sum_{\mathfrak{t}=1}^{\mathfrak{T}_\jmath} \sum_\imath f_\jmath \Lambda_{\imath \tilde{\mathfrak{t}}(\jmath,\mathfrak{t})} m_\imath\left(\jmath, \mathfrak{t}\right) h_{\imath\jmath\tilde{\mathfrak{t}}(\jmath,\mathfrak{t})} q_{\imath\jmath\tilde{\mathfrak{t}}(\jmath,\mathfrak{t})} n_{\jmath\mathfrak{t}} \mathcal{I}_\jmath.$$

3. Average surplus

$$\frac{\sum_\imath V_{\imath 1} \mathcal{I}_\imath + \sum_\jmath W_\jmath \mathcal{I}_\jmath}{\sum_\imath \mathcal{I}_\imath + \sum_\jmath \mathcal{I}_\jmath},$$

where $W_\jmath$ is the simulated passenger value of $\jmath$ based on (16) if not subject to passenger commitment, and (18) otherwise. Specifically, we draw $\widetilde{NS} = 100$ logistic shocks for ξ_j. For each shock $\widetilde{ns} = 1, \ldots, \widetilde{NS}$, we first compute the optimal leaving time $\mathfrak{t}_\jmath^{\star\widetilde{ns}}$ as the minimum of $\mathfrak{T}_j$ and $\mathfrak{t}$ that satisfies

$$o_\jmath\left(\mathfrak{t}\right) < \gamma_\jmath\left(\zeta_x x_\jmath - \zeta_f f_\jmath + \zeta^{\widetilde{ns}}\right) < o_\jmath\left(\mathfrak{t}+1\right).$$

We then compute the value function as

$$\begin{aligned}
W_\jmath = \frac{1}{\widetilde{NS}} \sum_{\widetilde{ns}=1}^{\widetilde{NS}} \Bigg(& \left(1-d_\jmath\right) \sum_{\mathfrak{t}=1}^{t_\jmath^{\star\widetilde{ns}}} \gamma_\jmath\left(\zeta_x x_\jmath - \zeta_f f_\jmath + \zeta^{\widetilde{ns}} - o_\jmath\left(\mathfrak{t}\right)\right)\left(1-\gamma_\jmath\right)^{\mathfrak{t}-1} \\
& + d_\jmath \sum_{\mathfrak{t}=1}^{\mathfrak{T}_\jmath} \gamma_\jmath\left(\zeta_x x_\jmath - \zeta_f f_\jmath + \zeta^{\widetilde{ns}} - o_\jmath\left(\mathfrak{t}\right)\right)\left(1-\gamma_\jmath\right)^{\mathfrak{t}-1} \Bigg).
\end{aligned}$$

4. Drivers

(a) Among drivers with departure times between 5:00 pm and 5:20 pm, the percentage of drivers who decide to wait after arrival,

$$\frac{\sum_\imath m_{\imath 1}\widetilde{\mathcal{I}}_\imath}{\sum_\imath \widetilde{\mathcal{I}}_\imath}.$$

(b) The search duration conditional on waiting after arrival,

$$\frac{\sum_\imath \sum_{\mathfrak{t}=1}^{\mathfrak{T}_\imath} m_{\imath\mathfrak{t}} \left(\mathfrak{t}-1\right) \Delta^{\text{drv}}\widetilde{\mathcal{I}}_\imath}{\sum_\imath \widetilde{\mathcal{I}}_\imath}.$$

(c) The search duration conditional on a match,

$$\frac{\sum_\imath \sum_{\mathfrak{t}=1}^{\mathfrak{T}_\imath} \sum_\jmath \Lambda_{\imath\mathfrak{t}} m_{\imath\mathfrak{t}} q_{\imath\jmath\mathfrak{t}} n_\jmath \left(\imath,\mathfrak{t}\right) \left(\mathfrak{t}-1\right) \Delta^{\text{drv}}\widetilde{\mathcal{I}}_\jmath}{\sum_\imath \sum_{\mathfrak{t}=1}^{\mathfrak{T}_\imath} \sum_\jmath \Lambda_{\imath\mathfrak{t}} m_{\imath\mathfrak{t}} q_{\imath\jmath\mathfrak{t}} n_\jmath \left(\imath,\mathfrak{t}\right) \widetilde{\mathcal{I}}_\jmath}.$$

(d) The average surplus is $\dfrac{1}{\sum_\imath \widetilde{\mathcal{I}}_\imath} \sum_\imath V_\imath \widetilde{\mathcal{I}}_\imath$.

5. For passengers, the percentage that waits, the conditional search duration and the average surplus are defined analogously to the driver's. The search duration conditional on matching is

$$\frac{\sum_\jmath \sum_{\mathfrak{t}=1}^{\mathfrak{T}_\jmath} \sum_\imath \Lambda_{\imath\tilde{\mathfrak{t}}(\jmath,\mathfrak{t})} m_\imath \left(\jmath,\mathfrak{t}\right) h_{\imath\jmath\tilde{\mathfrak{t}}(\jmath,\mathfrak{t})} q_{\imath\jmath\tilde{\mathfrak{t}}(\jmath,\mathfrak{t})} n_{\jmath\mathfrak{t}} \left(\mathfrak{t}-1\right) \Delta^{\text{psg}}\mathcal{I}_\jmath}{\sum_\jmath \sum_{\mathfrak{t}=1}^{\mathfrak{T}_\jmath} \sum_\imath \Lambda_{\imath\tilde{\mathfrak{t}}(\jmath,\mathfrak{t})} m_\imath \left(\jmath,\mathfrak{t}\right) h_{\imath\jmath\tilde{\mathfrak{t}}(\jmath,\mathfrak{t})} q_{\imath\jmath\tilde{\mathfrak{t}}(\jmath,\mathfrak{t})} n_{\jmath\mathfrak{t}} \mathcal{I}_\jmath}.$$

F.3 Choose $h_{\imath\jmath\mathfrak{t}}$

Consistent with the information assumption about the designer in Section 4.2.2, we do not choose $h_{\imath\jmath\mathfrak{t}}$ for each $\imath, \jmath$ and $\mathfrak{t}$. It is also not computationally feasible to do so. We group driver and passengers and assign the same $h_{\imath\jmath\mathfrak{t}}$ to those in the same group. The grouping is based on the observed driver and passenger characteristics.

1. Route popularity. We measure the popularity of a trip using the number of passenger requests that travel to and from the same pair of 2 km-by-2 km squares as the route over all days in our sample. The motivation is that drivers across these groups differ in the expected number of compatible passengers and therefore the effects of additional waiting. Similarly, passengers across different groups face different distributions of drivers and should differ in their assessments of the values of waiting. An agent is in one of the popularity groups $\mathcal{G}_1^{\text{pop}}, \ldots, \mathcal{G}_5^{\text{pop}}$ $[0,1]$, $(1,2]$, $(2,5]$, $(5,8]$, $(8,\infty]$.

2. Time. We also classify the time periods of each agent based on the corresponding time-to-departure $T_\imath - \Delta^{\text{drv}}\mathfrak{t}$ (for a driver $\imath$) or $T_\jmath - \Delta^{\text{psg}}\mathfrak{t}$ (for a passenger $\jmath$), which may be in one of groups (in unit of minutes) $\mathcal{G}_1^{\text{dept}}, \ldots, \mathcal{G}_5^{\text{dept}}$: $[0,5]$, $(5,7.5]$, $(7.5,10]$, $(10,20]$ and $(20,\infty]$.

3. Driver-passenger compatibility. We classify each $\imath$-$\jmath$ pair into two groups based on whether compatibility score is greater than 80%, $\mathcal{G}_1^{\text{comp}}, \mathcal{G}_2^{\text{comp}}$.

The algorithm chooses the following sets of parameters

1. Driver route popularity and move time. The algorithm chooses $h_{11}^{\text{drv}}, h_{12}^{\text{drv}}, \ldots, h_{55}^{\text{drv}}$ for each combination of $\mathcal{G}_1^{\text{pop}} \ldots$ and $\mathcal{G}_1^{\text{dept}} \ldots$.

2. Passenger route popularity and time. Similarly, the algorithm chooses $h_{11}^{\text{psg}}, h_{12}^{\text{psg}}, \ldots, h_{55}^{\text{psg}}$.

3. Compatibility. The algorithm chooses h_1^{comp} and h_2^{comp}.

For $h_{\imath\jmath\mathfrak{t}}$, we use $\mathfrak{g}(\imath)$ to denote the popularity group index corresponding with $\imath$, $\mathfrak{g}(\imath,\mathfrak{t})$ to denote the departure time group index corresponding with $\imath$ and the corresponding period $\mathfrak{t}$,$\tilde{\mathfrak{t}}_\jmath(\imath,\mathfrak{t})$ for the passenger $\jmath$'s period when $\imath$ searches in her period $\mathfrak{t}$ and $\jmath$ is a passenger in the choice set, and use $\mathfrak{g}(\imath,\jmath)$ to denote the compatibility group index for $\imath$-$\jmath$ pair. We construct $h_{\imath\jmath\mathfrak{t}}$ as

$$h_{\imath\jmath\mathfrak{t}} = h^{\text{drv}}_{\mathfrak{g}(\imath)\mathfrak{g}(\imath,\mathfrak{t})} \cdot h^{\text{psg}}_{\mathfrak{g}(\jmath)\mathfrak{g}\left(\jmath,\tilde{\mathfrak{t}}_\jmath(\imath,\mathfrak{t})\right)} \cdot h^{\text{comp}}_{\mathfrak{g}(\imath,\jmath)}.$$

In our implementation, the optimization algorithm chooses $h_{11}^{\text{drv}}, h_{12}^{\text{drv}}, \ldots, h_{55}^{\text{drv}}$, $h_{11}^{\text{psg}}, h_{12}^{\text{psg}}, \ldots, h_{55}^{\text{psg}}$ and h_1^{comp} and h_2^{comp} between 0 and 1 to maximize one of the quantities in Section F.2. We use the surrogate algorithm in MATLAB for optimization.

F.4 Multiple Equilibria

The input to our algorithm is the vector of initial passenger masses, $n_{\jmath\mathfrak{t}}, \mathfrak{t} = 1, \ldots, \mathfrak{T}_\jmath$ for each simulated $\jmath$. While we use the initial values estimated from their implied empirical distributions in data for our main results, we can also vary the initial input to explore the multiplicity of the equilibria. Specifically, we use the grouping from Section F.3, where the indices $(\imath,\mathfrak{t})$ of each $n_{\imath\mathfrak{t}}$ are associated with two groups $\mathcal{G}^{\text{pop}}_{\mathfrak{g}(\imath)}$ and $\mathcal{G}^{\text{dept}}_{\mathfrak{g}(\imath,\mathfrak{t})}$. For a given vector of nonnegative real numbers, $\mathring{n}_{11}, \ldots, \mathring{n}_{55}$, we set the initial input passenger mass as

$$n_{\imath\mathfrak{t}} = \mathring{n}_{\mathfrak{g}(\imath)\mathfrak{g}(\imath,\mathfrak{t})},$$

and use the algorithm in F.1 to compute the corresponding equilibrium solution and the number of matches based on the formula in F.2. We choose the values of $\mathring{n}_{11}, \ldots, \mathring{n}_{55}$ to maximize or minimize the number of matches through the surrogate minimizer in MATLAB. In our experiments with many starting values, we find multiple equilibria, but they are quantitatively similar.[26] For example, the maximum number of matches across the equilibria we find is 422.01, relative to the baseline 421.87, which are based on initial passenger masses estimated from data (Appendix F.1).[27]

[26] This exercise does not amount to a complete enumeration of all possible equilibria. Any solution to the set of ordinary differential equations and the maximization problems, collected in Appendix D, is an equilibrium. Given that directly solving the large number of ordinary differential equations is computationally prohibitive, we simplify the problem by focusing on equilibria computable through the iterative procedure in Section F.1. This exercise can alternatively be framed as searching within the refined set of equilibria that are fixed points of the mapping from the space of passenger masses to itself defined by the procedure in Appendix F.1.

[27] Our convergence criterion is for the difference in driver and passenger masses to be within 10^{-6} between iterations.

G Comparing Equilibrium Predictions and Simulations

In this section, we examine whether the statistics in Appendix F.2 based on the equilibrium definition can approximate those from simulated markets. In a simulated market, there are a discrete number of drivers and passengers. We first simulate their routes, departure times and unobserved heterogeneity. Then drivers receive move opportunities that arrive stochastically. Drivers and passengers receive shocks and take actions consistent with the equilibrium strategy, thus also changing the number and composition of agents stochastically. The simulation proceeds as follows:

1. We assume that drivers and passengers arrive at the Poisson rates 77.6 drivers/minute and 31.77 passengers/minute. We simulate their arrival times, departure times, routes and the finite unobserved types, and solve for the equilibrium, as in Appendix F.1.

2. For a passenger, we simulate her logistic shock, and solve for her optimal leaving time as in Section 4.4, taking the equilibrium match rate in the first step as given. Passengers are removed from the market after their optimal leaving time.

3. A simulated driver moves immediately upon arrival and can move at most once in every 5 minutes. In every 5-minute interval after the driver arrival, we simulate a potential move time randomly in the interval according to the uniform distribution. We sequentially simulate driver actions based on the clock time of the arrival times and potential move times. With the estimated probability in Section A.6, a driver receives an opportunity to move at a potential move time. Given the move opportunity either upon arrival or at a potential move time, the driver observes a set of waiting passengers. We simulate a driver preference shocks ν_{ij} for each waiting passenger. The driver then uses the value functions computed based on (SE.1) and decide whether to choose a passenger, wait, or leave the market. If the driver chooses a passenger, both the driver and passenger are immediately removed. If the driver chooses to leave without a match, the driver is removed. If the driver chooses to wait or the move opportunity does not arrive, the driver stays in the market until the next potential move time, and this decision process repeats.[28] Any remaining drivers that reach their departure times are removed.

We repeat the steps 2 and 3 100 times. Table SG.1 compares the average of the statistics from 100 simulations to the equilibrium statistics. The equilibrium model predicts longer waiting time for drivers. The differences of other statistics between the two calculations are within 5%.

[28] We generate uniform random variables and compare them with the logit choice probabilities to simulate decisions.

Table SG.1. Compare Equilibrium Predictions and Simulated Market Outcomes

	Equilibrium Prediction	Simulated Market Outcomes
Number of Matches*	421.87	412.93
Total Revenue ($)*	2019.85	1961.49
Driver**		
% Wait After Arrival	42.90	43.16
Search Duration | Wait After Arrival	20.66	16.56
Search Duration | Matched	4.87	5.05
Passenger*		
% Wait After Arrival	80.18	80.06
Search Duration | Wait After Arrival	6.67	6.90
Search Duration | Matched	5.52	5.67

*: Calculated based on passengers arriving between 4:30 pm and 5:00 pm.
**: Calculated based on drivers with departure times between 5:00 pm and 5:20 pm.